Conodont succession and biofacies in upper Frasnian formations (Devonian) from the southern and central parts of the Dinant Synclinorium (Belgium) - (Timing of facies shifting and correlation with late Frasnian events)

by Pierre BULTYNCK, Stefan HELSEN & Joanna HAYDUCKIEWICH

Abstract

Early *rhenana*, Late *rhenana* and *linguiformis* Conodont Zones are recognised in the upper Frasnian Neuville, Valisettes and Matagne Formations of southern Belgium, and documented by their index-taxa. The age of the base of the Matagne Formation shifts from the Early and Late *rhenana* Zones in the southern Dinant Basin into the *linguiformis* Zone in the more northerly Philippeville Massif. In the first area conodont biofacies analyses reveal a deepening of the shelf below the base of the diachronic Matagne Formation; within the lower part of the Matagne shales biofacies analyses indicate shallowing depositional conditions followed by a progressive deepening. The Lower Kellwasser Event is situated close to the base of the Matagne Formation in the southern part of the Dinant Synclinorium and at the base of the Valisettes Formation in the Philippeville Massif. The Upper Kellwasser Event is correlated with the base of the Matagne Formation in the latter area.

Key-words: Conodonts, biostratigraphy, biofacies, late Frasnian, Belgium

Résumé

Les Zones inférieure et supérieure à *Palmatolepis rhenana* et la Zone à *P. linguiformis*, toutes identifiées par la présence de l'espèce-guide, sont reconnues dans les Formations de Neuville, des Valisettes et de Matagne, appartenant au Frasnien supérieur du sud de la Belgique. La base de la Formation de Matagne est diachronique. Au bord sud du Synclinorium de Dinant, elle se situe dans un intervalle couvrant le sommet de la Zone à *P. rhenana* inférieure et la base de la Zone à *P. rhenana supérieure*. Dans le Massif de Philippeville, plus au nord, elle appartient à la Zone à *P. linguiformis*.

L'étude de la succession des biofaciès à conodontes dans la première région, indique un approfondissement de la plate-forme continentale sous la base de la Formation de Matagne; dans la partie inférieure de cette formation, l'environnement redevient moins profond puis progressivement plus profond. Au bord sud du Synclinorium de Dinant, l'événement Kellwasser inférieur est proche de la base de la Formation de Matagne et dans le Massif de Philippeville il se situe à la base de la Formation des Valisettes, dans cette dernière région l'événement Kellwasser supérieur correspond à la base de la Formation de Matagne.

Mots-clefs: Conodontes, biostratigraphie, biofaciès, Frasnien, Belgique

Introduction

In the last decades the biostratigraphy of the upper Frasnian strata in the type-localities in southern Belgium has been discussed in several studies; those on conodonts include BULTYNCK & MARTIN, 1995; COEN & COEN-AUBERT, 1974; HELSEN & BULTYNCK, 1992; MOURAVIEFF, 1970, 1974, 1982; SANDBERG *et al.* 1988, 1992; among others, on ostracodes CASIER, 1975, 1989, 1992, on goniatites MATERN, 1931 and MOURAVIEFF, 1970, on brachiopods SARTENAER, 1974, GODEFROID & HELSEN, in press. and on rugose corals, COEN & COEN-AUBERT, 1974; COEN-AUBERT, 1994. Since the start of a new regional geologic mapping program in the 1990s renewed attention has been paid to the definition, stratigraphical position and correlation of the many lithological units in the Devonian (BOULVAIN *et al.* 1993; BULTYNCK *et al.* 1991; GODEFROID *et al.* 1994).

In southern Belgium Devonian sediments are chiefly represented by neritic facies, and the stratigraphic ranges of taxa used in zonations that are established in pelagic facies, are more than often incomplete. As a result, problems may rise when applying standard biozones, such as the palmatolepid-based Late Devonian conodont zonation. Because of the lack of *Palmatolepis gigas* in the Frasnian of Belgium, MOURAVIEFF (1970) defined the *Ancyrognathus triangularis* Zone (s.l.) by grouping the *An. triangularis* Zone (s.s.) and the Lower *Palmatolepis gigas* Zone of ZIEGLER (1962). In addition, his extended Upper *Pa. gigas* Zone comprised the Upper *Pa. gigas* Zone (s.s.) and the Uppermost *Pa. gigas* Zone, because of the lack of *Pa. linguiformis*. The accuracy of conodont biochronology depends largely on the frequency of index-taxa, as well as of typical specimens . Still other problems arise in Frasnian conodont studies when comparing the KLAPPER (1988, 1990), KLAPPER & FOSTER (1993) KLAPPER *et al.* (1996) and ZIEGLER & SANDBERG (1990) biozonations. The troublesome comparison between the two sets of zonations is to some degree the consequence of a different palmatolepid taxonomy. However, objectively synonymised taxa (e.g., *Palmatolepis subrecta* = *Palmatolepis winchelli*) still have a different stratigraphic range in the two zonations.

In this paper several type-localities have been studied and restudied in order to more precisely locate the Frasnian Early *rhenana,* Late *rhenana* and *linguiformis* Con-

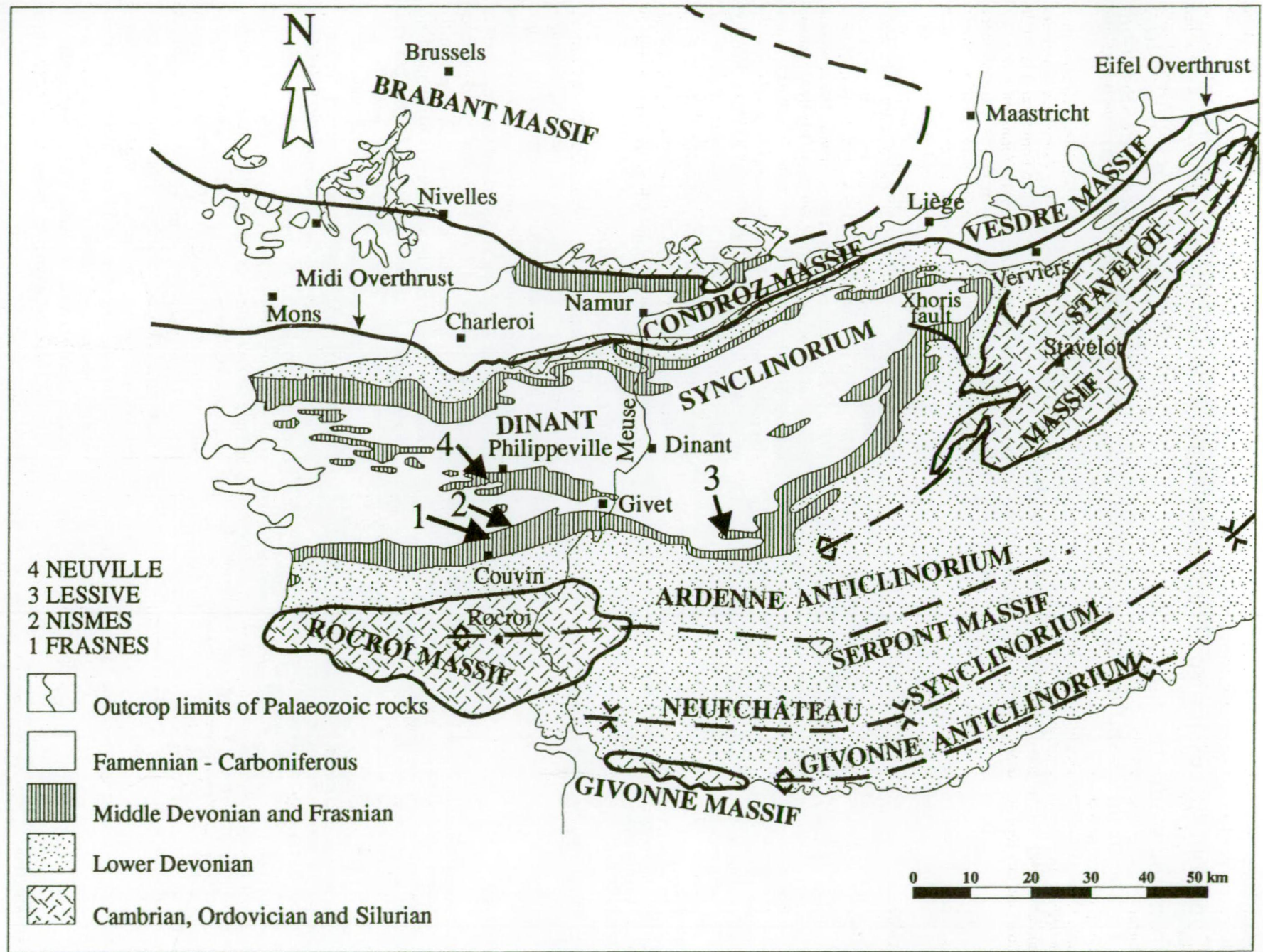Pierre BULTYNCK, Stefan HELSEN & Joanna HAYDUCKIEWICH

Fig. 1a – Geological setting and location of the studied sections.

odont Zones in Belgium. In addition, it is the aim to document the late Frasnian extinction event by means of conodont biofacies and lithofacies, and to correlate them with the Kellwasser Events.

Location and geologic setting of the studied sections

Being part of the Variscan fold belt, Middle and Upper Devonian rocks in southern Belgium are deformed in a series of anticlines and synclines, frequently overturned to the south and associated with inverse faulting. Among the studied sections, the outcrops at Frasnes, Lessive and Nismes are located

on the southern flank of the Dinant Synclinorium; the strata at Neuville are exposed on the southern flank of the Philippeville Massif, a major anticlinal structure in the central part of the Synclinorium (Fig. 1a). In the type-area the Frasnian succession is approximately 400 m thick and includes at least three distinct levels of limestone mounds (TSIEN, 1974). To the east, in the Lessive area 365 m of Frasnian strata are represented by shales and some inferior limestone beds (COEN, 1977).

In the southern and central parts of the Dinant Synclinorium the upper Frasnian is represented by the Valisettes and Matagne Formations, which overlie the Neuville Formation (Fig. 2). In the Philippeville Massif, the Neuville Formation covers the Philippeville Formation which comprises a series of dark, thin-bedded limestones and reef lentils, and a massif biostromal unit. At Neuville the Philippeville Formation is up to 113 m thick (BOULVAIN et al. 1993). The Neuville Formation is represented by some 15-25 m of typically nodular shales, with only few inferior nodular and argillaceous limestone beds. According to this definition, it appears that SANDBERG et al. (1992: fig. 6) took the lower boundary of the Neuville Formation in the Frasnes area some 11 m too low. The Valisettes Formation is characterised by dark-grey, locally calcareous shales and measures some 90-100 m in the Philippeville Massif (BOULVAIN et al. 1993), but is reduced to less than 10 m in the more southern Frasnes-Nismes area (COEN-AUBERT, 1994) or may be entirely missing. As carbonate nodules are in general uncommon in the Valisettes Formation, these rocks can be distinguised easily from the characteristic nodular shales of the Neuville Formation. The lower limit of the Valisettes Formation is defined in the Neuville railway section at the base of
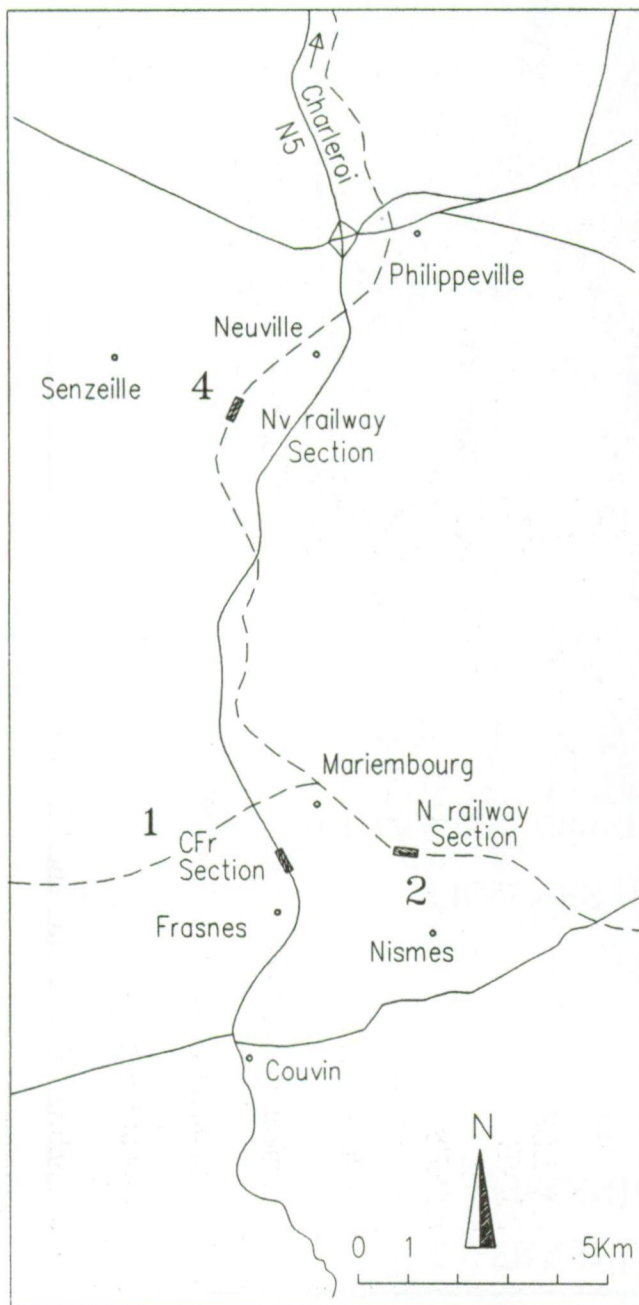

Fig. 1b – Location of the Frasnes, Nismes and Neuville sections; location of localities 1, 2 and 4 in the Dinant Synclinorium is shown on Fig. 1a.
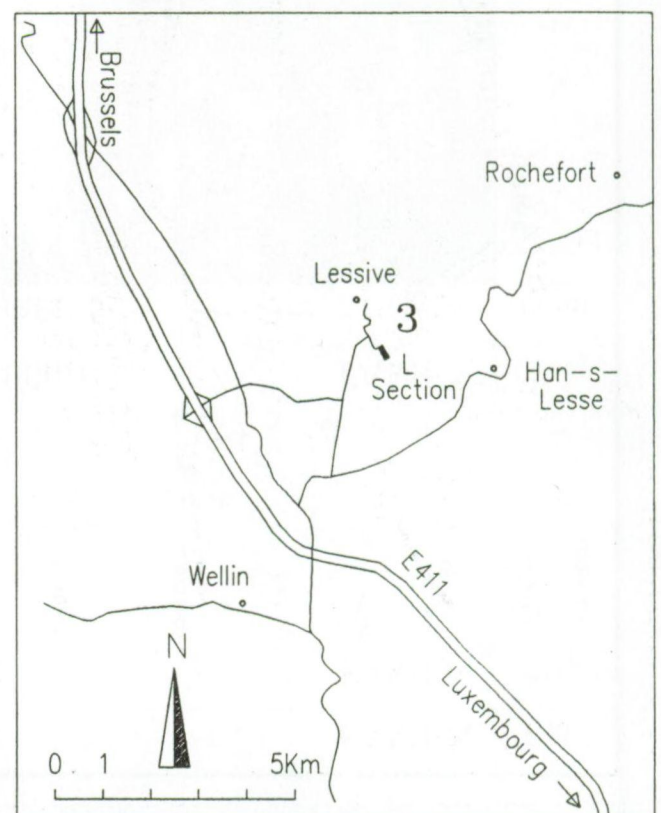

Fig. 1c – Location of the Lessive Section; location of locality 3 in the Dinant Synclinorium is shown on Fig. 1a.
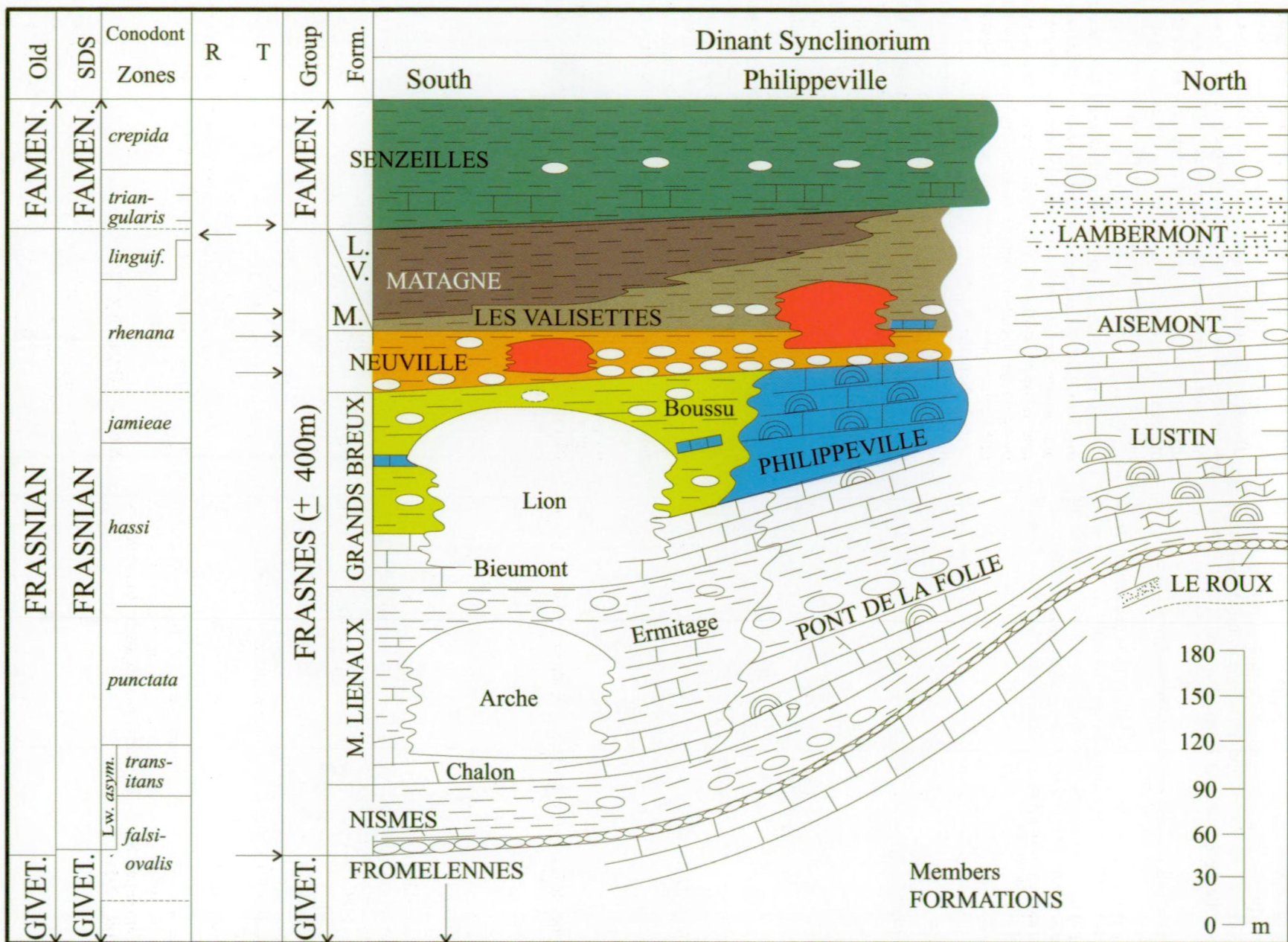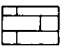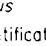
Fig. 2 – Generalized lithostratigraphic cross-section of upper Givetian to lower Famennian strata across the Dinant Synclinorium; the studied stratigraphic interval and area shown in color.

Old	SDS	Conodont Zones	R	T	Group	Form.	Dinant Synclinorium
FAMEN.	FAMEN.	crepida			FAMEN.		South — Philippeville — North
		trian-gularis				SENZEILLES	
		linguif.				L. / L.V.	LAMBERMONT
		rhenana				MATAGNE / LES VALISETTES / M.	AISEMONT
						NEUVILLE	
FRASNIAN	FRASNIAN	jamieae			FRASNES (± 400m)	GRANDS BREUX	Boussu / PHILIPPEVILLE / LUSTIN
		hassi					Lion / Bieumont
		punctata				M. LIENAUX	Ermitage / PONT DE LA FOLLE / LE ROUX
							Arche
	Lw. asym.	trans-itans					Chalon
GIVET.	GIVET.	falsi-ovalis			GIVET.	NISMES	
						FROMELENNES	Members FORMATIONS

180
150
120
90
60
30
0 — m

SYMBOLS AND ABBREVIATIONS FOR FIGURES

▨	Shale	𝕝	Receptaculids
▨	Fissile blackish shale	ℐ	Rugose corals
⬭	Nodular shale	⬥	Hexagonaria
		⬭	"Phillipsastrea"
	Subnodular limestone	⬭	Brachiopods
	Limestone	⋓	Fenstellids
	Dark subnodular limestone	⬭	Gastropods
⬟	Domical stromatoporoids	⬭	"Buchiola"
⬬	Laminar stromatoporoids	☋	Orthoconic cephalopods
Y	Ramose stromatoporoids	⬭	Goniatites
		⊗	Crinoids

I : *Icriodus*   P : *Polygnathus*   Pa : *Palmatolepis*
Bel : *Belodella*   An : *Ancyrognathus*   Anl : *Ancyrolepis*.
Ad : *Ancyrodella*   ● : species identification is sure
● : cf.identification   o : aff.identification   —— : stratigraphic range
Ancyrodella curvata : ⬤ eary form , ● early + late form ,
                        ⬤ late form , ✦ late + latest form

---

the fine shales overlying the last nodular limestone bed of the Neuville Formation. Reddish, massive limestone mounds occur in both Neuville and Valisettes Formations (BOULVAIN, 1993). At least 50 m thick in the Frasnes area, the younger Matagne Formation comprises a succession of fine, dark greenish brown to black shales and dark limestones (GOSSELET, 1871). These shales are rich in pyrite, and apart from a few tiny and thin-shelled benthonic elements, the faunas consist chiefly of pelagic organisms, indicating hypoxic bottom conditions during sedimentation. Ostracodes, tentaculites (CASIER, 1975, 1989, 1992), and small cephalopods (MATERN, 1931; MOURAVIEFF, 1970) are generally preserved as pyritised molds, while the small characteristic bivalve *Buchiola* is commonly found as impressions. In the stratotype at Nismes the lower boundary of the Matagne Formation has been defined at the base of the first limestone bed with abundant goniatites, orthocones and *Buchiola*, i.e., bed 84 of HELSEN & BULTYNCK (1992) (*Commission Nationale de Stratigraphie*, unpub. report). Only in the Senzeilles trench, temporary filled in between 1993-1995, is the upper boundary of the Matagne Formation with the Famennian Senzeilles Formation exposed (BULTYNCK & MARTIN, 1995).

FRASNES (Figs. 3 to 6)

At Frasnes the road section along the Philippeville-Couvin highway was sampled. This section is commonly referred to as "Contournement à Frasnes" (CFr). In addition to the section on the west side where the base of the Matagne Formation is no longer exposed (SARTENAER, 1974), the gently northward dip-

ping strata on the east roadside were sampled (CFrW, CFrE, Fig. 3). In the CFrW section SARTENAER (1974) recognised six lithological units of which units 1 and 2 likely belong to the middle Frasnian Grand Breux Formation and units 3 and 4 to the Neuville Formation. Starting with a series of dark fossiliferous limestone beds, units 5 and 6 probably represent the Matagne Formation. In the Neuville Formation VANDELAER (unpub.) identified three metabentonite horizons labeled Mercurius 1and 3 and Venus 3. Correlation of the first two horizons with the metabentonites in the Frasnes railway cut (SANDBERG *et al.* 1992, fig. 9) and, possibly, in the Ave-et-Auffe section in the Lessive area, is based on the REE pattern. The relative abundance of apatite and the REE pattern of the Venus 3 metabentonite enables a detailed correlation between sections in the Frasnes area (CFrW, railway cut and southern access road to the Lion Quarry) and at Lompret, some nine km south-west of Frasnes. The base of the Matagne Formation has been sampled for conodonts by MOURAVIEFF (1974) and COEN (unpub.)(Fig. 5). In the CFrE section the equivalents of SARTENAER (1974)'s units 4-6 are recognised, forming an anticlinal structure plunging to the east and probably complicated by faulting (Fig. 3).

On the west side, samples CFrW1to 6 were taken in a succession of green nodular shales and grey nodular limestones (units 3 and 4 of SARTENAER, 1974; Fig. 3). A seventh sample in a dark-grey fossiliferous limestone, most likely from the basal part of the Matagne Formation, was not *in situ*. In the heavy fraction of some of the CFrW samples (e.g., CFrW6) grains of sphalerite of 0.5-1.0 mm across are very abundant. Of the 14 samples taken on the eastern side three are from nodular limestones of the Neuville Formation (CFrE1A,1C,1D). The dark limestone beds, lenses and nodules from CFrE2 to 15-6 are assigned to the Matagne Formation (Figs. 3 and 5). The Valisettes Formation is not clearly represented. Based on their lithostratigraphical position, CFrW1 to 6 are considered to be older than CFrE1A.

NISMES (Figs. 7 to 9)

The lithostratigraphic succession and conodonts from this section, located along the Mariembourg-Olloy railway, were studied by MOURAVIEFF (1970) and HELSEN & BULTYNCK (1992)(Fig. 6). The alternation of calcareous shales and limestones, including a massive limestone lens, has been considered as the Neuville Formation. Some 3.5 m of the overlying, greenish fine shales, identified by HELSEN & BULTYNCK (1992) as the lowest part of the Matagne Formation, are here assigned to the Valisettes Formation. As a result, the Matagne Formation comprises the upper nine m of the lithological succession at Nismes. In addition to the HELSEN & BULTYNCK (1992) samples, five new samples were taken at stratigraphically important horizons, e.g., near the Valisettes-Matagne boundary (Figs. 8 and 9).

NEUVILLE (Figs. 10 to 13)

At Neuville, the Charleroi-Couvin railway cut was sampled (Fig. 10). In this section the middle and upper Frasnian Philippeville, Neuville, Valisettes and Matagne Formations and the Famennian Senzeilles Formation are exposed. BOUCKAERT *et al.* (1970) described the section as a succession of seven lithological units, interrupted twice by less important inverse faults. The generally northwards dipping limestones and shales are thus considered to form a more or less continuous succession on

Pierre BULTYNCK, Stefan HELSEN & Joanna HAYDUCKIEWICH

Fig. 3 – Location of the Frasnes sections (CFrW, CFrE).
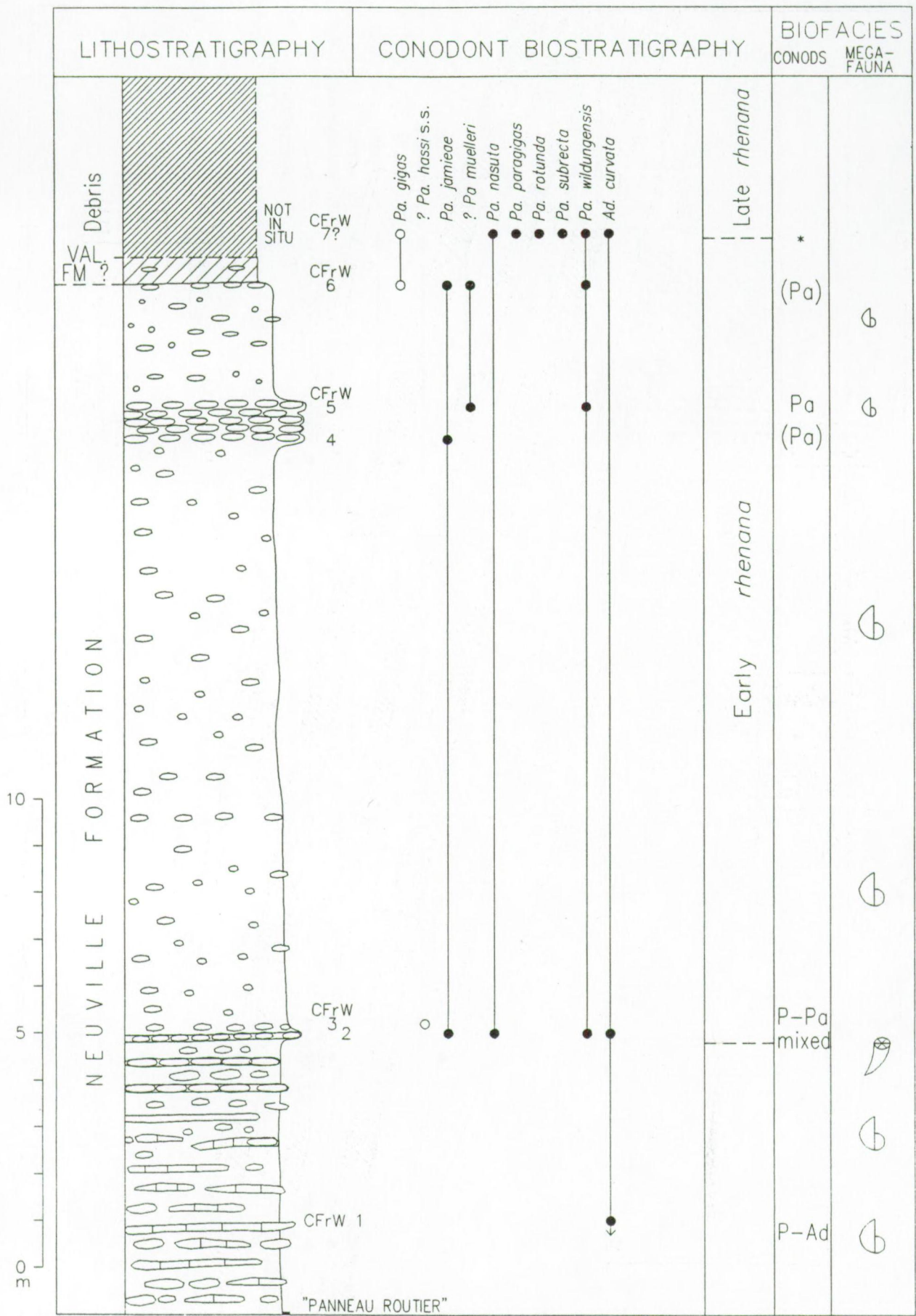
Fig. 4 – Stratigraphy and biofacies of the Frasnes-W section (CFrW).
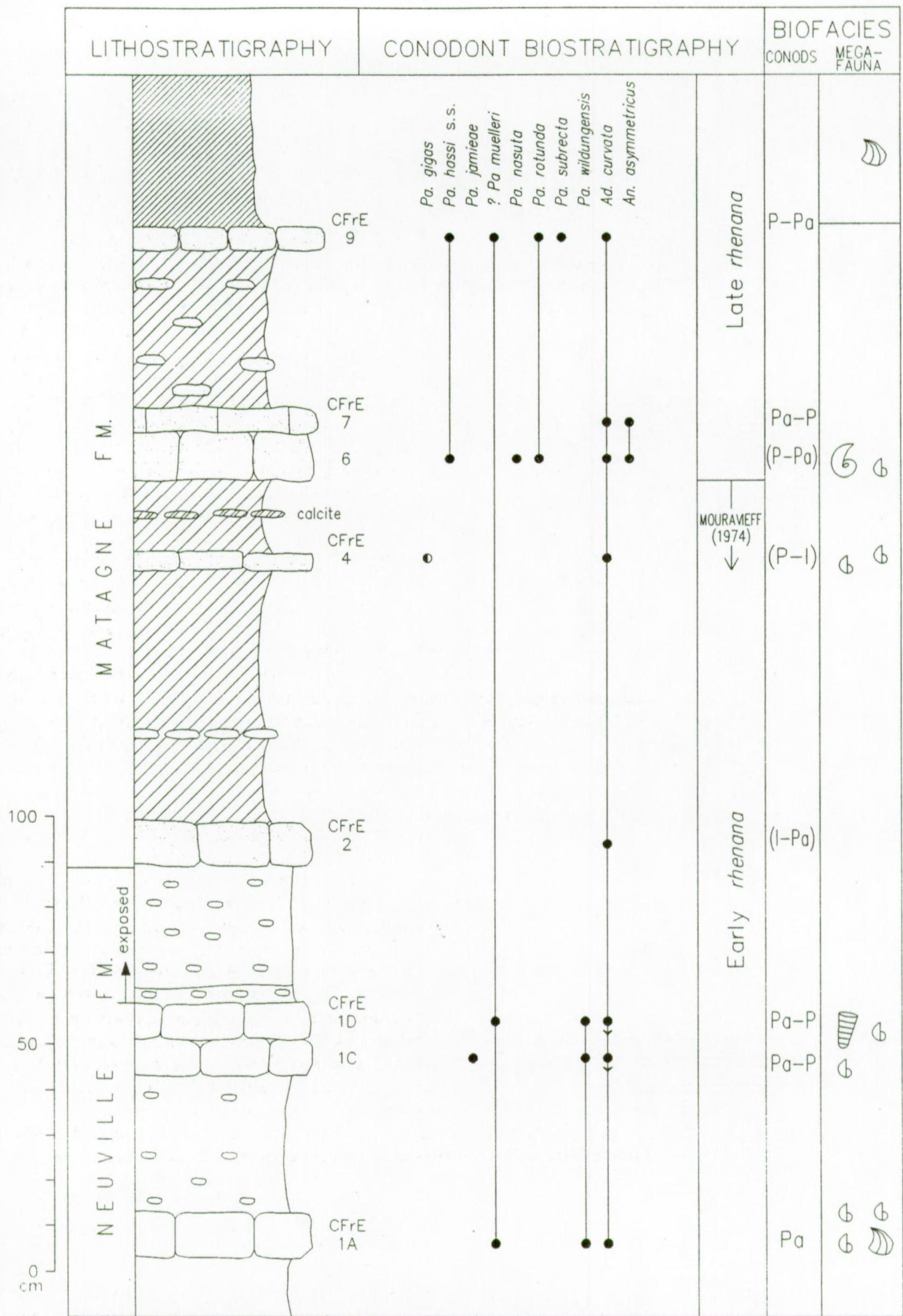
Fig. 5 – Stratigraphy and biofacies of the Frasnes-E section (CFrE).
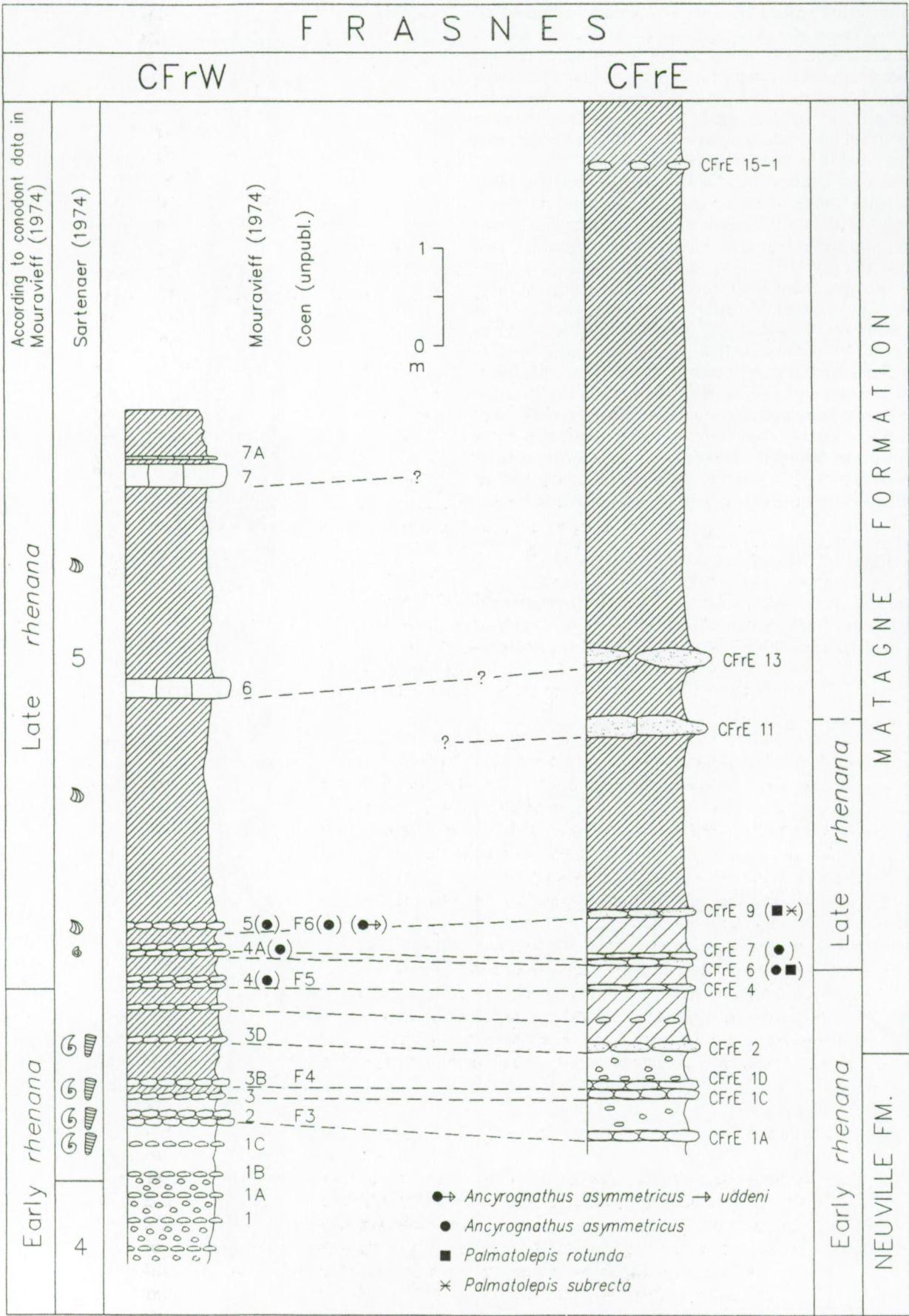
Fig. 6 – Bio- and lithostratigraphical correlation of the Frasnes sections, completed with data from MOURAVIEFF (1974), SARTE-
NAER (1974) and COEN (unpublished).

the north flank of an anticline composed of thick-bedded reefal-biostromal limestones. The suggestion that faulting has not resulted in a repetition of lithological units implies that the re-appearance of the Matagne facies in the outcrop needs to be explained by the return of depositional conditions favorable for the sedimentation of black shales. According to BOUCKAERT *et al.* (1970) only the nodular strata of the fifth unit are supposed to be repeated in an undulating anticline.

At the same section, SARTENAER (1974) described nine lithological units, some of them repeated more than six times. BOULVAIN *et al.* (1993) introduced the Philippeville Formation for the reefal-biostromal limestones at Neuville, and assigned the overlying 16 m of nodular shales and limestones to the Neuville Formation. According to these authors, the younger Valisettes Formation, about 100 m thick, comprises fine darkgrey-greenish shales in its lower part, green or reddish nodular limestones (considered as debris flows from a nearby red mudmound) and shales in the middle part and fine blackish shales (9 m thick) at the top. The overlying nodular sequence and dark shales (between 452 - 601 m; SARTENAER, 1974), separated by a fault from the Senzeilles Formation, are not discussed by BOULVAIN *et al.* (1993). The fine black shales at the top of the Valisettes Formation are now assigned to the Matagne Formation.

Biostratigraphical data from the lower units of the succession are published by COEN & COEN-AUBERT (1976), MOURAVIEFF (1974) and BOULVAIN *et al.* (1993). A detailed conodont sampling of the whole section was carried out by HAYDUKIEWICH (1989: unpub.). It is in this study that the *linguiformis* Conodont Zone was documented for the first time in Belgium by its index-
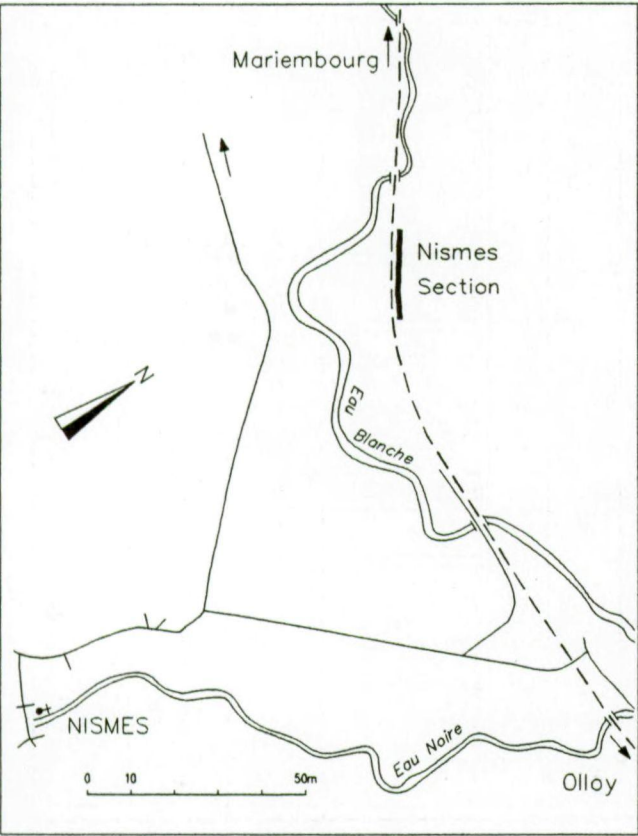
Fig. 7 – Location and sketch of the Nismes section (N).
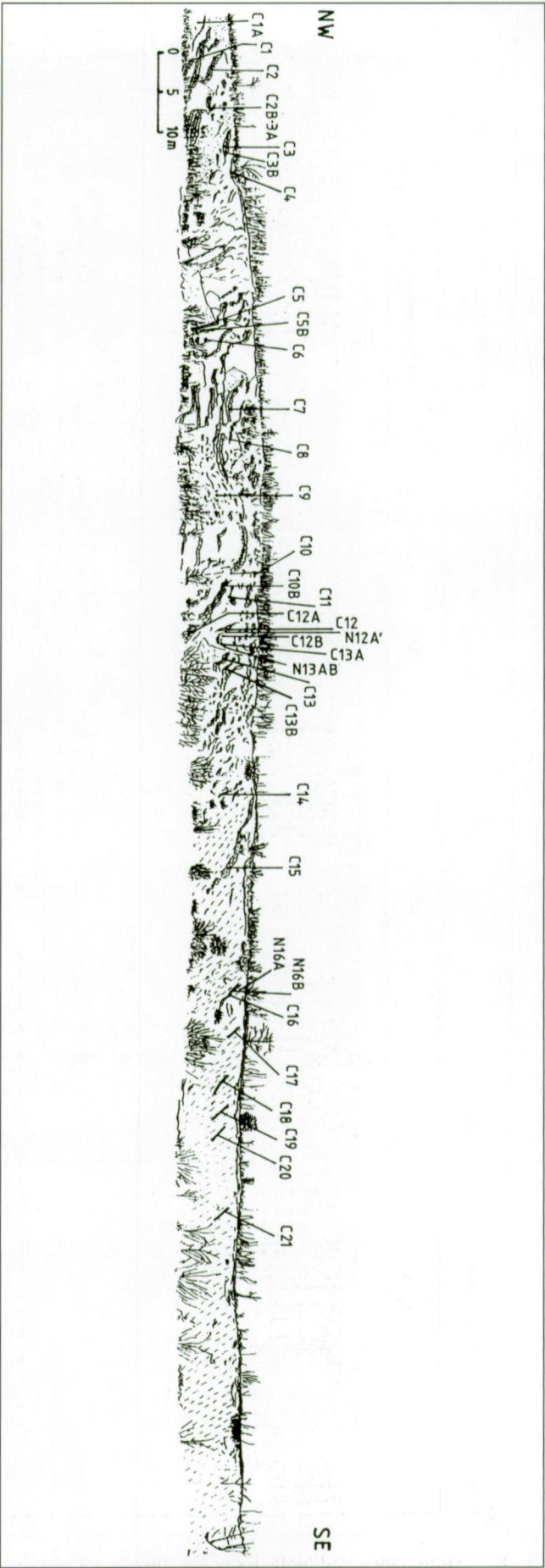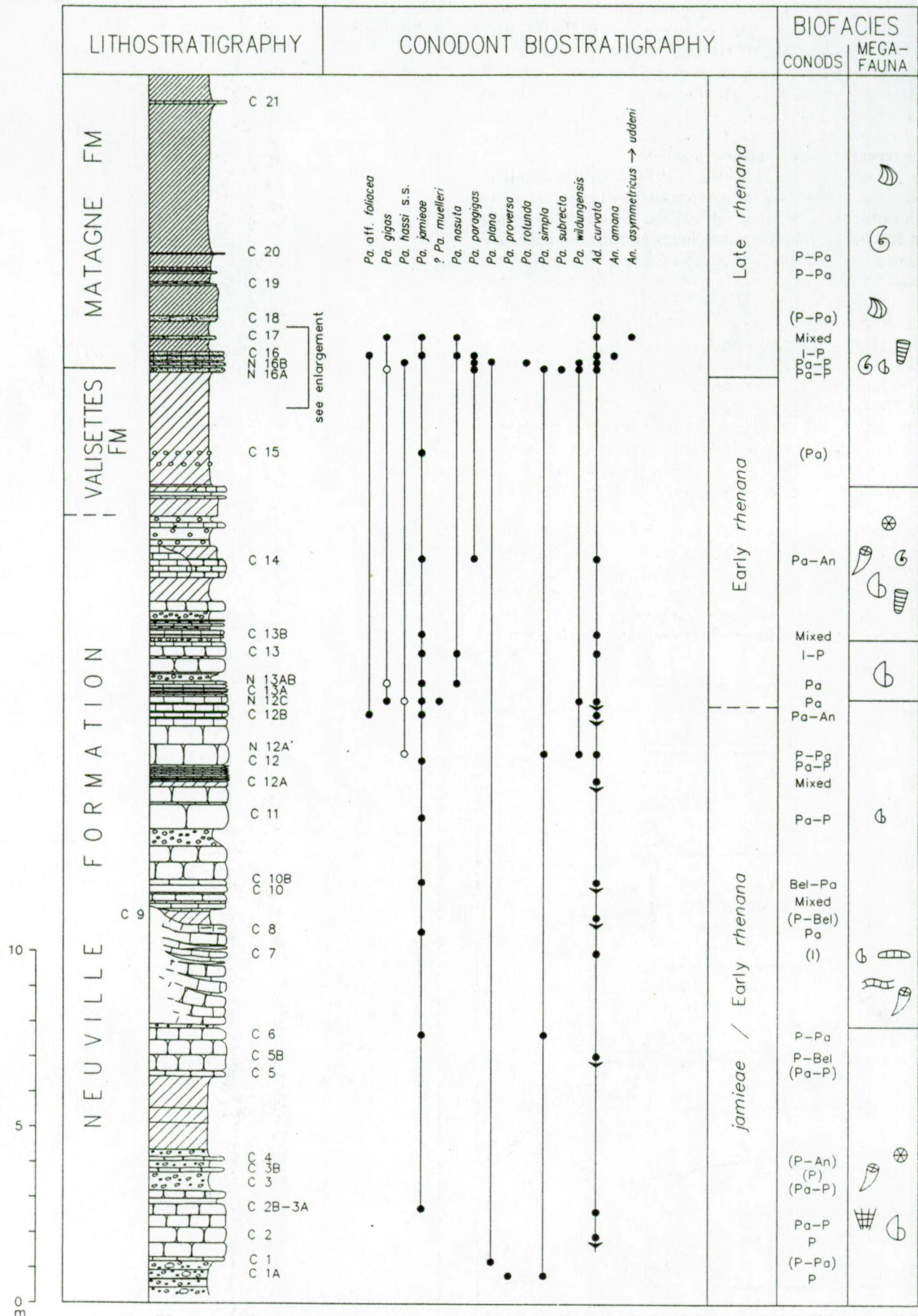
Fig. 8 – Stratigraphy and biofacies of the Nismes section (N).
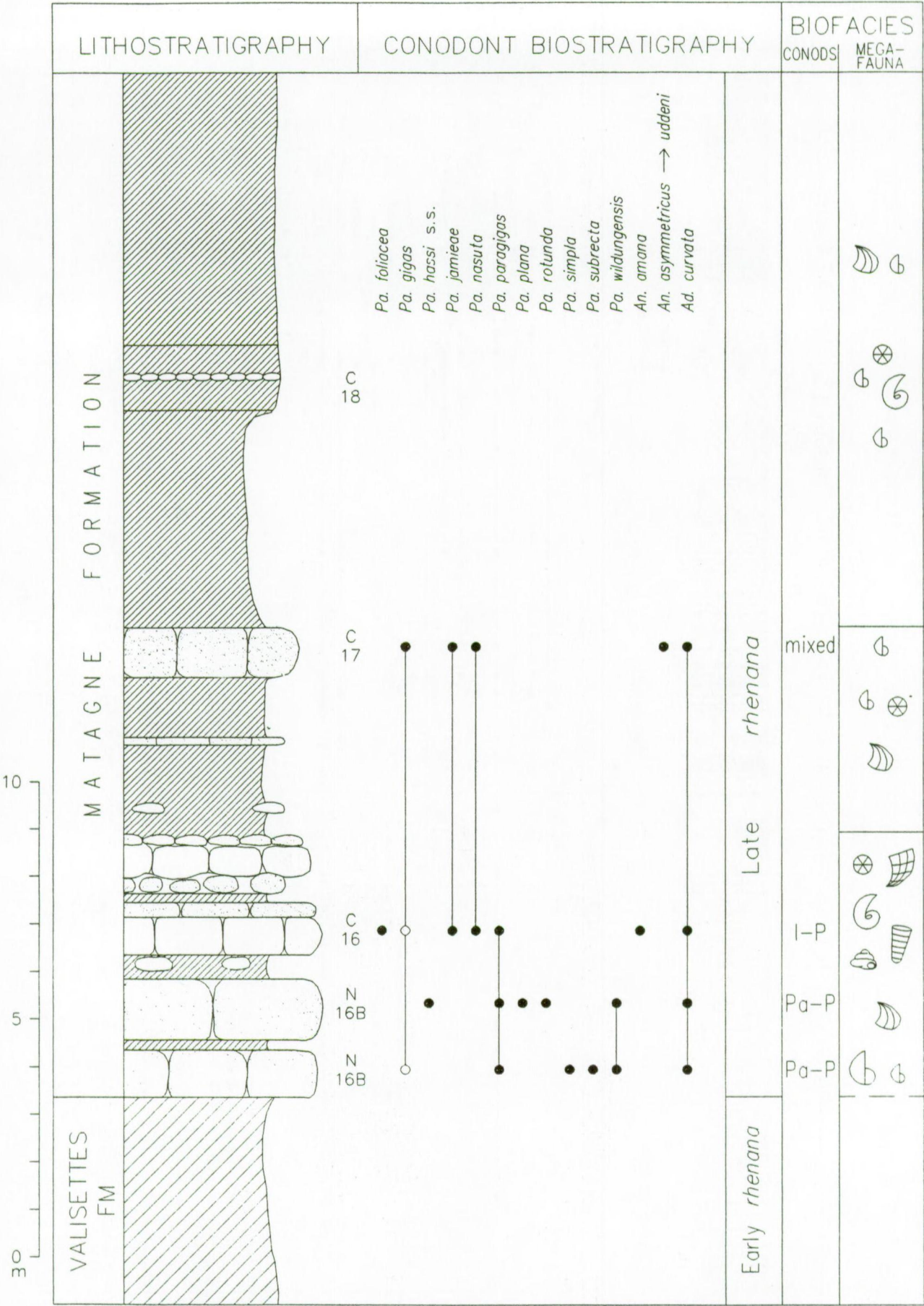
Fig. 9 – Stratigraphy and biofacies of the Nismes section (N), detail of Early-Late *rhenana* transition.
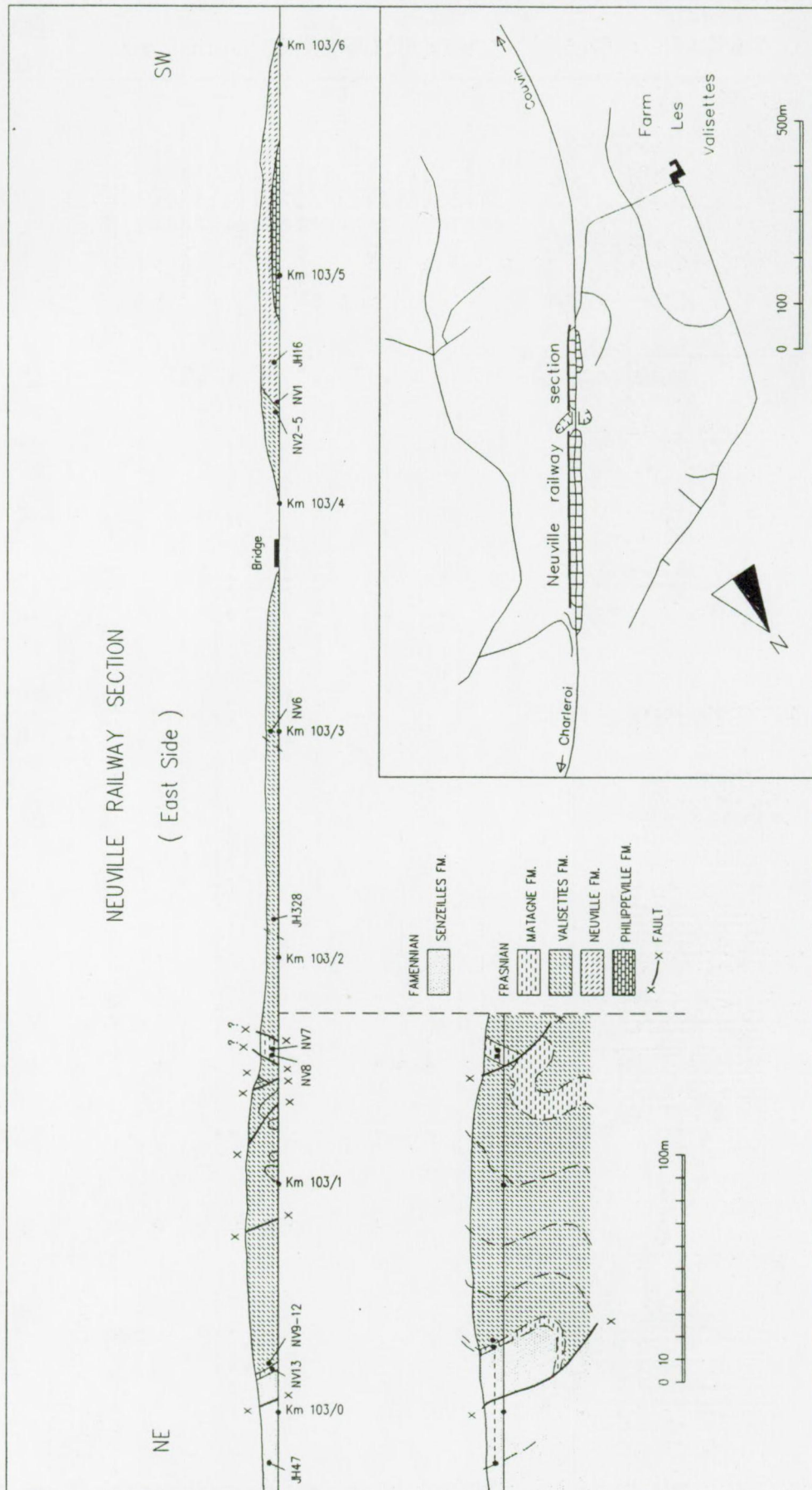
Fig. 10 – Location and sketch of the Neuville section (Nv).

Fig. 11 – Stratigraphy and biofacies of the Neuville section (Nv).
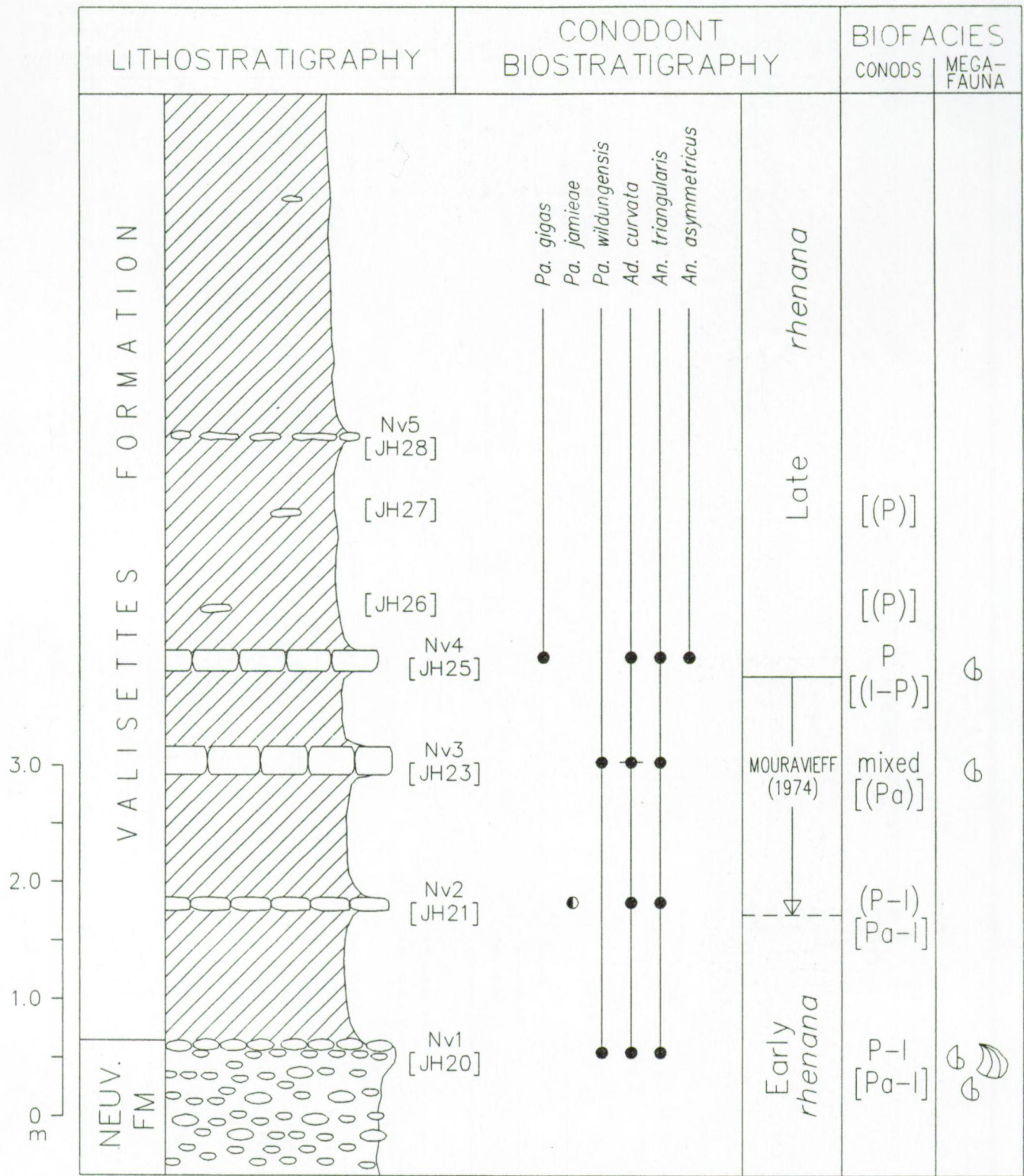
Fig. 12 – Stratigraphy and biofacies of the Neuville section (Nv), detail of Early-Late *rhenana* transition.

fossil. Similar to BOUCKAERT *et al.* (1970), HAYDUKIEWICH (1989: unpub.) considered the lithological succession as continuous, without any repetition. The conodont data of this unpublished study are revised and completed within the present paper (Figs. 11 to 13). In the Neuville Formation nine

thin clayey beds were identified as possible metabentonite horizons (VANDELAER, unpub.). Mineralogical and geochemical analyses may prove these beds to enable high resolution correlation with other sections in the Frasnian of southern Belgium.
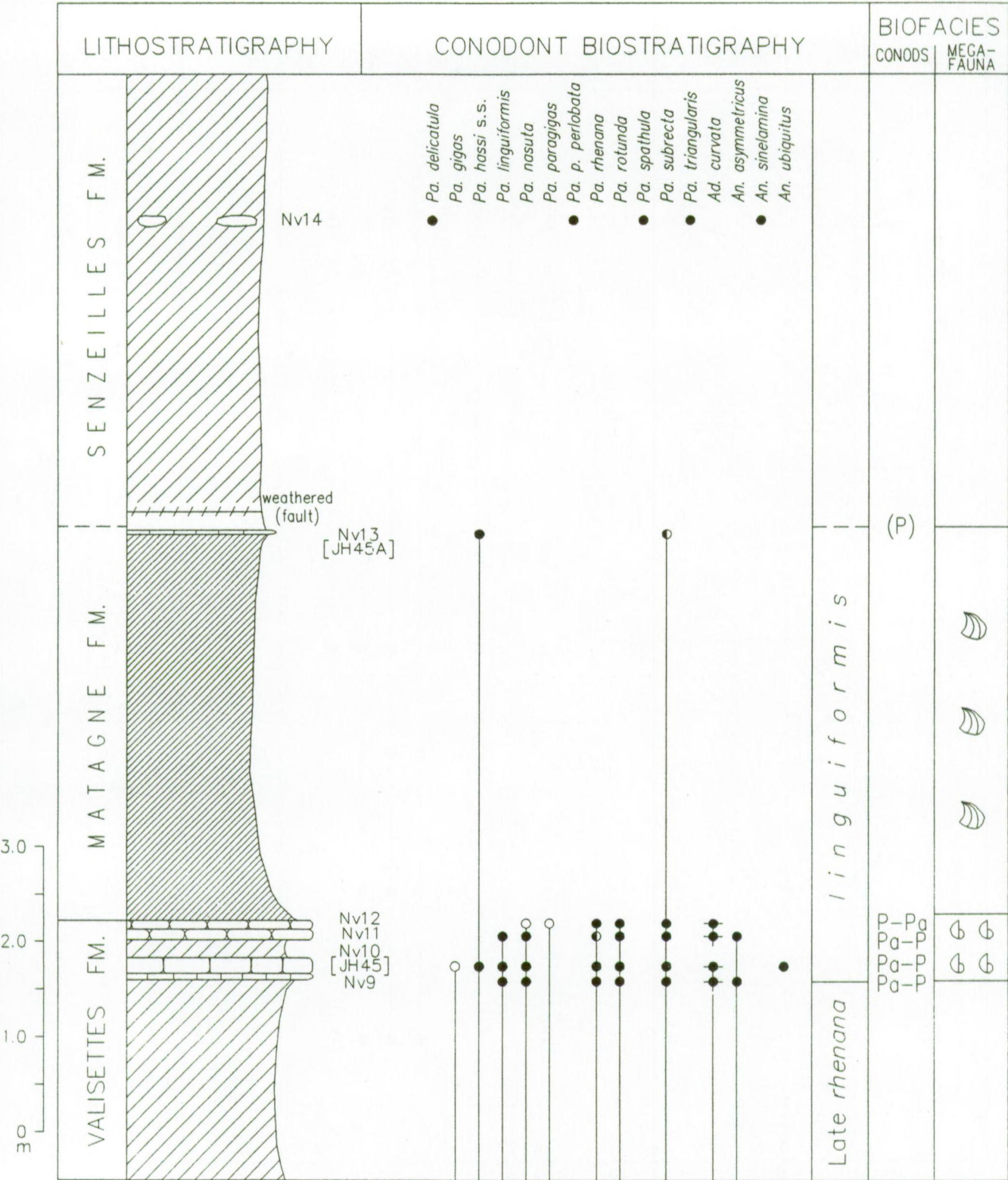
Fig. 13 – Stratigraphy and biofacies of the Neuville section (Nv), detail of Late *rhenana-linguiformis* transition.

LESSIVE (Figs. 14 and 15)

Parallel to the Cobri River, the Lessive section comprises several isolated outcrops along the east side of the paved road linking the hamlets of Al Fosse and Au Roké (Fig. 14). A preliminary study of the Lessive section was already carried out by COEN (1977 a). Apparently, the 48°S dipping strata constitute the overturned northern limb of a N85°E striking anticline.

In the Lessive outcrops three major lithological units are
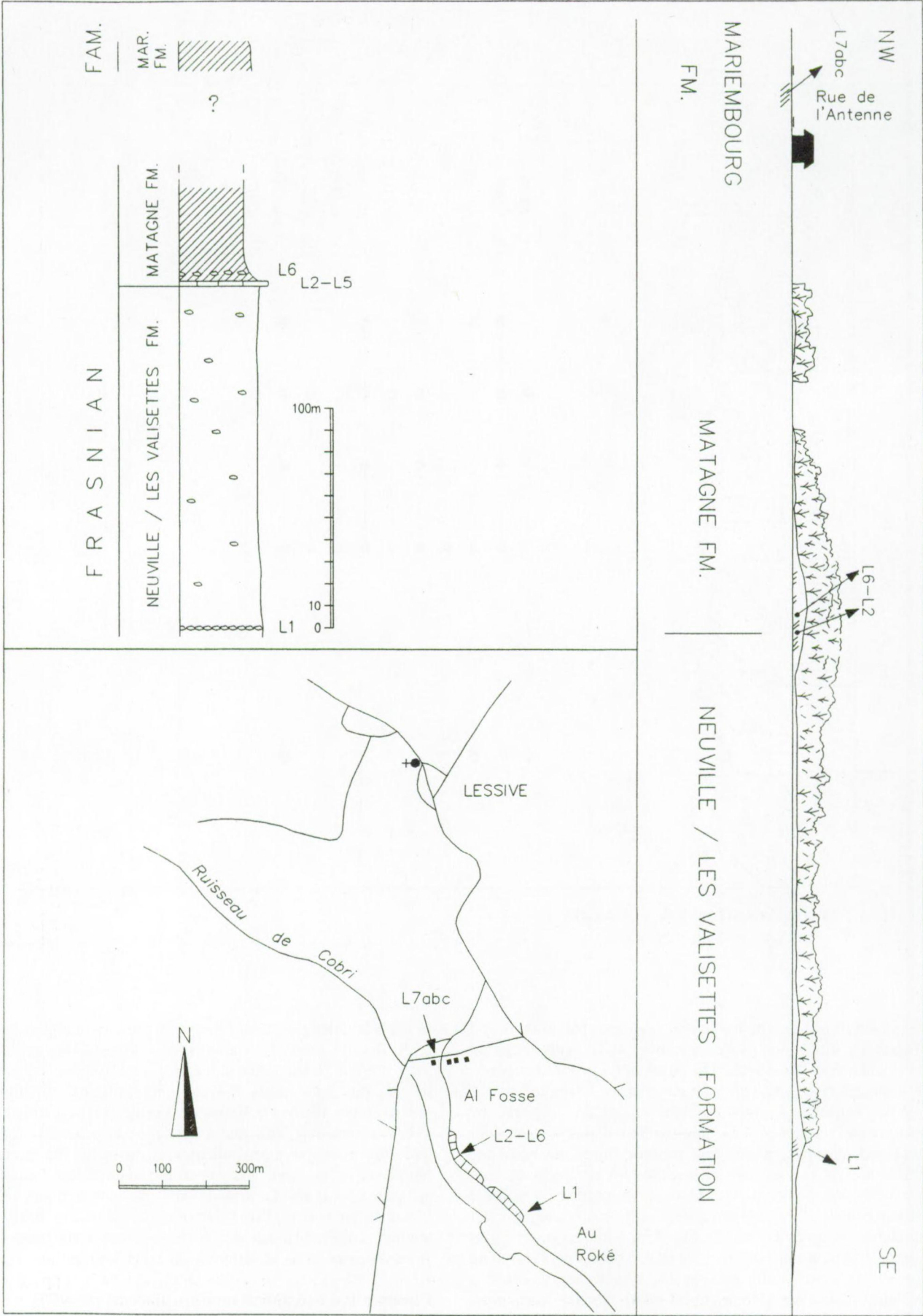
Fig. 14 – Location and sketch of the Lessive section (L).
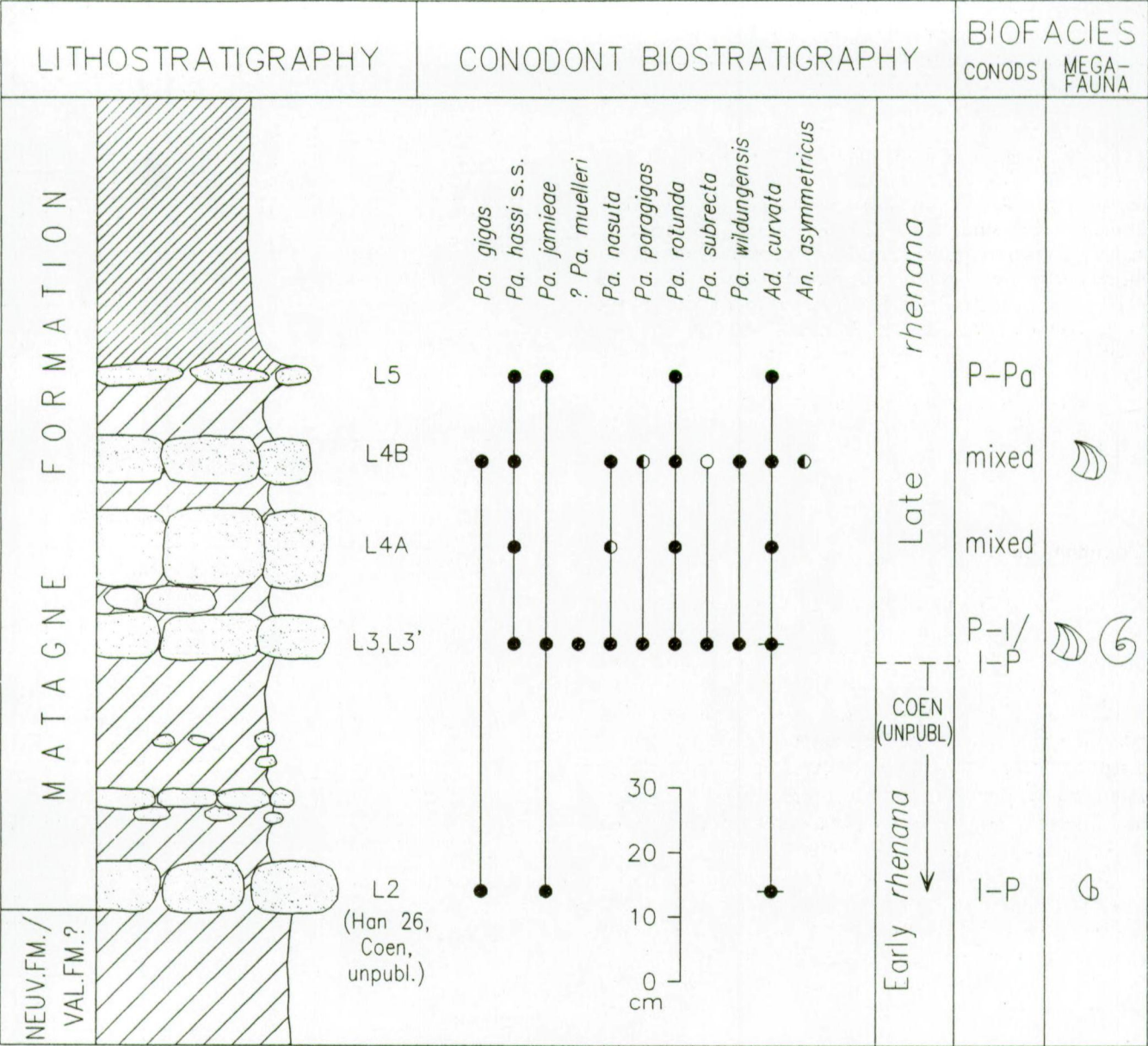
Fig. 15 – Stratigraphy and biofacies of the Lessive section (L).

recognised (Fig. 14). The lower unit is at least 150 m thick and comprises a succession of fine, greenish shales with occasionally nodular limestone beds. The basal strata of the succession are exposed in a small abandoned quarry. Attributed to the Neuville/Valisettes Formation, these shales are followed by approximately 50 m of dark fine-grained shales with a well-developed cleavage, and a few inferior limestone beds and nodular horizons at the base. This second lithostratigraphic unit probably corresponds to the Matagne Formation, the basal limestone beds of which have been sampled intensively for conodonts (samples L2 to L5; Fig. 15). After an interruption of some 150 m, a third lithological unit is observed. Consisting of greenish, occasionally nodular and silty shales, this unit is attributed to the lower Famennian Mariembourg Formation. These rocks were only temporarily exposed at the construction site of a house. However, similar rocks are sporadically exposed

to the north along the Cobri River. Of the three samples labeled L7A, B and C, only L7A was taken *in situ*. On the geological map of FORIR (1900) strata along the Cobri River are considered to constitute two nearly E-W striking anticlinal structures in 'Fr1m' rocks (Neuville/Valisettes Formation), separated by a syncline exposing 'Fr2' strata (Matagne Formation). As a result, the geologic map indicates erroneously the transition between 'Fr1m' and 'Fr2' near the site of the Famennian samples L7A,B and C. In addition to the new samples, unpublished Lessive conodont collections of M. COEN have been studied. Labeled Han26 to 29, these samples are most likely from the same beds as samples L2, L3, L4A and L5.

Preservation and abundance of conodont elements

At the W and E side of the Frasnes road cut most samples were

productive, with a maximum yield of 392 relatively well-preserved conodont elements per kg in CFrW3 (Table 1). Many barren samples are from limestone lenses and nodules within the Matagne Formation (CFrE11, CFrE13, CFrE15-1 through 15-6). At Nismes conodonts are very abundant near the base of the Matagne Formation, particularly in bed C16 with 3965 elements per kg (Table 3). Most of the Neuville samples yield less than 100 conodont elements per kg, several of them being barren (Tables 4a and 4b). The richest samples are to be found in the youngest strata of the Frasnian series, containing large and well-preserved palmatolepids. At Lessive conodont elements are relatively poorly preserved, regarding the number of broken specimens. Of the 11 samples analysed, four showed to be unproductive (Table 5). Conodont elements are most abundant in samples L3', L4A and L4B, exceeding 4390 elements per kg in sample L4A. Differences in the concentration of conodont elements may be expected within a single bed as documented by L3', which is actually from the same horizon as L3.

Conodont biostratigraphy

Key-species to late Frasnian conodont biozonation are to be sought chiefly among the palmatolepids (ZIEGLER & SANDBERG, 1990). Other conodont genera recognised include *Ancyrodella*, *Ancyrognathus*, *Belodella*, *Icriodus*, *Mehlina* and *Polygnathus*. In this study taxonomic identification is based on the Pa elements, the Pb, S and M elements being counted only. *Polygnathus* species with a relative wide platform, distinctly ornamented with ridges and /or eventually nodes are put together in the *P.* group A (i.e., *P. aequalis*, *P. alatus* and *P. webbi*), whereas the *P.* group B includes narrow and less ornamented platformed species, such as *P. aspelundi*, *P. decorosus* and *P. pacificus*. Icriodids are represented by the *Icriodus alternatus* group comprising *I. praealternatus* and *I. alternatus alternatus*, *I. alternatus helmsi*, *I. symmetricus* and *I. aff. excavatus*.

FRASNES (Tables 1, 2)

Among the conodont elements in the CFrW samples 1to 6 from the Neuville Formation, well-preserved palmatolepids are rather scarce. Sample CFrW2 has the lowest occurrence of *Pa. jamieae* and *Pa. nasuta* and one specimen in CFrW3 shows affinities with *Pa. hassi* s.s. (= *Pa. hassi* sensu KLAPPER & FOSTER, 1993). According to these authors the entry of the last taxon coincides with that of *Pa. bogartensis* (= *Pa. rotunda* sensu ZIEGLER & SANDBERG, 1990). *Pa. hassi* s.l. (= less typical *Pa. hassi* specimens, sensu ZIEGLER & SANDBERG, 1990) is found in CFrW2-5 and in CFrW7. This last sample, not exactly *in situ*, is a dark-grey limestone which is most likely from one of the beds at the base of the Matagne Formation. *Pa. wildungensis* is present in CFrW2,5 to 7. *Pa.* aff. *gigas* occurs in CFr6 and 7. *Pa. paragigas*, *Pa. subrecta* and *Pa. rotunda* all have their first appearances in CFrW7. *Ancyrodella curvata*, recognised in CFrW1,2 and 7 includes both early and late forms. As a result, samples CFrW2 to

Table 1 – Conodont distribution in the Frasnes-W section (CFrW).

	CFrW1	CFrW2	CFrW3	CFrW4	CFrW5	CFrW6	CFrW7
Sample weight (kg)	2.5	2.5	2.5	2.5	2	2	
Fraction dissolved (kg)	1.08	1.18	1.05	1.06	1.17	0.76	
Nr. elements	99	297	412	19	85	19	x
Nr. elements/kg diss.	92	252	392	18	73	25	
Icriodus (Pa el.)	1	15	12		2	1	x
I. a. alternatus		12	7				x
I. praealternatus					1	1	x
I. symmetricus	1				1		x
I. sp.		3	5				
Polygnathus (Pa el.)	19	49	106		1	2	x
P. group A	12	13	7		1	1	x
P. group B	7	36	99			1	x
Palmatolepis (Pa el.)	3	48	70	11	41	13	x
Pa. aff. gigas						1	x
Pa. hassi s.s.		3?	1?				x
Pa. hassi s.l.		7	1	1	3		x
Pa. jamieae		1		1		1	
?Pa. muelleri					1	1	x
Pa. nasuta		1					x
Pa. paragigas							x
?Pa. punctata							x
Pa. rotunda							x
Pa. subrecta							x
Pa. wildungensis		5			8	2	x
Pa. sp.	3	31	68	9	30	7	x
Ancyrodella (Pa el.)	4	4					x
A. curvata early f.	1	1					x
A. curvata late f.		1					x
A. cf. gigas		1					
A. nodosa		1					x
A. sp.	2						x
Ancyrognathus (Pa el.)	3	47	5	3	11		x
An. triangularis	2	11	3	1	3		
An. sp.	1	36	2	2	8		x
Belodella sp.	3	16	41		2		x
M elements	2	3	20				x
Pb, S elements	64	115	158	5	28	3	x

CFrW6 are considered to belong to the Early *rhenana* Zone, whereas CFrW7 likely falls within the Late *rhenana* Zone. The presence of *Ancyrognathus triangularis* suggests that CFrW7 is older than the middle Late *rhenana* Zone (cf. KLAPPER, 1990: fig. 1). Because index-species are lacking in CFrW1, only a broad age range can be assigned to this sample (Fig. 4).

Also on the eastern side of the Frasnes highway section well-identifiable palmatolepids are relatively scarce. However, two populations of *Palmatolepis* are recognised. In the stratigraphically lowest part of the section (CFrE1A,1C,1D from the Neuville Formation), *Pa. hassi* s.l., *Pa. muelleri?*, *Pa. jamieae* and *Pa. wildungensis* are found. Lacking typical palmatolepid Pa elements, CFrE2 from the lowest part of the Matagne Formation separates the first group of samples from the

Table 2 – Conodont distribution in the Frasnes-E section (CFrE). Samples CFrE15-1 through CFrE15-6, with dissolved fractions less than 0.3 kg and devoid of conodonts, are not shown in this table.

	CFrE1A	CFrE1C	CFrE1D	CFrE2	CFrE4	CFrE6	CFrE7	CFrE9	CFrE11	CFrE13
Sample weight (kg)	3.5	1.5	1.5	2	3	3.5	5	3	4	2.5
Fraction dissolved (kg)	2.75	1.08	1.05	1.1	2.4	2.85	4	2.4	2.8	1.9
Nr. elements	468	90	102	38	121	417	120	322	20	15
Nr. elements/kg diss.	170	83	97	35	50	146	30	134	7	8
Icriodus (Pa el.)	**5**	**3**	**5**	**14**	**36**	**37**	**5**	**1**	**1**	**2**
I. a. alternatus	2	2	2	2	6	7	2	2	1	2
I. praealternatus	2	2	3	9	2	2	2	2	2	2
I. symmetricus	5	3	2	5	16	26	2	2	2	2
I. sp.					14	4	5	1		
Polygnathus (Pa el.)	**30**	**19**	**23**	**3**	**41**	**120**	**23**	**121**	**5**	**7**
P. group A	30	17	22	2	4	8		11	3	3
P. group B		2	1	1	37	112	23	110	2	4
P. sp.										
Palmatolepis (Pa el.)	**264**	**48**	**57**	**5**	**13**	**92**	**35**	**94**	**11**	**3**
Pa. cf. gigas					1					
Pa. hassi s.s.						1	3	1		
Pa. hassi s.l.		2	1		4	4	4			
Pa. jamieae		1								
Pa. muelleri	47?		1?					2		
Pa. nasuta						2				
Pa. rotunda						1		13	1	
Pa. subrecta								2		
Pa. wildungensis	50	4	3							
Pa. sp.	167	41	52	5	8	84	28	76	10	3
Ancyrodella (Pa el.)	**25**	**2**	**8**	**2**	**7**	**33**	**8**	**22**	**1**	
A. curvata				2	2	9				
A. curvata early f.	9	1	3	6	6	7	1	2		
A. curvata late f.	1					2	2	12		
? A. gigas		1								
A. lobata	3							1		
A. nodosa	6		3			5	1			
A. sp.	6		2		5	10	4	7	1	
Ancyrognathus (Pa el.)	**20**		**3**	**1**	**1**	**9**	**6**	**8**		
An. asymmetricus						3	2			
An. triangularis	8					2		2		
An. sp.	12		3	1	1	4	4	6		
Belodella sp.		1	2			11	1			1
M elements	4			2		4		1		
Pb, S elements	120	17	24	11	23	132	42	75	2	2

second group, which includes CFrE4,6,7,9. Characteristic constituents of the second population of palmatolepids are *Palmatolepis* cf. *gigas, Pa. hassi* s.s., *Pa. nasuta, Pa. rotunda* and *Pa. subrecta.* The occurrence of *Ancyrognathus asymmetricus* in CFrE6 and 7 suggests that the base of the Late *rhenana* Zone is below CFrE6 (Fig. 5). Both present in CFrE9, *Ancyrognathus triangularis* and *Ancyrodella lobata* may indicate that the succession between CFrE6 and 9 may be older than the middle Late *rhenana* Zone. *Ancyrodella curvata* is again represented by both forms, the late form being more abundant in CFrE7 to 9. Since samples CFrE13 and CFrE15-1 to 15-6 were devoid of characteristic conodont elements, no precise information can be given on the relative age of

the younger part of the Matagne shales. MOURAVIEFF (1974) and COEN (unpub.) reported the first occurrence of *Ancyrognathus asymmetricus* in the sixth limestone bed within unit 5 of SARTENAER (1974). This bed is considered to correspond to CFrE4, which places the lower boundary of the Late *rhenana* Zone some 20 cm lower (Fig. 6).

The above conodont data indicate that at Frasnes the middle and upper parts of the nodular limestones and shales of the Neuville Formation should be assigned to the Early *rhenana* Zone and not to the Late *rhenana* Zone as indicated by SANDBERG *et al.*, 1993. Apparently, the base of the Matagne Formation does not coincide with the lower boundary of the Late *rhenana* Zone, as the first

Table 3 – Conodont distribution in the Nismes section (N).

	C1A	C1	C2	C2B-C3A	C3	C3B	C4	C5	C5B	C6	C7	C8	C9	C10	C10B	C11	C12A	C12	N12A'	C12B	N12C	N13AB	C13	C13B	C14	C15	N16A	N16B	C16	C17	C18	C19	C20	C21
Sample weight (kg)		2.14	2	2.5		2.4	2.43		2.46	2.5	2	2.39	2.5		2.5		2.41	3		2.5	2.5	2.5		2.46	2.5	3	2	2.5	2.5	2.5	2.5	2.5	2.5	2.5
Fraction dissolved (kg)	1.4	1.32	1.98	4	1.5	1.6	1.67	2	1.9	1.96	2	1.5	2.29	2.45	2.2	2.47	2.2	2.36	3	2.3	1.85	1.82	2.28	2.2	2.36	1.22	3	2	2.45	1.91	1.41	2.24	2.25	1.49
Nr. elements	77	60	209	519	33	13	17	27	93	61	4	222	56	121	205	46	84	127	169	428	597	263	757	121	1321	25	480	485	9715	1590	49	419	146	6
Nr. elements/kg diss.	55	45	106	130	22	8	10	14	49	31	2	148	24	49	93	19	38	54	56	186	323	144	332	55	560	20	160	243	3965	832	35	187	65	4
Icriodus (Pa el.)	1	1	2	20		1		1	1	8	1	3	1	15	9		6	2	10	14	10	4	192	4	12		22	53	4223	181	1	22	1	
I. a. alternatus				6						1			1	1	1		4		8	7		1	70	2	1		7	4	101	120				
I. expansus		1																																
I. aff. expansus													1						3															
I. praealternatus				9				1	5	1		1	13	8			2	2	2	2	10	3	53	1	4		5	11	557	7			1	
I. symmetricus	1		2	4			1			1		2								1			10	1			10	38	778	125	1		12	
I. sp.				1						2													51		7				1563	33			10	
Polygnathus (Pa el.)	35	12	85	63	4	9	3	5	34	16		14	12	13	15	6	12	23	54	28	46	10	89	3	52		70	113	1278	287	11	144	32	1
P. group A	14	5	21	24		5	1		6	5		2	3	3	2	1	1	5	1	10	10	4	39		9		52	80	144	14		43		
P. group B	8	2	7	19	2			1	17	5		5	3	4	5		4	11	53	6	36	6	22	1	8		18	33	828	201	6	98	30	
P. sp.	13	5	57	20	2	4	2	4	11	6		7	6	6	8	5	7	7		12			28	2	35				306	72	5	3	2	1
Palmatolepis (Pa el.)	8	11	2	174			1	7	4	14		145	2	21	31	13	14	29	45	97	252	140	69	27	615	15	199	197	455	235	6	34	32	
Pa. aff. foliacea																					5								11					
Pa. gigas																					8											2		
Pa. aff. gigas																						1				1			1					
Pa. hassi s.s.																			2?		4?							1						
Pa. hassi s.l.			1	32		1	3		5	10	1	8	8	4	5	5	4	28	15				29	7	155	1	3	8	5	51	3	14	7	
Pa. aff. hassi																			8		6	9					19	17						
Pa. jamieae				10					2			11				4	2		1	6	10	1	1	3	25	2				10	7			
?Pa. muelleri																					2													
Pa. nasuta																						2	1							1	2			
Pa. paragigas																								1			8	3	5					
Pa. aff. paragigas																											2							
Pa. plana		3																							1									
Pa. proversa	4																																	
Pa. punctata		1										1		1																1				
Pa. cf. rhenana																														1				
Pa. rotunda																												1						
Pa. simpla	1								1									1											1					
Pa. subrecta																											2							
Pa. wildungensis																			1		1						10	2						
Pa. sp.	3	7	1	132			4	4	6			122	1	12	17	7	9	23	29	56	221	127	38	17	434	11	147	64	422	172	3	20	25	
Ancyrodella (Pa el.)			2	3	5				4	3		3	1		6		1	2	3	4	4	1	3	7	41		26	20	127	72	2	13	5	
A. curvata early f.				1	1				1	1		1			1						1		1				5	5	2		1			
A. curvata late f.			2							1												1		4	5		2	8	80	9		6	4	
A. curvata		1						1							2							1								16				
A. gigas																									1									
A. ioides																				1		1												
A. lobata																	1								1		2	1	10			1		
A. nodosa																				1				2	24		10	2	11	18			5	
A. sp.			1		4			3	2	1					3				2	1	3	1		1	11		7	4	26	27	1	1	1	
Ancyrognathus (Pa el.)	3	1	3	49	5		3		2						2	2	4	4	5	33	43	13	36	11	144	3	17	23	145	12	1	2		
An. amana																												6						
An. asymmetricus --> uddeni																																1		
An. irregularis						2																												
An. seddoni						1																												
An. triangularis				27					1							1	2	3	1	3	19	12	24	6	122	3	3	11	78	2		2		
An. tsiensi	2	1	1		2		1																							4	4			
An. sp.	1		2	22		2		1			1				1		1	3	2	14	31	7	12	5	42		14	12	58	4	1			
***Belodella* sp.**		1					1	5	5		4	10	15	58		14	6	5	8	2	2	4	3		30		2	8	10	2		3	4	
M elements				3									3							2	10	10	10	4	8		7	3	209	12		4		
Pb, S elements	30	35	114	207	19	3	10	13	43	15	3	53	27	57	84	25	33	61	45	178	230	90	354	62	419	7	137	68	3268	782	28	197	72	5

Table 4a, b – Conodont distribution in the Neuville section (Nv). The presence of the phyletically latest form of *Ancyrodella curvata* among the other late forms is indicated with * .

	JH1	JH2	JH7	JH9	JH10	JH11	JH13	JH15	JH16	JH17	JH18	JH20	NV1	JH21	NV2	JH23	NV3	JH25	NV4	JH26	JH27	JH29	JH32	NV6
Sample weight (kg)	3	3	2	2	2	2	2	2	2	2	2	2	1.5	2	3	2	2.5	2	2.5	2	2	2	2	2
Fraction diss.(kg)													1.05		1.9		1.2		1.6					0.62
Nr. elements	1	6	69	13	46	117	31	51	27	25	21	58	730	46	37	19	57	13	147	11	21	36	38	85
Nr. elem./kg. diss.*	3	2	35	7	23	59	16	26	14	13	11	29	695	23	19	10	48	7	92	6	11	18	19	137
Icriodus (Pa el.)		5	15		1	12	6	3	1		2	4	151	2	7		8	3	2	1		4	3	4
I. alternatus group													72											
I. a. alternatus										1			14		6		2	3	2					
I. a. helmsi										1												1	1	
I. cornutus																								
I. aff. *excavatus*		5	5		1	7	6	3																
I. praealternatus												4	10	2			4					3		4
I. symmetricus						5				1			55		1		2		1					
I. sp.			10																					2
Polygnathus (Pa el.)	1	1	42	9	16	48	12	34	15	13	14	7	204	9	17	2	16	2	71	8	11	3	11	28
P. group A						7	12	2	11	3	2	4	4	2	6		11		36	2	9		1	12
P. group B	1	1	12	6	6	28	9	3	7	6	6		200	2	11		5		35		2		6	16
P. sp.			30	3	3	6	1	20	5	7	6	3			5	2		2			6	3	4	
Palmatolepis (Pa el.)					8	6	2			2		22	23	11	1	11	7		6			15	1	2
Pa. barba						2																		
Pa. aff. *crepida*																								
Pa. delicat.+ protorhom.																								
Pa. gigas																			1					
Pa. aff. *gigas*																								
Pa. hassi s.s.																								
Pa. hassi s.l.					1	2	1				1			3			2		2	2				
Pa. aff. *hassi*																1								
Pa. aff. *jamieae*																								
Pa. cf. *jamieae*														1										
Pa. linguiformis																								
Pa. nasuta																								
Pa. aff. *nasuta*																								
Pa. cf. *nasuta*																								
Pa. aff. *paragigas*																								
Pa. p. perlobata																								
Pa. proversa						1																		
Pa. quadrantinodosalobata																								
Pa. aff. *quadrantinodosalobata*																								
Pa. rhenana																								
Pa. cf. *rhenana*																								
Pa. rotunda																								
Pa. aff. *rotunda*																								
Pa. spathula																								
Pa. subrecta																								
Pa. cf. *subrecta*																								
Pa. tenuipunctata																								
Pa. cf. *tenuipunctata*																								
Pa. triangularis																								
Pa. wildungensis												6	6				1							
Pa. cf. *wildungensis*																	5							
Pa. wolskajae																								
Pa. sp.			2		7	1	1			2		15	17	7	1	4	5		3	2		15	1	2
Ancyrodella (Pa el.)					1	1	1			1			8	4	3	1	2	1	10		1	3		1
A. curvata early f.										1			1	1										
A. curvata late/lst.* f.						1							5		2		2	1	5			2		1
A. nodosa													1	3		1			3	1	1			
A. sp.					1	1							1			1			2					
Ancyrognathus (Pa el.)								1	1		1	7	20	5	1		2	1	5			2	1	2
An. asymmetricus																			3					
An. coeni-tsiensi group						1				1														
An. sinelamina																								
An. sinelobus																								
An. triangularis												3	14		1		1		1					1
An. cf. *triangularis*																								
An. tsiensi																						2		
An. aff. *tsiensi*																								
An. cf. *tsiensi*								1				4		1										
An. ubiquitus																								
An. sp.								1			1		6	4			1	1	1				1	1
Ancyrolepis cruciformis																								
Mehlina* aff. *gradata													1											
***Belodella* sp.**													4				1		1					
M elements			3					2					47				1					3		2
Pb, S elements			10	4	17	49	10	13	8	8	4	20	292	15	8	8	21	6	52		6	8	20	48

JH32B	JH34	JH35	JH37	JH38	NV7	NV8	JH39	JH40	JH41	JH42	JH42A	JH43	JH44	NV9	JH45	NV10	NV11	NV12	JH45A	NV13	NV14	JH46A	JH47	
2	3	2	2	2	2	2.3	2	3	2	2	2	3	2	2	2.5	3	3	2	2	2	3	2	2	Sample weight (kg)
					0.15	1.47								1.3		2.1	2	16		2	2			Fraction diss.(kg)
16	4	5	231	23	2	68	126	509	75	1917	49	4	20	444	300	330	380	466	18	6	77	6	120	Nr. elements
8	1	3	116	12	13	46	63	170	38	959	25	1	10	342	120	157	190	291	9	3	39	3	110	Nr. elem./kg. diss.*
			43			2	12			3			2	4										**Icriodus (Pa el.)**
										2				1										*I. alternatus* group
			40			2	5							3										*I. a. alternatus*
																					2			*I. a. helmsi*
																					1			*I. cornutus*
																								I. aff. excavatus
										1														*I. praealternatus*
			3				2																	*I. symmetricus*
							5						2								1			*I. sp.*
			26	2		20	39	170	6	318	23	1	2	109	95	94	105	193	4	5	16	9		**Polygnathus (Pa el.)**
			7	2		16	15	67	1	43	9		1	47	15	17	18	33	2	4	6	8		P. group A
			3			4	3	40		100	3			62		77	87	160		1				P. group B
			16				21	63	5	175	11	1	1		80				2		10	1		P. sp.
9	2	1	2	11		18	36	165	17	1118	24		5	239	137	190	205	179	3	1	55	4	68	**Palmatolepis (Pa el.)**
																								Pa. barba
																							2	*Pa. aff.* **crepida**
																					10			*Pa. delicat.+protorhom.*
																								Pa. gigas
																1								*Pa. aff. gigas*
							1	1		2						2		1						*Pa. hassi* s.s.
							1																	*Pa. hassi* s.l.
							3																	*Pa. aff. hassi*
										1														*Pa. aff. jamieae*
																								Pa. cf. jamieae
														3	2	2	2							*Pa. linguiformis*
								1		44	3			8		12	1							*Pa. nasuta*
														3			4							*Pa. aff. nasuta*
							1						1											*Pa. cf. nasuta*
																	1							*Pa. aff. paragigas*
																					7			*Pa. p. perlobata*
																								Pa. proversa
																							15	*Pa. quadrantinodosal.*
																					1			*Pa. aff. quadrantinodosal.*
										3				8		3		2						*Pa. rhenana*
										10							3							*Pa. cf. rhenana*
3								2	1	11				3	3	6	6	6						*Pa. rotunda*
1																								*Pa. aff. rotunda*
																					4			*Pa. spathula*
2			2	4			5	27	2	252	11			116	55	105	120	108						*Pa. subrecta*
																			1					*Pa. cf. subrecta*
																							8	*Pa. tenuipunctata*
																					2			*Pa. cf. tenuipunctata*
																					2			*Pa. triangularis*
																								Pa. wildungensis
																								Pa. cf. wildungensis
																							1	*Pa. wolskajae*
3	2	1	7			18	25	134	14	800	10		4	101	73	59	73	58	1	1	30	3	42	*Pa. sp.*
1						1	7	4	1	37			1	23	8	4	11	5						**Ancyrodella (Pa el.)**
																								A. curvata early f.
1						1	6	2	1	19*				15*	5	1	7*	3						*A. curvata* late/lst.* f.
																								A. nodosa
							1	2		18			1	8	3	3	4	2	1					*A. sp.*
			2	1		2	1	10		23	1		1	4	3	2	3				2			**Ancyrognathus (Pa el.)**
								8		9				1			2							*An. asymmetricus*
																								An. coeni-tsiensi group
																					2			*An. sinelamina*
										1														*An. sinelobus*
																								An. triangularis
							1																	*An. cf. triangularis*
										1														*An. tsiensi*
			2																					*An. aff. tsiensi*
																								An. cf. tsiensi
																	1							*An. ubiquitus*
				1		2		2		12	1		1	3	3	2	1							*An. sp.*
																							2	**Ancyrolepis cruciformis**
														3										**Mehlina aff. gradata**
						1				4				11	3	6	11	10						**Belodella sp.**
			8							6	3								2					**M elements**
5	1	4	150	9	2	25	30	160	50	410	4	3	9	55	50	34	45	45	11		2	1	40	Pb, S elements

Matagne beds still belong to the Early *rhenana* Zone. The succeeding shales and limestones of the Matagne Formation, up to sample CFrE-11, are assigned to the Late *rhenana* Zone.

NISMES (Table 3)

Palmatolepids are present in most samples, but zonally important key-species are rather scarce. According to HELSEN & BULTYNCK (1992), the lowest part of the succession (C1A,1,2) may correspond either to the Late *hassi* or to the *jamieae* Zone, although the first occurrence of *Palmatolepis jamieae* is in C2B-3A.

Re-examination of the ancyrodellids showed the presence of phyletically late forms of *Ancyrodella curvata* in C2B-3A and may indicate a younger age, i.e., Early *rhenana* Zone, according to ZIEGLER & SANDBERG (1990). *Icriodus alternatus alternatus* occurs in the same sample. *Pa.* aff. *hassi* s.s. and *Pa. wildungensis* make their entry in N12A'. The first appearances of *Pa. gigas* and of ? *Pa. muelleri* is in N12C (Fig. 8). In addition, *Pa. paragigas* has been found in C14, N16A,B and C16. Consequently, the positively documented lower boundary of the Early *rhenana* Zone in the Nismes section, previously defined in sample C13 by the index *Palmatolepis nasuta* (HELSEN & BULTYNCK, 1992), should be situated stratigraphically lower in sample N12C. The available conodont data thus indicate, at least for the upper part of the Neuville Formation at Nismes, an Early *rhenana* age, which agrees with the biostratigraphic interpretation at Frasnes.

Other stratigraphically important species are *Pa. subrecta* in N16A and *Pa. rotunda* in N16B, indicating the lower limit of the Late *rhenana* Zone between samples C15 and N16A (Figs. 8 and 9). MATERN (1931) and MOURAVIEFF (1970) reported from the N16A,B beds a do I (β) γ goniatite fauna, including Manticoceratidae and Tornoceratidae. The occurrence of *Ancyrognathus triangularis* in C17 to C19 implies that this part of the succession is no younger than the middle Late *rhenana* Zone. The presence of *An. amana* in bed C16 and of *An. asymmetricus* in C17 agrees with the above data, indicating that the lower limit of the Late *rhenana* Zone is at the base of the Matagne Formation. The underlying shales, attributed to the Valisettes Formation, thus best correspond to the late Early *rhenana* Zone.

NEUVILLE (Table 4a, b)

At Neuville palmatolepids are relatively rare throughout the lower two-thirds of the succession (samples JH1-Nv8). The Philippeville Formation and the lowest part of the Neuville Formation are not well dated by conodonts. *Pa. barba* occurs in JH11, assigning the major part of the Neuville Formation to the Early *rhenana* Zone (Fig. 11). The entry of *Pa. wildungensis* is somewhat higher, i.e. at the base of the Valisettes Formation (JH20, Nv1). The first appearance of *Pa. gigas* is in

Nv4. The first occurrence of the Late *rhenana* Zone conodonts *Pa. rotunda* and *Pa. subrecta* is in JH32B. The first specimens of *Pa. hassi* s.s. are found in JH39, those of *Pa. rhenana* occur from JH42 onwards. Based on the first appearance of the namesake *Palmatolepis* species, the base of the *linguiformis* Zone is placed between JH44 and Nv9 (Fig. 12). In the interval Nv9-Nv11 *Pa. linguiformis* was recorded for the first time in Belgium by HAYDUKIEWICH (see BULTYNCK & MARTIN, 1995). Additional evidence for the *linguiformis* Zone is from *Ancyrognathus ubiquitus* in JH45. *An. asymmetricus*, recovered as incomplete specimens in Nv4, but found well-preserved in samples from overlying beds, indicate the lower limit of the Late *rhenana* Zone between Nv3 and Nv4 (Fig. 12). The occurrence of *An. asymmetricus* at the base of the Valisettes Formation agrees well with the findings of MOURAVIEFF (1974) and COEN & COEN-AUBERT (1974). The presence of *An. triangularis* in Nv1-Nv6 places this part of the succession in the early part of the Late *rhenana* Zone. The early form of *Ancyrodella curvata* is found in JH17, Nv1 and JH21 only, while the late form is present throughout nearly the entire succession. *Icriodus alternatus alternatus* and *I. alt. helmsi* occur as low as JH18. As mentioned above, fine blackish Matagne shales appear twice in the lithological succession. Surprisingly, the lower interval of Matagne shales is underlain and overlain by rocks of the Valisettes Formation which are assigned to the Late *rhenana* Zone. The upper interval (Fig. 13) overlies limestone beds with a typical *linguiformis* Zone conodont fauna and is separated at the top by a fault contact from greenish Senzeilles shales, assigned to the *triangularis* and Early to Middle *crepida* Zones, based on *Pa. delicatula, Pa. perlobata perlobata, Pa. protorhomboidea, Pa. spathula* and *Pa. triangularis* in Nv14, and on *Pa. quadrantinodosalobata, Pa. tenuipunctata* and *Pa. wolskajae* in JH46A and 47.

Although conodont evidence suggests a more or less continuous succession, the broad similarities in lithology and thickness between the lower and upper intervals of Matagne shales and between both underlying shale-limestone successions, as well as the distribution of atrypoids (GODEFROID & HELSEN, in press), all suggest that there is a major repetition within the succession at Neuville. This repetition may have been produced by faulting as the grey-greenish shales overlying the lower interval of fine, dark shales are somewhat mylonitised and disrupted by fault planes (Fig. 10). If this interpretation should be right, the lower interval of Matagne shales should be assigned to the *linguiformis* Zone as well. This is not impossible, because index-species are lacking in samples Nv7 and 8. However, the conodont biofacies is strikingly different below the lower Matagne interval (scarcity of palmatolepids) and above it (rich in palmatolepids: JH40,42 and Nv9 to 12). The scarcity of palmatolepids and the lack of *Pa. linguiformis* below the lower Matagne interval may perhaps be related to shallow-marine proximal mudmound facies (i.e., Bulants Mudmound), unlike the overlying succession with abundant palmatolepids,

which was supposedly deposited in deeper marine settings. However, the presence of *Pa. linguiformis*, indicating pelagic depositional environments for at least some beds, implies an important fault displacement above the lower interval of Matagne shales. That interpretation seems unlikely for the unconformities in the section and the local tectonic framework.

Another temporary exposure of upper Frasnian and lower Famennian rocks was along the Charleroi-Couvin highway south of Philippeville. According to COEN (1977 b), 16.5 m of nodular limestones and shales, representing the Neuville Formation, are overlain by 86 m of fine greyish shales and reddish nodular limestones that can be assigned to the Valisettes Formation. On top of this series some 10 m of dark-green to blackish shales, rich in pyrite and with abundant *Buchiola*, are considered as Matagne shales. Some 5 m above this last unit, green nodular shales yield a Famennian microfauna with *Pa. triangularis*, *Pa. delicatula* and *Pa. subperlobata*.

From the above, it is apparent that the lithological succession at Neuville is still a questionable one. New evidence may help clarify the depositional history of the Matagne shales; whether they constitute an unique deposition in time, or a returning facies due to a combination of various sedimentological conditions.

LESSIVE (Table 5)

The lowest occurrences of *Palmatolepis gigas* and *Pa. paragigas* are respectively in sample L2 and sample L3'. *Pa. hassi* s.s. is found in samples L3 through L5,? *Pa. muelleri* in L3 only and *Pa. jamieae* in L2, L3 and L5. Characteristic *Pa. wildungensis* specimens are from L3' and L4B. *Pa. nasuta* is recognised in samples L4A and L4B and *Pa. rhenana* in L4B. The entry of *Pa. rotunda* in L3 and that of *Pa. subrecta* in L3' marks the lower boundary of the Late *rhenana* Zone between L2 and L3 (Fig. 15). Additional evidence for this age comes from *Ancyrognathus asymmetricus* in L4B. The stratigraphical ranges of *An. triangularis* (L2 to L5), of *Ancyrodella nodosa*, of the early form of *Ad. curvata* (L3' to L4B) and of *Icriodus praealternatus* (L2 to L4B) suggest that the succession between L3 and L5 probably corresponds to the lower to middle part of the Late *rhenana* Conodont Zone. As a result, the base of the Matagne Formation (L2) should still be of Early *rhenana* age. However, the occurrence of *Pa. subrecta* in the COEN sample Han26 (most likely from the same bed as L2) may indicate also that the base of the Matagne Formation is included in the Late *rhenana* Zone. As samples L1 and L6 were not productive, no information on the biostratigraphic position of the adjacent lower and upper parts of the succession can be given. Of the samples L7A,B,C only the second yielded conodonts and among them, *Palmatolepis termini* indicates a Middle to Late *crepida* age. As a result, the *linguiformis*, *triangularis* and Early *crepida* Zones are not recognised in the Lessive section.

Table 5 – Conodont distribution in the Lessive section (L). L7b was not sampled *in situ*.

	L2	L3	L3'	L4a	L4b	L5	L7b
Sample weight (kg)	2	2.69	2	3.5	2	2.21	2
Fraction dissolved (kg)	0.65		2	0.985	2	2.1	1
Nr. elements	486	60	1185	4329	1520	90	x
Nr. elements/kg diss.*	748	22	593	4395	760	43	
Icriodus (Pa el.)	**136**	**18**	**293**	**698**	**216**	**3**	**x**
I. alternatus group	68		126	89			
I. a. alternatus	9	2	3	8	1		
I. praealternatus	6	1	11	1	1		
I. symmetricus	19	15	153	350	194	1	
I. sp.	34			250	20	2	x
Polygnathus (Pa el.)	**53**	**16**	**528**	**491**	**520**	**27**	**x**
P. group A	1		4	4	12	1	
P. group B	34	14	524	487	508	26	x
P. sp.	18	2					
Palmatolepis (Pa el.)	**41**	**10**	**51**	**463**	**277**	**36**	**x**
Pa. gigas	1				4		
Pa. hassi s.s.					6	3	
Pa. hassi s.l.		1		9	22	2	
Pa. aff. hassi			2			2	
Pa. jamieae	6	1				5	
?Pa. muelleri		4					
Pa. nasuta					9		
Pa. cf. nasuta				1			
Pa. paragigas			2				
Pa. cf. paragigas					2		
Pa. quadrantinodosalob.							x
Pa. rotunda		1	1	14	3	4	
Pa. subrecta			3				
Pa. aff. subrecta					3		
Pa. termini							x
Pa. wildungensis			5		1		
Pa. sp.	34	3	38	439	227	26	x
Ancyrodella (Pa el.)	**6**	**3**	**23**	**81**	**39**	**2**	
A. curvata				13	8		
A. curvata early f.			17	2	2		
A. curvata late f.	2	3	2	7	12	1	
A. nodosa				11	6		
A. sp.	4		4	48	11	1	
Ancyrognathus (Pa el.)	**7**	**2**	**12**	**82**	**29**	**2**	
An. cf. asymmetricus					3		
An. triangularis	3		4	16	6	1	
An. tsiensi		1		3			
An. sp.	4	1	8	63	20	1	
Mehlina aff. gradata				**4**			
Belodella sp.	**1**		**5**	**22**	**58**	**2**	
M elements	34		34	248	36		
Pb, S elements	208	12	239	2240	345	18	x

Conodont biofacies

Conodont biofacies of strata surrounding lower and middle Frasnian mudmounds in the type area, Belgium are discussed by VANDELAER *et al.* (1989) and SANDBERG *et al.* (1992). In the present paper conodont biofacies are

mainly derived from the percentages of Pa elements of the genera *Ancyrodella*, *Ancyrognathus*, *Icriodus*, *Palmatolepis* and *Polygnathus*; in a few cases percentages of the genus *Belodella* are also taken into account. The population of Pa elements in most of the samples used for biofacies analyses, is large enough to draw statistically justified conclusions. If this is not the case, biofacies names are mentioned between brackets. The conodont biofacies are mainly named following the methodology of ZIEGLER & SANDBERG (1990).

FRASNES (Tables 6 and 7)

Among the Frasnes-W samples two groups are distinguished (Table 6). In the first group, comprising the samples CFrW1 to CFrW3, *Polygnathus* is abundant. The second group of samples (CFrW4 to CFrW6) is characterised by the dominance of *Palmatolepis*. The relative importance of *Polygnathus* decreases considerably from 58% in CFrW1 to zero in CFrW4, and then slightly increases again towards 13% in CFrW6. On the other hand, *Palmatolepis* shows an increasing trend, from 33% in CFrW1 towards 81% in CFrW6. Associated *Ancyrognathus* Pa elements are important in CFrW2,

CFrW4 and CFrW5, ranging around 20%. *Ancyrodella* reaches its maximum abundance in CFrW1 (12%). The percentage of *Belodella* is significant in the first group of samples, with a maximum of 18% in CFrW3. *Icriodus* is generally present, though less important (0-9%). Biofacies are polygnathid-ancyrodellid, mixed, and polygnathid-palmatolepid in samples CFrW1 through CFrW3. Palmatolepid biofacies are observed in CFrW4-6, including samples poor in conodont elements. Mixed faunas are generally considered to result from sedimentological mixing by downslope transport (SANDBERG *et al.* 1992).

The Frasnes-E samples start with a dominance of *Palmatolepis* of respectively 77%, 66% and 58% in CFrE1A,1C and 1D (Table 7). In sample CFrE2 *Icriodus* is numerically the most important genus (56%). With relative abundances of 30-49%, *Polygnathus* is important, if not dominant in the samples CFrE4, 6, 7, and 9. *Palmatolepis* is again important in CFrE4 through CFrE11 (30-45%). It can be concluded that biofacies change gradually from palmatolepid into palmatolepid-polygnathid in the nodular shales of the Neuville Formation. Icriodid-palmatolepid and polygnathid-icriodid biofacies characterise the base of the Matagne Formation. In the following succession biofacies are changing towards polygnathid-palmatolepid and palmatolepid-polygnathid biofacies. Mixed biofacies are from CFrE13 which has, however, a numerically smaller conodont population.

NISMES (Table 8)

In the Nismes section conodont biofacies tend to change rapidly. This is partly due to the presence of a mudmound in the Neuville Formation, which may have created a peculiar environment. With the exception of samples C2B-C3A, C3 and C5 (the last two being less significant due to the small number of Pa elements), *Polygnathus* is the most common genus in samples C1A to C6. Relative abundances range between 34-90%. Numerically, *Palmatolepis* is generally second in importance, but in C2B-C3A it becomes the dominant genus with a relative abundance of 56%. With less than 10% icriodids are of minor importance in the series of samples C1A to C5. In

Table 6 – Relative importance of conodont genera the Frasnes-W section (%), *n* being the absolute total of Pa elements and *Belodella*.
Names biofacies: P: polygnathid, Ad: ancyrodellid, Pa: palmatolepid, mix: mixed. Biofacies between ( ) are based on populations of less than 30 Pa elements, and are thus less significant.

	CFrW1	CFrW2	CFrW3	CFrW4	CFrW5	CFrW6
Belodella	9	9	18	0	3	0
Icriodus	3	9	5	0	4	6
Polygnathus	58	27	45	0	2	13
Ancyrodella	12	2	0	0	0	0
Ancyrognathus	9	26	2	21	19	0
Palmatolepis	9	27	30	79	72	81
n	33	179	234	14	57	16
Biofacies	P-Ad	mix	P-Pa	(Pa)	Pa	(Pa)

Table 7 – Relative importance of conodont genera in the Frasnes-E section (%), *n* being the absolute total of Pa elements and *Belodella*.
Names biofacies: I: icriodid, P: polygnathid, Pa: palmatolepid, mix: mixed. Biofacies between ( ) are based on populations of less than 30 Pa elements, and are thus less significant.

	CFrE1A	CFrE1C	CFrE1D	CFrE2	CFrE4	CFrE6	CFrE7	CFrE9	CFrE11	CFrE13
Belodella	0	<1	2	0	0	4	<1	0	0	8
Icriodus	1	4	5	56	37	12	6	<1	5	16
Polygnathus	9	26	24	12	42	40	30	49	29	53
Ancyrodella	7	3	8	8	7	11	10	9	5	0
Ancyrognathus	6	0	3	<1	<1	3	8	3	0	0
Palmatolepis	77	66	58	20	13	30	45	38	61	23
n	344	73	98	25	98	302	78	246	18	13
Biofacies	Pa	Pa-P	Pa-P	(I-Pa)	P-I	P-Pa	Pa-P	P-Pa	(Pa-P)	(mix)

Table 8 – Relative importance of conodont genera in the Nismes section (%), *n* being the absolute total of Pa elements and *Belodella*. Samples proceeded by 'N' are new samples; 'C-samples' are from HELSEN & BULTYNCK (1992). Names biofacies: An: ancyrognathid, B: belodellid, I: icriodid, P: polygnathid, Pa: palmatolepid, mix: mixed. Biofacies between ( ) are based on populations of less than 30 Pa elements, and are thus less significant.

	C1A	C1	C2	C2B-C3A	C3	C3B	C4	C5	C5B	C6	C7	C8	C9	C10	C10B	C11
Belodella	0	0	1	0	0	0	0	7	17	13	0	2	38	23	48	0
Icriodus	2	4	2	7	0	10	0	7	2	17	100	2	4	23	7	0
Polygnathus	75	48	89	20	31	90	43	36	63	34	0	8	46	21	12	29
Ancyrodella	0	0	2	1	38	0	0	0	7	6	0	2	4	0	5	0
Ancyrognathus	6	4	4	16	31	0	43	0	4	0	0	0	0	0	2	9
Palmatolepis	17	44	2	56	0	0	14	50	7	30	0	86	8	33	26	62
n	47	25	95	309	13	10	7	14	54	47	1	169	26	62	121	21
Biofacies	P	(P-Pa)	P	Pa-P	(mix)	(P)	(P-An)	(Pa-P)	P-Bel	mix	(I)	Pa	(P-Bel)	mix	Bel-Pa	(Pa-P)

	C12A	C12	N12A'	C12B	N12C	N13AB	C13	C13B	C14	C15	N16A	N16B	C16	C17	C18	C19	C20
Belodella	37	9	4	4	<1	1	1	5	3	0	<1	2	<1	<1	0	1	6
Icriodus	10	3	8	8	3	2	49	7	1	0	7	13	68	23	5	10	1
Polygnathus	20	35	44	15	13	16	22	6	6	0	21	27	20	36	52	66	43
Ancyrodella	2	3	3	2	1	<1	<1	13	5	0	7	5	2	9	9	6	7
Ancyrognathus	7	6	4	18	12	8	9	20	16	17	5	5	2	1	5	1	0
Palmatolepis	24	44	37	53	70	82	18	49	69	83	59	48	7	30	29	16	43
n	59	66	122	184	357	170	393	55	894	18	336	414	6238	789	21	218	74
Biofacies	mix	Pa-P	P-Pa	Pa-An	Pa	Pa	I-P	mix	Pa-An	(Pa)	Pa-P	Pa-P	I-P	mix	(P-Pa)	P-Pa	P-Pa

C6 the abundance of 17% was reached. *Ancyrodella* and *Ancyrognathus* are of minor importance as well, but peaks of 30-40% are noted in the numerically smaller samples C3 and C4. In summary, conodont biofacies in this first series of samples are polygnathid and combinations with polygnathids.

A second series of samples (C7 to C10A) is from a massif mudmound fringe and its super- and subjacent bedded limestones. Palmatolepid-rich samples (86% in C8) alternate with assemblages rich in *Polygnathus* (up to 46%) and in *Belodella* (up to 48% in C10B). In fact, *Belodella* is also of minor importance in C5B and in C12A. Samples with mixed assemblages, e.g., yielding shallow-marine *Belodella* and deep-marine *Palmatolepis*, may be considered as downslope deposits.

Samples C12 to C16B are rich in palmatolepids (37-83%) with the exception of C13, wich has only 18% *Palmatolepis*. As a result, several of them indicate palmatolepid biofacies. *Polygnathus* is well represented in this part of the succession, but is more abundant than *Palmatolepis* in C12A' (44%) and in C13 (22%) only. The relative abundance of *Icriodus* is less than 10% in this part of the succession, with the exception of C13 (49%) and N16B (13%). Because of the relative importance of *Icriodus* and *Polygnathus* C13 is assigned to the icriodid-polygnathid biofacies. *Ancyrognathus* reaches peaks of relative abundance up to 20%.

In the extremely rich sample C16 (6238 Pa elements) *Icriodus* is by far the most common genus (68%). Because *Polygnathus* with a relative abundance of 20% is second in importance, the sample is assigned to the

icriodid-polygnathid biofacies. Mixed assemblages of *Polygnathus* (36%), *Palmatolepis* (30%) and *Icriodus* (23%) characterise C17. In the samples C18 to C20 *Polygnathus* (43 to 66%) and *Palmatolepis* (16 to 43%) determine the polygnathid-palmatolepid biofacies. In the interval C16 to C20 *Polygnathus* is especially represented by species with smooth and narrow platforms. DRUCE (1973) and SCHUMACHER (1976) associated these conodonts, such as the constituting species of the *Polygnathus* group B, with chiefly shallow-subtidal facies. Suggesting conodont biofacies analyses at species level, KLAPPER & LANE (1985) considered some *Polygnathus* species with narrow platforms, i.e., *P. decorosus*, as characteristic for the palmatolepid biofacies. As a result, at least a part of the *P.* group B constituents may be assigned to the palmatolepid biofacies.

NEUVILLE (Table 9)

Because most of the samples in the Neuville section revealed impoverished conodont faunas, especially in the lowest and middle part of the succession, biofacies analysis are not always reliable. As a result, differences in conodont biofacies may be observed between some of the JH samples and the additional Nv samples that are from the same beds.

In the lowest part of the succession (JH1 to JH35) the number of Pa elements (= *n*) is generally less than 30. Only in the Nv1 sample more than 100 Pa elements were recovered. Biofacies are determined by the relative abundance of polygnathids, which may reach up to more than 70% in the numerically large Nv4 and Nv6 samples. In

Table 9 – Relative importance of conodont genera in the Neuville section (%), *n* being the absolute total of Pa elements and *Belodella*.
Names biofacies: I: icriodid, P: polygnathid, Pa: palmatolepid, mix: mixed. Biofacies between ( ) are based on populations of less than 30 Pa elements, and are thus less significant.

	JH1	JH2	JH7	JH9	JH10	JH11	JH13	JH15	JH16	JH17	JH18	JH20	NV1	JH21	NV2
Belodella	0	0	0	0	0	0	0	0	0	0	0	0	1	0	0
Icriodus	0	83	25	0	4	18	29	8	6	0	12	6	37	6	24
Polygnathus	100	17	72	100	61	72	57	89	88	81	82	18	49	29	59
Ancyrodella	0	0	0	0	4	1	5	0	0	6	0	0	2	13	11
Ancyrognathus	0	0	0	0	0	0	0	3	6	0	6	18	5	16	3
Palmatolepis	0	0	3	0	31	9	9	0	0	13	0	58	6	36	3
n	1	6	59	9	26	67	21	37	17	16	17	38	410	31	29
Biofacies	(P)	(I)	P	(P)	(P-Pa)	P	(P-I)	P	(P)	(P)	(P)	Pa-P	P-I	Pa-P	(P-I)

	JH23	NV3	JH25	NV4	JH26	JH27	JH29	JH32	NV6	JH32B	JH34	JH35	JH37	JH38	NV8	JH39
Belodella	0	3	0	1	0	0	0	0	0	0	0	0	0	0	0	0
Icriodus	0	22	43	2	9	0	14	19	11	0	0	0	59	0	5	13
Polygnathus	18	44	29	75	73	92	11	69	76	9	33	0	35	14	46	40
Ancyrodella	9	6	14	11	0	8	14	0	3	9	0	0	0	0	2	7
Ancyrognathus	0	6	14	5	0	0	7	6	5	0	0	0	3	7	5	2
Palmatolepis	73	19	0	6	18	0	47	6	5	82	67	100	3	79	42	38
n	11	36	7	95	11	12	28	16	37	11	3	1	73	14	43	96
Biofacies	(Pa)	mix	(I-P)	P	(P)	(P)	(mix)	(P-I)	P	(Pa)	(Pa-P)	(Pa)	I-P	(Pa)	P-Pa	P-Pa

	JH40	JH41	JH42	JH42A	JH43	JH44	NV9	JH45	NV10	NV11	NV12	JH45A	NV13	NV14	JH46A	JH47
Belodella	0	4	2	0	0	0	3	1	2	3	2	0	0	0	0	0
Icriodus	0	0	<1	0	0	18	0	1	0	0	8	0	0	3	0	2
Polygnathus	49	24	21	55	100	18	28	43	32	32	46	57	83	21	20	10
Ancyrodella	1	4	2	0	0	9	6	3	1	3	1	0	0	0	0	0
Ancyrognathus	3	0	1	2	0	9	1	1	<1	1	0	14	0	3	0	0
Palmatolepis	47	68	74	43	0	46	62	51	64	61	43	29	17	73	80	86
n	349	25	1501	42	1	11	386	270	296	336	419	7	6	75	5	80
Biofacies	P-Pa	(Pa-P)	Pa	P-Pa	(P)	(mix)	Pa-P	Pa-P	Pa-P	Pa-P	P-Pa	(P-Pa)	(P)	Pa	(Pa)	Pa

the richer samples JH20 and JH21 (*n*>30) the relative abundance of palmatolepids exceeds the 30%. *Icriodus* is relatively important (>20%) in some of the numerically large samples, i.e., JH7 at the base of the Neuville Formation and Nv1 to 3 near the Neuville-Valisettes boundary. *Ancyrodella*, *Ancyrognathus* and *Belodella* seldom make up more than 10% of the conodont population. Sample JH37 yields an unusually high percentage of *Icriodus* (59%), and thus with *Polygnathus* (35%) constitute an icriodid-polygnathid biofacies.

The interval JH38 to JH45a reveals palmatolepid-polygnathid biofacies, with exception of JH43 and 44, which belong to polygnathid and mixed biofacies; they are less significant however, because of the small number of conodonts. In the larger samples (*n*>30) contributions of *Palmatolepis* range between 38-74%; relative abundances of *Polygnathus* range between 21 and 55%. Other conodont genera (*Icriodus*, *Ancyrognathus*, *Ancyrodella* and *Belodella*) are of minor importance.

The two Famennian samples are characterised by pelagic palmatolepid biofacies (80 to 86% of *Palmatolepis*).

LESSIVE (Table 10)

It appears that the relative importance of the deeper marine palmatolepids varies from sample to sample, but overall increases towards sample L5, where it reaches 50%. The number of associated *Ancyrodella* and *Ancyrognathus* Pa elements remains less important, ranging up to 6%. On the other hand, the relative abundance of *Icriodus* decreases dramatically from 56% in sample L2 to 4% in sample L5. *Polygnathus*, chiefly species of group B, represents a substantial percentage in any of the samples L2 to L5, reaching a peak of relative abundance in L3' (58%), L4b (39%) and L5 (37%). Ranging up to 3%, *Belodella* and *Ozarkodina* are numerically less important genera.

Following ZIEGLER & SANDBERG (1990), samples L2 and L3 are placed in the icriodid-polygnathid biofacies, and sample L3' in the polygnathid-icriodid biofacies. Furthermore, L4a and L4b yield a mixed biofacies, and L5 is assigned to the palmatolepid-polygnathid biofacies. The shift from icriodid-polygnathid, and polygnathid-icriodid to palmatolepid-polygnathid biofacies as a result

Table 10 – Relative importance of conodont genera and some species in the Lessive section (%), *n* being the absolute total of Pa elements and *Belodella*. Names biofacies: I: icriodid, P: polygnathid, Pa: palmatolepid, mix: mixed.

	L2	L3	L3'	L4a	L4b	L5
Belodella	<1	0	<1	1	4	3
Icriodus	56	38	32	38	16	4
Ozarkodina	0	0	0	<1	0	0
Polygnathus	22	33	58	27	39	37
Ancyrodella	2	6	2	4	3	3
Ancyrognathus	2	4	1	4	2	3
Palmatolepis	17	19	6	25	20	50
n	244	48	912	1841	1331	72
Biofacies	I-P	I-P	P-I	mix	mix	P-Pa

of the increasing relative abundance of pelagic *Palmatolepis* and the decrease of neritic *Icriodus*, reveals a progressive deepening of the shelf. Rich in *Palmatolepis*, the lower Famennian sample L7b is assigned to the palmatolepid biofacies.

Interpretation of conodont biofacies and correlation with the Lower and Upper Kellwasser Horizons (Fig. 16)

EARLY *RHENANA* ZONE

Most of the lower and middle part of the Neuville Formation (*jamieae*?-Early *rhenana* Zone) is characterised by polygnathid biofacies (i.e., CFrW and Neuville sections). The associated megafauna includes brachiopods, crinoids, gastropods and fish remains. At Nismes a more peculiar setting related to the development of a mud-mound yields biofacies rich in *Belodella*, *Icriodus* and fish remains, alternating or mixed with assemblages rich in pelagic palmatolepids. Fish remains, however, are not restricted to the shallow-marine conodont biofacies in the studied area. They may be equally important in palmatolepid and palmatolepid-polygnathid biofacies (e.g., CFrE1A-1C).

In the southern parts of the Dinant Basin polygnathid biofacies gradually change into palmatolepid-dominated biofacies towards the top of the Neuville Formation (C11 to C15 at Nismes and CFrW3 to 6 at Frasnes). At Neuville, in the more northerly Philippeville Massif and actually 10 km north of Frasnes (during Frasnian times the distance may have been more than 20 km), the number of conodont elements is too small to make sound interpretations. However, the available data from this section suggests that polygnathid-dominated biofacies persist throughout the entire Neuville Formation. At Nismes and Frasnes (CFrE) the uppermost part of the Neuville Formation (and the shales attributed to the strongly reduced Valisettes Formation at Nismes) yield a pelagic fauna of goniatites and orthocones. Apparently, the upper part of the Neuville Formation is deposited in a slightly deepening shelf environment.

Conodont biofacies show a similar succession across the Early-Late *rhenana* boundary in the southern part of the Dinant Basin (Frasnes, Nismes, Lessive). During the late Early *rhenana* Zone, represented by the upper part of the Neuville Formation, and the locally reduced Valisettes Formation, the deeper water palmatolepid biofacies is characteristic (e.g., CFrE1A, C15). However, towards the Early-Late *rhenana* boundary, at the base or slightly above the base of the Matagne Formation, a shallowing upwards trend may be observed as conodont biofacies change into palmatolepid-polygnathid biofacies.

LATE *RHENANA* ZONE

In the early part of the Late *rhenana* Zone in the southern Dinant Basin, represented by the lowest part of the Matagne Formation, icriodid-polygnathid and polygnathid-icriodid biofacies indicate more shallow-marine habitats. In the CFrE succession these biofacies are preceded by the icriodid-palmatolepid combination, which is, however, based on a smaller number of specimens. At Nismes and Lessive, mixed biofacies, still rich in icriodids, separate the icriodid-dominated biofacies from the polygnathid-palmatolepid and palmatolepid-polygnathid biofacies that are characteristic for the overlying Matagne shales and associated nodular limestones. Based on the available conodont data, it appears that a dramatic change in biofacies took place at the base of the Late *rhenana* Zone at Frasnes and Lessive, and within this zone at Nismes (beds with icriodid-polygnathid and polygnathid-icriodid populations). However, since sample 4 of MOURAVIEFF (1970) and sample Han26 of COEN (unpub.) already lowered placing of the Early-Late *rhenana* boundary at Frasnes and Lessive, additional sampling in these sections may lower it even more, suggesting a maximum shallowing (icriodid-rich beds) within the early Late *rhenana* Zone. This would agree well with the timing for the Lower Kellwasser Horizon (LKW). It has already been argued that, at least at Nismes, the LKW or its equivalent, could be traced within the Matagne shales (e.g., BUGGISCH, 1972: 62; HELSEN & BULTYNCK, 1992: 152). In the ''Matagne facies'' the number of fauna groups that flourished in the Neuville Formation is reduced. Characteristic megafossils in the Matagne Formation include small, smooth-shelled brachiopods, ostracodes, tentaculites, goniatites and a few gastropods and foraminifers. The bivalve *Buchiola* is characteristic for the Matagne shales as well, although its early occurrences are already in the Neuville Formation (CFrE1C, Nv1).

LINGUIFORMIS ZONE

Considering data from Hony and Sinsin (eastern part of the Dinant Synclinorium) SANDBERG *et al.* (1988) concluded that the Late Frasnian extinction event, the Upper Kellwasser Horizon (UKW), occurred in the Matagne

Fig. 16 – Correlation of the Frasnes (CFrW and CFrE), Nismes (N), Neuville (Nv) and Lessive (L) sections, showing the position of the Lower and Upper Kellwasser Horizons (LKW, UKW).

shale equivalent, assigned to the *linguiformis* Zone on the basis of the occurrence of *Ancyrognathus ubiquitus*. These authors demonstrated an eustatic fall within the *linguiformis* Zone by an important decrease in palmatolepids and an increase in *Polygnathus* and *Icriodus*, finally resulting in a polygnathid-icriodid biofacies. Although their conodont populations are somewhat different, the lithological succession assigned to the *linguiformis* Zone at Hony and at Neuville are very similar. At both places some 70 cm of shelly limestones with brachiopods and some thin shaley intercalations, and yielding an abundant conodont fauna, are succeeded by shales with impoverished faunas. At Neuville these shales are dark and fine, and assigned to the Matagne Formation. The overlying greenish shales are attributed to the Famennian based on conodonts (Nv14), and thus dated post-event. SCHINDLER (1993) stated that the effect of the UKW on the biota is more pronounced than that of the LKW. This was recognised in the Neuville section, especially for the brachiopod and coral faunas.

Systematic Palaeontology

Representatives of most taxa mentioned in the range charts and distribution tables (1-5) are figured in Plates 1-8. Some of the taxa from the Nismes section (*Ancyrodella ioides, Ancyrognathus irregularis, A. seddoni, Icriodus expansus, Palmatolepis* aff. *P. foliacea, P. plana, P. punctata* and *P. simpla*) were figured in HELSEN & BULTYNCK (1992, pls. 1-3) and are not refigured herein. Most taxa are only briefly discussed in the light of the taxonomy of Frasnian *Ancyrognathus* and *Palmatolepis* species proposed by KLAPPER (1990), KLAPPER & FOSTER (1993), SANDBERG, ZIEGLER, DREESEN & BUTLER (1992) and ZIEGLER & SANDBERG (1990).

Palmatolepis wildungensis is described in detail. Synonymies are limited to the original reference or to figured or taxonomically discussed specimens from Frasnian sections in Belgium. All discussions and descriptions refer to Pa elements. In our discussions or descriptions of Pa elements of *Palmatolepis* the platform, excluding lobe, is designated as "main part of the platform". All figured specimens are reposited at the Institut royal des Sciences naturelles de Belgique, under catalogue numbers I.R.Sc.N.B. N° b 3285 - b 3390.

Genus *Ancyrodella* ULRICH & BASSLER, 1926

Ancyrodella curvata (BRANSON & MEHL, 1934)
Pl. 5, Figs. 8-10; Pl. 6, Figs. 1-3.

* 1934   *Ancyrognathus curvata* BRANSON & MEHL, p. 241, pl. 19, figs. 6, 11.

DISCUSSION: KLAPPER (1988) and ZIEGLER & SANDBERG (1990) distinguish early and late forms/morphotypes in *A. curvata*, respectively with a weakly defined outer lateral lobe and with a distinctly developed outer lateral lobe. The late form is herein restricted to specimens with a pronounced outer lateral lobe and with a nearly right angle between the outer anterolateral carina and the outer

posterolateral carina (Pl. 6, Figs. 1, 2). We also recognise a latest form characterised by a more posteriorly orientated outer lateral lobe and with a clearly obtuse angle (up to 115°) between the outer anterolateral carina and the outer posterolateral carina (Pl. 5, Figs. 8-10). The holotype of *A. curvata* belongs to the latest form. In the sections studied herein the latest form is recorded from the upper part of the Late *rhenana* Zone and from the *linguiformis* Zone.

Genus *Ancyrognathus* BRANSON & MEHL, 1934

Ancyrognathus amana MÜLLER & MÜLLER, 1957
Pl. 7, Figs. 9-11.

* 1957   *Ancyrognathus amana* n. sp. - MÜLLER & MÜLLER, p. 1095, pl. 138, fig. 5.
p 1973   *Ancyrognathus triangularis triangularis* YOUNQUIST-COEN, fig. 3, n° 13.
1990   *Ancyrognathus amana* MÜLLER & MÜLLER, 1957 - KLAPPER, pp. 1001, 1003, figs. 2.1-2.6.
1992   *Ancyrognathus amana* MÜLLER & MÜLLER, 1957 - SANDBERG, ZIEGLER, DREESEN & BUTLER, p. 54, pl. 10, figs. 1-4.

DISCUSSION: Specimens assigned here to *A. amana* correspond perfectly to the holotype and the specimens figured by KLAPPER (1990) and SANDBERG *et al.* (1993). KLAPPER (1990) includes in *A. amana* two specimens of *A. triangularis* figured by MOURAVIEFF (1982, pl. 6, figs. 1-2). However, according to the diagnosis of SANDBERG *et al.* (1993) we do not include these specimens in *A. amana* because the posterior platform is relatively long in comparison to the lateral lobe.

The *A. amana* specimens from the present study occur in the oldest part of the Matagne Formation (Late *rhenana* Zone) and therefore the species is not restricted to a backmound facies as mentioned by SANDBERG *et al.* (1993).

Ancyrognathus asymmetricus (ULRICH & BASSLER, 1926)
Pl. 7, Figs. 1-5.

* 1926   *Palmatolepis asymmetrica* n. sp. - ULRICH & BASSLER, p. 50, pl. 7, fig. 18.
1970   *Ancyrognathus asymmetrica* (ULRICH & BASSLER) - BOUCKAERT & MOURAVIEFF, pl. 7, figs. 7-12.
1973   *Ancyrognathus asymmetricus* (ULRICH & BASSLER) - COEN, fig. 3 - n° 16-18; fig. 4 - n° 4, 7; fig. 5 - n° 1-3; pl. 1, figs. 6, 7.
p 1982   *Ancyrognathus asymmetricus* (ULRICH & BASSLER, 1926) - MOURAVIEFF, pl. 6, figs. 5, 7, 8; pl. 7, figs. 5-7.
1982   *Ancyrognathus asymmetricus* - TOURNEUR, fig. 5 - n° 112.
p 1990   *Ancyrognathus asymmetricus* (ULRICH & BASSLER, 1926) - KLAPPER, pp. 1003, 1004, figs. 4.3, 4.4, 4.6-4.16; fig. 6.10.

1993   *Ancyroides asymmetricus* (ULRICH & BASSLER, 1926) - SANDBERG, ZIEGLER, DREESEN & BUTLER, pp. 58-59, pl. 6, figs. 7-9.

p 1993   *Ancyroides leonis - Ancyroides asymmetricus* - SANDBERG, ZIEGLER, DREESEN & BUTLER, pl. 6, fig. 6.

DISCUSSION: Identification is restricted to specimens with a fixed blade on the right side of the platform, terminating abruptly and offset from the carina. The anterior part of the carina is incomplete or only weakly indicated. Specimens with a distinct convex bulge in the inner platform margin are considered to be transitional between *A. asymmetricus* and *A. uddeni* (Pl. 7, figs. 6-8).

Ancyrognathus asymmetricus (ULRICH & BASSLER, 1926) - Ancyrognathus uddeni (MILLER & YOUNGQUIST, 1947)
Pl. 7, Figs. 6-8.

p 1990   *Ancyrognathus asymmetricus* (ULRICH & BASSLER, 1926) - KLAPPER, pp. 1003, 1004, fig. 4.7; figs. 6.4, 6.7 (only).

DISCUSSION: The platform is less rounded than in typical *A. uddeni* specimens. See also under *A. asymmetricus*.

Ancyrognathus coeni KLAPPER, 1990 - Ancyrognathus tsiensi MOURAVIEFF, 1982 group
Pl. 9, Figs. 9, 10.

DISCUSSION: A few specimens under this designation are somewhat similar to *A. coeni* and slender specimens of *A. tsiensi* figured by KLAPPER (1990, e.g. fig. 12.7). The platform is elongated and narrow, with marginal ridges or nodes. The fixed blade is centrally positioned, high and declining either abruptly or gradually into the anterior carina. The anterior carina is straight or slightly sinuous. The posterior carina is slightly to strongly deflected inwards. The denticles of the carina are relatively high. The lateral lobe is short and the secondary carina meets the anterior carina at a right angle. The two last mentioned characteristics separate the specimens under discussion from *A. coeni* and *A. tsiensi*. The specimens occur in the Neuville Formation (Early *rhenana* Zone) at Neuville.

Ancyrognathus sinelobus (SANDBERG, ZIEGLER & DREESEN, 1992)
Pl. 6, Fig. 5.

* 1992   *Ancyroides sinelobus* n. sp. SANDBERG, ZIEGLER & DREESEN-SANDBERG, ZIEGLER, DREESEN & BUTLER, pp. 57, 58, pl. 10, figs. 7, 8.

DISCUSSION: The only specimen in our collection is from the upper part of the Valisettes Formation (Late *rhenana* Zone) at Neuville.

Ancyrognathus triangularis YOUNGQUIST, 1945
Pl. 6, Figs. 6, 7.

* 1945   *Ancyrognathus triangularis* n. sp. - YOUNGQUIST, pp. 356-357, pl. 54, fig. 7.

DISCUSSION: In our material of *A. triangularis* occur wide specimens with a nearly triangular platform outline and with a nearly straight posterior platform margin (Pl. 6, Fig. 6) and also more elongate specimens with a deeper sinus in the posterior margin (HELSEN & BULTYNCK, 1992, pl. 1, fig. 9). As mentioned in the diagnosis of KLAPPER (1990) our specimens show an obtuse angle between the posterior and secondary carinae.

Ancyrognathus tsiensi MOURAVIEFF, 1982
Pl. 6, Fig. 11.

p 1982 *   *Ancyrognathus tsiensi* n. sp. - MOURAVIEFF, pp. 104-106, pl. 4, fig. 7; pl. 5, figs. 2-7, 11.

DISCUSSION: This species occurs only in small numbers in our collections. Our identification of *A. tsiensi* is based on these specimens from the figured type material mentioned here above. The fixed blade is central or nearly central, very high and declining abruptly to the uninterrupted anterior carina. The secondary carina is at an acute or nearly right angle to the posterior carina (see MOURAVIEFF, pl. 5, fig. 4 and pl. 4, fig. 7).

The specimen figured herein (Pl. 6, Fig. 8) is identified as *A.* aff. *A. tsiensi* because of the sinuous outline of the posterolateral lobe and the narrow posterior platform.

Genus Ancyrolepis ZIEGLER, 1959

Ancyrolepis cruciformis ZIEGLER, 1959
Pl. 7, Fig. 12.

* 1959   *Ancyrolepis cruciformis* n. sp. - ZIEGLER, pp. 78-80, pl. 7, figs. 1-4.

DISCUSSION: In the holotype of the species the inner lateral lobe is anteriorly and posteriorly demarcated by a shallow sinus. In our specimens the inner lateral lobe is absent or only weakly developed. However, in one of the figured type specimens (pl. 7, fig. 1) the inner lateral lobe is not clearly demarcated either. Therefore we include our specimens in the range of variation of *A. cruciformis*.

Genus Icriodus BRANSON & MEHL, 1938

Icriodus alternatus alternatus BRANSON & MEHL, 1934
Pl. 8, Fig. 22.

* 1934   *Icriodus alternatus* BRANSON & MEHL n.sp. - BRANSON & MEHL, pp. 225-226, pl. 13, figs. 4-6.

DISCUSSION: Typical *I. alternatus alternatus* specimens are common from within the Early *rhenana* Zone. SANDBERG, ZIEGLER, DREESEN & BUTLER (1992) mention the earliest occurrence within the Late *rhenana* Zone of the Frasnes area.

Icriodus alternatus helmsi SANDBERG & DREESEN, 1984
Pl. 8, Fig. 23.

* 1984   *Icriodus alternatus helmsi* n. subsp. - SANDBERG & DREESEN, p. 159, pl. 2, figs. 1-4, 6, 7.

DISCUSSION: An isolated specimen of *I. alternatus helmsi* was recorded from the top of the Neuville Formation at Neuville, just below the earliest occurrence of *Ancyrognathus asymmetricus*. ZIEGLER & SANDBERG (1990) mention the earliest occurrence in the later half of the Late *rhenana* Zone. In Belgium the taxon is common from the Early *triangularis* Zone on.

Icriodus aff. *I. excavatus* WEDDIGE, 1984
Pl. 8, Figs. 18-21.

aff. * 1984   *Icriodus excavatus* n. sp. - WEDDIGE, p. 208, pl. 1, fig. 9-22.
aff. 1987   *Icriodus excavatus* WEDDIGE, 1984 - BULTYNCK, pp. 158-159, pl. 6, figs. 21-25.
? 1992   *Icriodus* cf. *I. retrodepressus* BULTYNCK, 1970 - SANDBERG, ZIEGLER, DREESEN & BUTLER, pp. 62, pl. 1, fig. 1.

DISCUSSION: The posteriormost 1-3 medial-row denticles lie in a depression and the extension of the medial-row denticles posterior of the spindle is relatively short. The outline of the spindle is slightly biconvex. The basal cavity is broadly expanded and nearly symmetrical. The holotype and paratypes of *I. excavatus* are from the early Givetian Bahram 1 - Subformation in NE Iran, they differ from our specimens by the strongly asymmetrical basal cavity expansion and the occurrence of short strongly biconvex forms in the range of variation. According to WEDDIGE (1984), *I. excavatus* ranges from the *varcus* Zone into the *Ancyrognathus triangularis* Zone. The specimens from the present study are from the Philippeville Formation and the lower part of the Neuville Formation at Neuville, below the earliest occurrence of *Ancyrognathus asymmetricus*.

Icriodus symmetricus BRANSON & MEHL, 1934
Pl. 8, Figs. 24, 25.

* 1934   *Icriodus symmetricus* BRANSON & MEHL n. sp. - BRANSON & MEHL, p. 226, pl. 13, figs. 1-3.

DISCUSSION: In the Frasnian sections from the present study the latest occurrence of the species is within the upper part of the Late *rhenana* Zone.

Genus *Palmatolepis* ULRICH & BASSLER, 1926

Palmatolepis barba ZIEGLER & SANDBERG, 1990
Pl. 1, Fig. 8.

* 1990   *Palmatolepis barba* n. sp. - ZIEGLER & SANDBERG, p. 48, pl. 4, figs. 3, 4, 8.

DISCUSSION: Two small specimens from the lower part of the Neuville Formation at Neuville are characterised by a narrow platform with a weakly developed platform ornamentation, a slightly anteriorly directed outer lateral lobe and a distinctly upward inclined posterior platform. The specimens correspond well to the juvenile specimen of *P. barba* figured by ZIEGLER & SANDBERG (ibidem, pl. 4, fig. 8). KLAPPER & FOSTER (1993) interpret the characteristics of *P. barba* as within the range of variation of *P. proversa*. However, in the latter species the outer lateral lobe is strongly directed anteriorly and the tip of the posterior platform is declined.

Palmatolepis aff. *P. foliacea* YOUNGQUIST, 1945

1992   *Palmatolepis foliacea* YOUNGQUIST, 1945 - HELSEN & BULTYNCK, pl. 3, figs. 8, 9.

DISCUSSION: Specimens from the Nismes section under this designation were assigned to *P. foliacea* by HELSEN & BULTYNCK (1992). They differ from *P. foliacea* by a less elliptical platform outline and a more developed outer lobe.

Palmatolepis gigas MILLER & YOUNGQUIST, 1947
Pl. 2, Fig. 7.

* 1947   *Palmatolepis gigas* n. sp. - MILLER & YOUNGQUIST, pp. 512-513, pl. 75, fig. 1.
p 1990   *Palmatolepis gigas gigas* MILLER & YOUNGQUIST, 1947 - ZIEGLER & SANDBERG, p. 54, pl. 7, figs. 1, 2, 5, 6; pl. 8, fig. 6, 7.
cf 1992   *Palmatolepis gigas gigas* MILLER & YOUNGQUIST, 1947 - HELSEN & BULTYNCK, pl. 3, fig. 11.
1993   *Palmatolepis gigas* MILLER & YOUNGQUIST, 1947 - KLAPPER & FOSTER, pp. 31, 32, fig. 18.9.
p 1993   *Palmatolepis winchelli* (STAUFFER, 1938) - KLAPPER & FOSTER, figs. 18.8, 18.9, 18.11;? figs. 18.1, 18.2, 18.10.

DISCUSSION: Specimens identified herein as *P. gigas* correspond to the diagnosis of *P. gigas gigas* of ZIEGLER & SANDBERG (1990), although we do not include in *P. gigas* all the specimens they figured under this designation. Contrary to the suggestion of KLAPPER & FOSTER (1993, p. 32) we do not include the holotype of *P. gigas* within the range of variation of *P. subrecta* (= *P. winchelli* sensu KLAPPER & FOSTER, 1993). The former species differs from *P. subrecta* by the development of a fortified rostrum, the more anterior position of the

outer lateral lobe and the different outline of the platform margin between its outer anterior end and the tip of the outer lateral lobe. Moreover, the anterior blade is characterised by a few high denticles.

Palmatolepis hassi MÜLLER & MÜLLER, 1957 s.s.
Pl. 2, Fig. 6; Pl. 3, Figs. 2-7.

* 1957   *Palmatolepis (Manticolepis) hassi* MÜLLER & MÜLLER, n. sp. - MÜLLER & MÜLLER, pp. 1102-1103, pl. 140, figs. 2-4;? pl. 139, fig. 2 = specifically indeterminable juvenile specimen.
1988   *Palmatolepis hassi* MÜLLER & MÜLLER form 4 - KLAPPER, p. 458, pl. 1, figs. 4-5.
p 1990   *Palmatolepis hassi* MÜLLER & MÜLLER, 1957 - ZIEGLER & SANDBERG, pp. 55-56, pl. 2, fig. 2 (only = refiguration of holotype);? pl. 2, fig. 5.
1993   *Palmatolepis hassi* MÜLLER & MÜLLER, 1957 - KLAPPER & FOSTER, p. 22, figs. 15.1-15.5, 15.8;? figs. 15.6, 15.7, 15.9, 18.12.

DISCUSSION: Most specimens assigned herein to *P. hassi* s.s. correspond perfectly to the holotype of that species and to the description of its Pa element by KLAPPER & FOSTER (1993, p. 22). The posterior half of the platform is wide, the outer lobe well developed and demarcated by deep sinuses. Most characteristic are the distinctly convex platform outline posterior of the outer lobe and the attenuating, pointed posterior platform end. The nodes on the platform surface are evenly distributed and in some specimens the outer lobe develops a secondary carina. The posterior carina is slightly curved inward. The blade is of medium height, gradually declining into the anterior carina. Although we follow the description of the Pa element of *P. hassi* by KLAPPER & FOSTER (1993) we stress some minor differences between the type material and the specimens from the Canning Basin (W. Australia) figured by the latter authors. In these specimens the interior of the platform is excavated, the platform margin tends to develop strong transversal ridges and the posterior carina is nearly straight. Moreover, the characteristic platform outline posterior of the outer lateral lobe is not developed in some figured specimens, they are mentioned with question - mark in our synonymy list.

Typical *P. hassi* specimens from the present study occur in the Late *rhenana* Zone, some specimens questionably referred to *P. hassi* (e.g. Pl. 3, Fig. 1) are from the Early *rhenana* Zone.

Palmatolepis hassi s.l. *sensu* ZIEGLER & SANDBERG, 1990
Pl. 2, Figs. 1-5.

p 1990   *Palmatolepis hassi* MÜLLER & MÜLLER, 1957 - ZIEGLER & SANDBERG, pp. 55-56, pl. 2, figs. 3, 4, 6, 8; pl. 12, figs. 10, 11.
1992   *Palmatolepis hassi* MÜLLER & MÜLLER, 1957 - HELSEN & BULTYNCK, pl. 3, fig. 5.

1992   *Palmatolepis hassi* MÜLLER & MÜLLER, 1957 - SANDBERG, ZIEGLER, DREESEN & BUTLER, pl. 2, figs. 1, 2.

DISCUSSION: Specimens under this designation correspond more or less to the concept of *P. hassi* according to ZIEGLER & SANDBERG (1990). They proposed a revised diagnosis of *P. hassi* including in the range of variation specimens with a narrow platform (ibidem, pl. 2, figs. 3, 6, 8; pl. 12, figs. 10, 11) and specimens with a wider platform (ibidem, pl. 2, fig. 4), however missing the distinctly convex platform outline posterior of the outer lobe and the attenuating, pointed posterior end. As discussed by KLAPPER, KUZ'MIN & OVNATANOVA (1996) it is evident that the two main morphotypes mentioned above are distinguishable from *P. hassi*. A taxonomic of revision the specimens herein designated as *P. hassi* s.l. is beyond the scope of the present paper, because they appear already in earlier Frasnian formations.

Palmatolepis jamieae ZIEGLER & SANDBERG, 1990
Pl. 1, Fig. 13.

1986   *Palmatolepis* sp. B - KLAPPER & FOSTER, pl. 2, figs. 6, 8.
1988   *Palmatolepis* sp. B of KLAPPER & FOSTER - KLAPPER, pl. 2, figs. 3-4.
* 1990   *Palmatolepis jamieae* n. sp. - ZIEGLER & SANDBERG, pp. 50-51, pl. 6, figs. 1-3, 5, 9, 10;? pl. 6, figs. 6, 8;? pl. 11, figs. 4-6; non pl. 6, figs. 4, 7 = *P. wildungensis*.
1992   *Palmatolepis jamieae* ZIEGLER & SANDBERG, 1990 - SANDBERG, ZIEGLER, DREESEN & BUTLER, pl. 3, figs. 3, 5.
1992   *Palmatolepis jamieae* ZIEGLER & SANDBERG, 1990 - HELSEN & BULTYNCK, pl. 3, figs. 6, 7.

DISCUSSION: The most characteristic specimens within the range of variation of *P. jamieae* belong to the second morphotype distinguished by ZIEGLER & SANDBERG (1990, p. 51) in which the outer lobe is poorly demarcated and the general platform outline tends to be pyriform (e.g. ZIEGLER & SANDBERG, 1990, pl. 6, figs. 9, 10; HELSEN & BULTYNCK, pl. 3, fig. 7). In some specimens from the type material (ZIEGLER & SANDBERG, 1990, pl. 6, figs. 6, 8) the lobe is well demarcated anteriorly and posteriorly and we prefer to exclude such forms from the range of variation of *P. jamieae*. See also the discussion of *P. wildungensis* herein.

Palmatolepis linguiformis MÜLLER, 1956
Pl. 5, Figs. 1, 2.

* 1956   *Palmatolepis (Palmatolepis) linguiformis* n. sp. - MÜLLER, pp. 24-25, pl. 7, figs. 1-7.
1990   *Palmatolepis linguiformis* MÜLLER, 1956 - ZIEGLER & SANDBERG, pp. 59-60 pl. 14, figs. 8-10.

1995   *Palmatolepis linguiformis* MÜLLER, 1956 - BUL-
TYNCK & MARTIN, 1995, p. 17, pl. 9, fig. 11.

DISCUSSION: Some specimens show a slight bulge in the outer platform margin. In specimens from the same sample the upper platform surface can be either more or less smooth or ornamented by nodes. The species occurs in small numbers in four grey-bluish limestone beds immediately below black Matagne shales in the Neuville section. BULTYNCK & MARTIN (1995, p. 17) included these beds in the Matagne Formation. However, according to the grey-bluish color these beds are herein assigned to the top of the Valisettes Formation.

Palmatolepis muelleri KLAPPER & FOSTER, 1993
Pl. 1, Fig. 12.

* 1993   *Palmatolepis muelleri* n. sp. - KLAPPER & FOSTER, pp. 22-24, figs. 16.2-16.9.
p 1996   *Palmatolepis muelleri* KLAPPER & FOSTER, 1993 - KLAPPER, KUZ'MIN & OVNATANOVA, pp. 147-148, figs. 8.1, 8.3 (only); non fig. 8.2 (= *P. wildungensis*).

DISCUSSION: A few specimens in our collections correspond relatively well to some of the figured paratypes of *P. muelleri*. The main part of the platform is oval-shaped, elongated with a narrow posterior tip. The outer lateral lobe is well developed, well demarcated by deep sinuses and is perpendicular to the long axis of the platform. The upper surface of the platform is equally covered with nodes. The anterior blade is high. *P. muelleri* differs from *P. nasuta* by the latter character and by the outline of the posterior platform with a distinctly narrowing tip. Some of the specimens herein assigned to *P. wildungensis* (e.g. Pl. 1, Fig. 3) are superficially similar to *P. muelleri*. However, the lobe is less demarcated in the former, the interior part of the platform is depressed and the platform margins are fortified.

Palmatolepis nasuta MÜLLER, 1956
Pl. 5, Figs. 3, 5-7.

* 1956   *Palmatolepis (Manticolepis) nasuta* n. sp. - MÜLLER, pp. 23-24, pl. 6, figs. 31-33 (only).
1982   *Palmatolepis gigas* MILLER & YOUNGQUIST, 1947 - MOURAVIEFF, pl. 7, fig. 15.
p 1990   *Palmatolepis rhenana nasuta* MÜLLER, 1956 - ZIEGLER & SANDBERG, p. 57, pl. 12, figs. 4-9; pl. 15, fig. 4 (only).
1992   *Palmatolepis rhenana nasuta* MÜLLER, 1956 - SANDBERG, ZIEGLER, DREESEN & BUTLER, pl. 2, fig. 7.
1992   *Palmatolepis rhenana rhenana* BISCHOFF, 1956 - ibidem, pl. 2, fig. 6.
1992   *Palmatolepis rhenana nasuta* MÜLLER, 1956 - HELSEN & BULTYNCK, pl. 3, fig. 13.

DISCUSSION: The main part of the platform is elongated and oval-shaped. The outer posterior platform is wider than the inner and its outline is slightly convex without a distinct constriction near the posterior tip. The outer lobe is strong, pointed, directed laterally and situated at mid-length of the platform. The blade declines gradually into the anterior carina and the posterior carina is nodose and straight to slightly curved inward. Specimens in our collections range from forms almost identical with the holotype (Pl. 5, Figs. 5-6) to more elongated forms (Pl. 5, Fig. 3) somewhat similar to *P. rhenana*. Differences with the latter species are discussed there.

Palmatolepis paragigas ZIEGLER & SANDBERG, 1990
Pl. 2, Figs 8, 9.

* 1990   *Palmatolepis gigas paragigas* n. subsp. - ZIEGLER & SANDBERG, p. 53, pl. 8, figs. 1-4, 9.
1990   *Palmatolepis gigas paragigas* ZIEGLER & SANDBERG, 1990 - SANDBERG, ZIEGLER, DREESEN & BUTLER, pl. 2, fig. 8.
1992   *Palmatolepis gigas paragigas* ZIEGLER & SANDBERG, 1990 - HELSEN & BULTYNCK, pl. 3, fig. 12.

DISCUSSION: The specimens identified herein as *P. paragigas* are characterised by a relatively narrow, elongated platform with a moderate rostrum and with a depressed interior, a short lobe and an anterior blade with a few high denticles. These characteristics are in agreement with the original diagnosis.

Palmatolepis proversa ZIEGLER, 1958
Pl. 1, Fig. 14.

* 1958   *Palmatolepis proversa* n. sp. - ZIEGLER, pp. 62-63, pl. 4, figs. 2, 7, 9-12 (only).
1982   *Palmatolepis proversa* ZIEGLER, 1958 - MOURAVIEFF, pl. 7, figs. 17,? 16.
1990   *Palmatolepis proversa* ZIEGLER, 1958 - ZIEGLER & SANDBERG, pp. 46-47, pl. 4, figs. 1, 2, 5, 6 (only).
1992   *Palmatolepis proversa* ZIEGLER, 1958 - *Palmatolepis barba* ZIEGLER & SANDBERG, 1990 - SANDBERG, ZIEGLER, DREESEN & BUTLER, pl. 2, fig. 9.
1992   *Palmatolepis proversa* ZIEGLER, 1958 - HELSEN & BULTYNCK, pl. 3, fig. 3.
1993   *Palmatolepis proversa* ZIEGLER, 1958 - KLAPPER & FOSTER, pp. 12-15, figs. 8.1, 8.2; figs. 9.1-9.8.

DISCUSSION: Specimens identified herein as *P. proversa* have a strong outer lateral lobe, distinctly directed anteriorly. Characteristically, the anterior margin of the outer lateral lobe meets the main part of the platform at an acute angle. The posterior end of the platform is arched downward. Differences with *P.barba* are discussed there.

P. proversa is rare in our collections, the species is only recorded from the lower part of the Neuville Formation in Neuville and Nismes (*jamieae*/Early *rhenana* Zones).

Palmatolepis rhenana BISCHOFF, 1956
Pl. 4, Fig. 12; Pl. 5, Fig. 4.

* 1956   *Palmatolepis rhenana* n. sp. - BISCHOFF, pp. 129-130, pl. 8, figs. 26-28, 30.
1970   *Palmatolepis gigas* MILLER & YOUNGQUIST - BOUCKAERT & MOURAVIEFF, pl. 7, fig. 1.
1990   *Palmatolepis rhenana rhenana* BISCHOFF, 1956 - ZIEGLER & SANDBERG, pp. 57-58, pl. 12, figs. 1-3; pl. 15, figs. 1, 3, 6,? 7.
non 1992   *Palmatolepis rhenana rhenana* BISCHOFF, 1956, early morphotype - SANDBERG, ZIEGLER, DREESEN & BUTLER, pl. 2, fig. 6 (= *P. nasuta*).
1993   *Palmatolepis rhenana* BISCHOFF, 1956 - KLAPPER & FOSTER, p. 24, fig. 16.1; figs. 17.3-17.10.
1996   *Palmatolepis rhenana* BISCHOFF, 1956 - KLAPPER, KUZ'MIN & OVNATANOVA, p. 1, figs. 8.7, 8.10, 8.13.

DISCUSSION: The two specimens figured herein are very close to the figured type material of *P. rhenana*. The main part of the platform is long and relatively narrow. The outer lateral lobe is very long and narrow. The platform margin posterior to this lobe is nearly rectilinear whereas the inner posterior platform margin shows a clear sinus. The platform surface is covered with uniform nodes and the carina is strongly sigmoidal. The free blade is long and high. The outline of the posterior platform, the outline of the lobe, the long and high free blade and the strongly sigmoidal carina distinguish *P. rhenana* from *P. nasuta*.

Most of our specimens of *P. rhenana* are very large (about 2 mm long) in comparison to other *Palmatolepis* taxa from the same samples.

Palmatolepis rotunda ZIEGLER & SANDBERG, 1990
Pl. 4, Figs. 1-11.

1970   *Palmatolepis subrecta* MILLER & YOUNGQUIST - BOUCKAERT & MOURAVIEFF, pl. 7, figs. 2-4.
1982   *Palmatolepis subrecta* MILLER & YOUNGQUIST, 1947 - MOURAVIEFF, pl. 7, fig. 14.
1986   *Palmatolepis* Sp. A - KLAPPER & FOSTER, pl. 1, fig. 4.
1988   *Palmatolepis bogartensis* (STAUFFER) - KLAPPER, p. 458, pl. 2, figs. 7-8.
* 1990   *Palmatolepis rotunda* n. sp. - ZIEGLER & SANDBERG, p. 62, pl. 10, figs. 1-5.
1993   *Palmatolepis bogartensis* (STAUFFER, 1938) - KLAPPER & FOSTER, pp. 17-18, figs. 13.4-13.16.
1996   *Palmatolepis bogartensis* (STAUFFER, 1938) - KLAPPER, KUZ'MIN & OVNATANOVA, pp. 140-143, fig. 8.6.

DISCUSSION: The figured specimens cover perfectly the range of variation of the elements of the multielement species *P. bogartensis* described by KLAPPER & FOSTER (1993). The intraspecific variation in these Pa elements is considerably larger than the one shown in the figured type material of *P. rotunda*. In most specimens from this type material the outline of the posterior platform is extremely rounded without development of a distinct posterior tip. *P. rotunda* is one of the more common *Palmatolepis* taxa during the Late *rhenana* Zone in the studied area.

Palmatolepis subrecta MILLER & YOUNGQUIST, 1947
Pl. 3, Figs. 8-13.

* 1947   *Palmatolepis subrecta* MILLER & YOUNGQUIST, n. sp. - MILLER & YOUNGQUIST, pp. 513-514, pl. 75, figs. 7-11.
1974   *Palmatolepis subrecta* MILLER, A.K. & YOUNGQUIST, W.L., 1947 - COEN & COEN-AUBERT, p. 3, fig, S.
p 1986   *Palmatolepis subrecta* MILLER & YOUNGQUIST - KLAPPER & FOSTER, pl. 2, fig. 7 (only).
p 1990   *Palmatolepis subrecta* MILLER & YOUNGQUIST, 1947 - ZIEGLER & SANDBERG, pp. 60-61, pl. 11, figs. 3,7-9, 11, 12 (only); pl. 15, fig. 8 (only).
non 1992   *Palmatolepis subrecta* MILLER & YOUNGQUIST, 1947 - SANDBERG, ZIEGLER, DREESEN & BUTLER, pl. 2, figs. 4, 5.
p 1993   *Palmatolepis winchelli* (STAUFFER, 1938) - KLAPPER & FOSTER, pp. 24-31, figs. 13.1, 13.2; figs. 18.3-18.7 (only).
1995   *Palmatolepis subrecta* MILLER & YOUNGQUIST, 1947 - BULTYNCK & MARTIN, p. 18, pl. 9, fig. 10.

DISCUSSION: In most specimens herein assigned to *P. subrecta* the platform anterior to the lobe is narrow and relatively long; the sinus between the anterior platform end and the rounded tip of the outer lateral lobe deepens very progressively; the lobe is short to moderate; the outer platform margin posterior to the lobe is convex, eventually with a sinus just anterior of the tip; the density of the nodes on the platform is higher towards the platform margins; the blade gradually declines into the slightly sigmoidal carina. In most of the specimens figured herein the lobe is less developed than in the lectotype, however within the range of variation also occur specimens with a stronger lobe (e.g. Pl. 3, Fig. 10 and BULTYNCK & MARTIN, 1995, pl. 9, fig. 10).

Palmatolepis wildungensis MÜLLER, 1956
Pl. 1, Figs. 1-7, 10, 11.

* 1956   *Palmatolepis (Manticolepis) wildungensis* n. sp. - MÜLLER, p. 22, pl. 5, figs. 21-24.
p 1956   *Palmatolepis (Manticolepis) triangularis* (SANNEANN 1955)? - MÜLLER, p. 50, pl. 2, fig. 19 (only).
p 1990   *Palmatolepis jamieae* n. sp. - ZIEGLER & SANDBERG, pp. 50-51, pl. 6, figs. 4, 7 (only).
p 1996   *Palmatolepis muelleri* KLAPPER, KUZ'MIN & OVNATANOVA, pp. 147-148, fig. 8.2 (only).

DESCRIPTION: *P. wildungensis* is characterised by a more or less triangular platform with fortified platform margins and a depressed interior. The mostly stubby outer lateral lobe is not well demarcated and is situated about midway

between the outer anterior platform end and the posterior tip. The outer platform margin, anterior and posterior of the lobe, is nearly straight with only a weak sinus anterior and posterior of the lobe. The upper platform surface, especially its margin, is ornamented by nodes. The anterior blade is high and declines more or less abruptly into the anterior carina. The anterior carina is straight and the posterior carina is straight or slightly curved inward.

DISCUSSION: On the one hand, ZIEGLER & SANDBERG (1990) regarded the holotype of *P. wildungensis* as "an atypical specimen of *P. rhenana nasuta*" and included the two figured paratypes of the former species in the range of variation of the new species *P. jamieae*. On the other hand KLAPPER & FOSTER (1993) considered the holotype of *P. wildungensis* "as a specifically indeterminate small Pa element" and they included the two figured paratypes in the new species *P. muelleri*. In our opinion the holotype and two paratypes of *P. wildungensis* figured by MÜLLER (1956) belong to one species and the three specimens show the characteristics mentioned in the description here above. This view is supported by the ontogenetic series figured herein (Pl. 1, Figs. 1-7). Furthermore, the weakly demarcated lobe and the depressed interior of the platform clearly distinguish *P. wildungensis* from both *P. muelleri* and *P. nasuta*. In representative specimens of *P. jamieae* (see discussion herein p. 58) the platform outline tends to be pyriform and the interior of the platform is not depressed.

Specimens from the present study occur in the Early *rhenana* Zone and in the lower part of the Late *rhenana* Zone.

Genus *Polygnathus* HINDE, 1879.

In the conodont faunas of the present study we formally recognised twelve *Polygnathus* taxa, seven of them are figured on Pl. 8, the other five were illustrated in HELSEN & BULTYNCK, 1992 (pl. 2). The taxa are not discussed herein and in the distribution tables 1 to 5 they are assembled in two groups, A and B. *Polygnathus* group A consists of taxa with a relatively wide platform, distinctly ornamented with ridges and/or eventually nodes. Group B includes taxa with a narrow, smooth or only weakly ornamented platform. A list of the *Polygnathus* taxa including the original reference and references to the specimens figured herein or in HELSEN & BULTYNCK (1992) is appended here below.

Polygnathus group A

Polygnathus aequalis KLAPPER & LANE, 1985, pp. 930-931, figs. 16.7-16.14; HELSEN & BULTYNCK, 1992, pl. 2, fig. 5.
Polygnathus alatus HUDDLE, 1934, p. 100, pl. 8, figs. 19-20; Pl. 8, Figs. 14-15; HELSEN & BULTYNCK, 1992, pl. 2, fig. 6.
Polygnathus brevis MILLER & YOUNGQUIST, 1947, p. 514, pl. 74, fig. 9; HELSEN & BULTYNCK, 1992, pl. 2, fig. 8.

Polygnathus evidens KLAPPER & LANE, 1985, pp. 935-936, figs. 20.1-20.8; Pl. 8, Fig. 16.
Polygnathus aff. *P. evidens*, Pl. 8, Figs. 13, 17.
Polygnathus independensis MÜLLER & MÜLLER, 1957, pp. 1088-1089, pl. 141, figs. 2, 9; HELSEN & BULTYNCK, 1992, pl. 2, fig. 10.
Polygnathus webbi STAUFFER, 1938, p. 439, pl. 53, figs. 25, 26, 28, 29; HELSEN & BULTYNCK, 1992, pl. 2, fig. 11.

Polygnathus group B

Polygnathus angustidiscus YOUNGQUIST, 1945, p. 365, pl. 54, fig. 2; HELSEN & BULTYNCK, pl. 2, fig. 7.
Polygnathus aspelundi SAVAGE & FUNAI, 1980, p. 812, pl. 2, figs. 1-33; Pl. 8, Figs. 5-6.
Polygnathus decorosus STAUFFER, 1938, p. 438, pl. 53, figs. 5, 6, 10, 15, 16; Pl. 8, Figs. 11-12; HELSEN & BULTYNCK, 1992, pl. 2, fig. 12 (erroneously assigned there to *P. xylus*).
Polygnathus pacificus SAVAGE & FUNAI, 1980, p. 811-812, pl. 2, figs. 6-17; Pl. 8, Figs. 7-9.
Polygnathus xylus STAUFFER, 1940, pp. 430-431, pl. 60, fig. 72; Pl. 8, Fig. 4.

Conclusions

Upper Frasnian deposits of the central southern part of the Dinant Synclinorium are represented by two different, partly synchronous fine shale sequences: the Valisettes Fm consisting of dark grey-greenish shales and the Matagne Fm characterised by fissile blackish to black shales. They surmount greenish-brownish nodular limestones and shales of the Neuville Fm.

1. The **Neuville Fm**, also characterised by the development of reddish mudmounds, is more or less uniformly represented in the whole area. The middle and upper parts belong to the Early *rhenana* conodont Zone and based on conodont biofacies, a clear deepening trend is recognised topwards. SANDBERG *et al.* (1992) assigned the upper part of this formation to the Late *rhenana* Zone, mainly on the basis of the first occurrence of *Palmatolepis subrecta*. However, the two figured specimens (ibidem: pl. 2, figs. 4-5) are not representative for *Pa. subrecta*, missing the characteristic "long narrow anterior platform", as mentioned in the revised diagnosis of ZIEGLER & SANDBERG (1990: 61). SANDBERG *et al.* (1992: pl. 2, fig. 6) also figure one specimen assigned to *Palmatolepis rhenana rhenana* (first occurrence defining the base of the Late *rhenana* Zone) from the Neuville Formation. This specimen differs from *Pa. rhenana rhenana* in missing "an extremely long, slender platform", as mentioned in the revised diagnosis of ZIEGLER & SANDBERG (1990: 58).

2. In the southern central part of the Dinant Synclinorium (Frasnes-Nismes-Lessive areas), the **Matagne Fm** mostly surmounts directly the Neuville Fm, and, if present, the Valisettes Fm is reduced to a few meters. The Neuville-Matagne contact is not abrupt, and the lowest part of the

Matagne Fm comprises lenticular dark limestone beds with brachiopods, orthoconic cephalopods and goniatites. The thickness of the overlying black shale sequence is at least 40 to 50 m. The base of the formation is just below or above the base of the Late *rhenana* Zone. Reddish mudmounds do not occur above the Neuville Fm in this area. The base of the Late *rhenana* Zone is demonstrated by the first occurrence of *Palmatolepis subrecta*, *P. rotunda*, *P. hassi* s.s. and *Ancyrognathus asymmetricus*.

3. At Neuville, in the more northerly (± 10 km) Philippeville Massif a thick sequence of at least 100 m of fine, dark grey-greenish shales belonging to the **Valisettes Fm** surmounts the Neuville Fm. The base of the Valisettes Fm is just above the Late *rhenana* Zone and coincides approximately with the base of the Matagne Fm in the southern area. Within the Valisettes Fm rich coral faunas and mudmounds occur. Two packages of black Matagne shales, each about 10 m thick and separated by a shale-limestone sequence about 60 m thick and assigned to the Valisettes Fm, occur in the upper part of the Neuville section. The second occurrence of Matagne shales surmounts brachiopod limestones with characteristic *linguiformis* Zone conodonts and is at the top separated by a fault contact from Senzeilles shales assigned to the *triangularis* and Early and Middle *crepida* Zones.

4. Biostratigraphically, the **Lower Kellwasser Horizon (LKW)** corresponds to the lowest part of the Matagne Formation in the southern Dinant Basin, though not necessarily to its base. It may be traced by dark limestone beds with abundant icriodid faunas, succeeded by fine blackish shales. The available conodont data at Neuville indicate the time equivalent of the LKW in the lower part of the Valisettes Formation, close to the base of the unit with fine dark grey-greenish shales. In the same section the **Upper Kellwasser Horizon (UKW)** is well documented by the second occurrence of the Matagne shales. From the Frasnes area to the Philippeville area the thickness of the Matagne Fm is reduced and its base shifts from the upper Early *rhenana*/lower Late *rhenana* Zones to the *linguiformis* Zone. The black shale sequence from the Frasnes area together with that in the Philippeville Massif correspond to the "Kellwasser Crisis", and do not represent an abrupt, short-lasting event.

5. Finally, we cannot pass without comments on the discrepancies between the Frasnian conodont taxonomy and "standard zonation" of ZIEGLER & SANDBERG (1990) on the one hand, and the Frasnian conodont species and ranges described by KLAPPER (1988, 1990) and by KLAPPER & FOSTER (1993) on the other hand. Although our conodont taxonomy is based on Pa elements, using the "standard zonation", we also took into account the description of the Pa elements and the range charts from the above mentioned KLAPPER and KLAPPER & FOSTER papers. We could not just "contemplate these and decide which zonation is more useful", as stated by SANDBERG *et al.* (1992: 30). We did not limit ourselves to one taxonomy and zonation: for the range of *Palmatolepis subrecta* our data best correspond to the results of ZIEGLER & SANDBERG (1990), while for the taxonomy of *Palmatolepis hassi* we distinguish a *Pa. hassi* s.l. and a *Pa. hassi* s.s., the latter corresponding to the diagnosis of KLAPPER & FOSTER (1993). Concerning *Palmatolepis wildungensis* none of the opinions expressed by both author groups were considered satisfactory.

Acknowledgements

References

BISCHOFF, G., 1956. Oberdevonische Conodonten (to 1) aus dem Rheinischen Schiefergebirge. *Notizblatt des Hessischen Landesamtes für Bodenforschung*, **86**: 115-137.

BOUCKAERT, J. & MOURAVIEFF, N. avec la collaboration de E. BLYSKOWSKA, 1970. Déviation de la ligne 132. Description géologique du raccord de Neuville. *Service Géologique de Belgique, Professional Paper*, 1970/8: 1-11.

BOULVAIN, F., 1993. Sédimentologie et diagenèse des monticules micrites "F2j" du Frasnien de l'Ardenne. *Service Géologique de Belgique, Professional Paper*, **260**: 1-427.

BOULVAIN, F., COEN, M., COEN-AUBERT, M., BULTYNCK, P., CASIER, L. & TOURNEUR, F., 1993. Les formations frasniennes du Massif de Philippeville. *Service géologique de Belgique, Professional Paper*, **259**: 1-37.

BRANSON, E.B. & MEHL., 1934. Conodonts from the Grassy Creek Shale of Missouri. *The University of Missouri Studies*, **8**(3): 171-259.

BUGGISCH, W., 1972. Zur Geologie und Geochemie der Kellwasserkalke und ihrer begleitenden Sedimente (Unteres Oberdevon). *Abhandlungen des Hessischen Landesamtes für Bodenforschung*, **62**: 1-68.

BULTYNCK, P., 1987. Pelagic and neritic conodont successions from the Givetian of pre-Sahara Morocco and the Ardennes. *Bulletin Institut royal des Sciences naturelles de Belgique, Sciences de la Terre*, **57**: 149-181.

BULTYNCK, P., COEN-AUBERT, M., DEJONGHE, L., GODEFROID, J., HANCE, L., LACROIX, D., PREAT, A., STAINIER, P., STEEMANS, Ph., STREEL, M. & TOURNEUR, F., 1991. Les formations du Dévonien Moyen de la Belgique. *Mémoires pour servir à l'Explication des Cartes Géologiques et Minières de la Belgique*, **30**: 1-106.

BULTYNCK, P. & MARTIN, F., 1995. Assessment of an old stratotype: the Frasnian/Famennian boundary at Senzeilles, southern Belgium. *Bulletin Institut royal des Sciences naturelles de Belgique, Sciences de la Terre*, **65**: 5-34.

CASIER, J.-G., 1975. Les ostracodes des schistes à aspect "Matagne" de la partie supérieure du Frasnien de l'affleurement protégé de Boussu-en-Fagne, Belgique. *Bulletin Institut royal des Sciences naturelles de Belgique, Sciences de la Terre*, **51**(9): 1-33.

CASIER, J.-G., 1989. Paléoécologie des ostracodes au niveau de la limite des étages Frasnien et Famennien, à Senzeilles. *Bulletin Institut royal des Sciences naturelles de Belgique, Sciences de la Terre*, **59**: 79-93.

CASIER, J.-G., 1992. Description et étude des ostracodes de deux tranchées traversant la limite historique Frasnien-Famennien dans la localité-type. *Bulletin Institut royal des Sciences naturelles de Belgique, Sciences de la Terre*, **62**: 109-119.

COEN, M., 1973. Facies, conodontes et stratigraphie du Frasnien de l'est de la Belgique, pour servir à une révision de l'étage. *Annales de la Société Géologique de Belgique*, **95**: 239-253.

COEN, M., 1977a. La Klippe du Bois Niau. *Bulletin Société belge de Géologie*, **86**: 41-44.

COEN, M., 1977b. Le Givetien et le Frasnien dans le contournement routier de Philippeville. Comparaisons avec la coupe de Neuville. *Annales de la Société Géologique de Belgique*, **100**: 23-30.

COEN, M. & COEN-AUBERT, M., 1974. Conodontes et coraux de la partie supérieure du Frasnien dans la tranchée du chemin de fer de Neuville (Massif de Philippeville, Belgique). *Bulletin Institut royal des Sciences naturelles de Belgique, Sciences de la Terre*, **50**(8): 1-7.

COEN-AUBERT, M., 1994. Stratigraphie et systématique des Rugueux de la partie moyenne du Frasnien de Frasnes-les-Couvin (Belgique). *Bulletin Institut royal des Sciences naturelles de Belgique, Sciences de la Terre*, **64**: 21-56.

FORIR, H. 1900. Carte Géologique de la Belgique à 1//40.000, n° 185 feuille Houyet - Han-sur-Lesse. *Institut Cartographique Militaire*, Bruxelles.

GODEFROID, J., BLIECK, A., BULTYNCK, P., DEJONGHE, L., GERRIENNE, P., HANCE, L., MEILLIEZ, F., STAINIER, P. & STEEMANS, P., 1994. Les formations du Dévonien Inférieur du Massif de la Vesdre, de la Fenêtre de Theux et du Synclinorium de Dinant (Belgique, France). *Mémoires pour servir à l'Explication des Cartes Géologiques et Minières de la Belgique*, **38**: 1-144.

GODEFROID, J. & HELSEN, S., (in press). The last Frasnian atrypoid brachiopods in southern Belgium. *Acta Palaeontologica Polonica*, **43**.

GOSSELET, J. 1871. Esquisse géologique du département du Nord et des contrées voisines. 1er fascicule: Terrains primaires. 107 pp. Lille.

HELSEN, S.. & BULTYNCK, P., 1992. Conodonts and megafauna from two sections at Nismes and Mariembourg (Frasnian of the southern flank of the Dinant Synclinorium, Belgium). *Annales de la Société Géologique de Belgique*, **115**: 145-157.

HINDE, G.J., 1879. On conodonts from the Chazy and Cincinnati Group of the Cambro-Silurian, and from the Hamilton and Genesee-Shale divisions of the Devonian, in Canada and the United States. *Quarterly Journal of the Geological Society of London*, **35**(3): 351-369.

HUDDLE, J.W., 1934. Conodonts from the New Albany Shale of Indiana. *Bulletins of American Paleontology*, **21**(72): 1-137.

KLAPPER, G., 1988. The Montagne Noire Frasnian (Upper Devonian) conodont succession. *In*: McMILLAN, N.J., EMBRY, A.F. & GLASS, D.J. (Editors). Devonian of the World. *Canadian Society of Petroleum Geologists*, **14**(3): 449-468.

KLAPPER, G., 1990. Frasnian species of the Late Devonian conodont genus *Ancyrognathus*. *Journal of Paleontology*, **64**(6): 998-1025.

KLAPPER, G. & FOSTER, C.T., 1986. Quantification of outlines in Frasnian (Upper Devonian) platform conodonts. *Canadian Journal of Earth Sciences*, **23**(8): 1214-1222.

KLAPPER, G. & FOSTER, C.T., 1993. Shape analysis of Frasnian species of the Late Devonian conodont genus *Palmatolepis*. *The Paleontological Society Memoir*. Supplement *Journal of Paleontologyy*, **67**(4), 32: 1-35.

KLAPPER, G., KUZ'MIN, A.V. & OVNATANOVA, N.S., 1996. Upper Devonian conodonts from the Timan-Pechora region, Russia, and correlation with a Frasnian composite standard. *Journal of Paleontology*, **70**(1): 131-151.

KLAPPER, G. & LANE, H.R., 1985. Upper Devonian (Frasnian) conodonts of the *Polygnathus* biofacies, N.W.T., Canada. *Journal of Paleontology*, **59**(4): 904-951.

MATERN, H. 1931. Die Goniatiten-Fauna der Schistes de Matagne in Belgien. *Bulletin Institut royal des Sciences naturelles de Belgique*, **7**(13): 1-15.

MILLER, A.K. & YOUNGQUIST, W., 1947. Conodonts from the type section of the Sweetland Creek Shale in Iowa. *Journal of Paleontology*, **21**(6): 501-517.

MOURAVIEFF, A.N. 1970. Conodontes du Frasnien de la Belgique. Biostratigraphie et aspects écologiques. *Unpublished PhD thesis U.C.L.* 140 pp. Leuven.

MOURAVIEFF, A.N., 1974. Excursion F. International Symposium on Belgian micropaleontological limits from Emsian to Visean, Namur 1974. Service Géologique de Belgique, Bruxelles, pp. 1-13.

MOURAVIEFF, A.N., 1982. Conodont stratigraphic scheme of the Frasnian of the Ardennes. *In*: Papers on the Frasnian-Givetian boundary. Subcommission on Devonian Stratigraphy. Geological Survey of Belgium, Brussels, pp. 101-118.

MÜLLER, K.J., 1956. Die Gattung *Palmatolepis*. *Abhandlungen der senckenbergischen naturforschenden Gesellschaft*, **494**: 1-70.

MÜLLER, K.J. & MÜLLER, E.M., 1957. Early Upper Devonian (Independence) conodonts from Iowa, Part I. *Journal of Paleontology*, **31**(6): 1069-1108.

SANDBERG, C.A. & DREESEN, R., 1984. Late Devonian icriodontid biofacies models and alternate shallow-water conodont zonation. *Geological Society of America, Special Paper*, **196**: 143-178.

SANDBERG, C.A., ZIEGLER, W., DREESEN, R. & BUTLER, J.L., 1988. Late Frasnian mass extinction: conodont event stratigraphy, global changes, and possible causes. *Courier Forschungsinstitut Senckenberg*, **102**: 263-307.

SANDBERG, C.A., ZIEGLER, W., DREESEN, R. & BUTLER, J.L., 1992. Conodont biostratigraphy around middle Frasnian Lion Mudmound (F2h). Frasnes, Belgium. *Courier Forschungsinstitut Senckenberg*, **150**, 87 pp.

SARTENAER, P., 1974. La Zone à *Caryorhynchus tumidus*, zone nouvelle de la partie supérieure du Frasnien. *Bulletin Institut royal des Sciences naturelles de Belgique, Sciences de la Terre*, **50**(6): 1-11.

SAVAGE, N.M. & FUNAI, C.A., 1980. Devonian conodonts of

probable early Frasnian age from the Coronados Islands of southern Alaska. *Journal of Paleontology*, **54**(4): 806-813.

SCHINDLER, E. 1993. Event-stratigraphic markers within the Kellwasser Crisis near the Frasnian/Famennian boundary (Upper Devonian) in Germany. *Palaeogeography, Palaeoclimatology, Palaeoecology*, **104**: 115-125.

SCHUMACHER, D., 1976. Conodont biofacies and paleoenvironments in Middle Devonian-Upper Devonian boundary beds, Central Missouri. *The Geological Association of Canada, Special Paper*, **15**: 159-169.

STAUFFER, C.R., 1938. Conodonts of the Olentangy Shale. *Journal of Paleontology*, **12**(5): 411-443.

STAUFFER, C.R., 1940. Conodonts from the Devonian and associated clays of Minnesota. *Journal of Paleontology*, **14**: 417-435.

TOURNEUR, F., 1982. Conodontes de trois "récifs de marbre rouge F2j" stratigraphie et écologie. *Bulletin de la Société belge de Géologie*, **91**: 91-102.

TSIEN, H.-H., 1974. Paleoecology of Middle Devonian and Frasnian in Belgium. International Symposium on Belgian micropaleontological limits from Emsian to Visean, Namur 1974, **12**: 1-53. Service Géologique de Belgique, Bruxelles.

ULRICH, E.O. & BASSLER, R.S., 1926. A classification of the tooth-like fossils, conodonts, with descriptions of American Devonian and Mississippian species. *Proceedings of the U.S. National Museum*, **68**(12): 1-63.

VANDELAER, E., VAN DORMAEL, C. & BULTYNCK, P., 1989. Biofacies and refinement of conodont succession in the Lower Frasnian (Upper Devonian) of the type area (Frasnes-Nismes, Belgium). *Courier Forschungsinstitut Senckenberg*, **117**: 321-351.

WEDDIGE, K., 1984. Zur Stratigraphie und Paläogeographie des Devons und Karbons von NE-Iran. *Senckenbergiana Lethaea*, **65**(1/3): 179-223.

YOUNGQUIST, W., 1945. Upper Devonian conodonts from the Independence Shale (?) of Iowa. *Journal of Paleontology*, **19**(4): 355-367.

ZIEGLER, W., 1958. Conodontenfeinstratigraphische Untersuchungen an der Grenze Mitteldevon/Oberdevon und in der Adorfstufe. *Notizblatt des Hessischen Landesamtes für Bodenforschung*, **87**: 7-77.

ZIEGLER, W., 1959. *Ancyrolepis* n. gen. (Conodonta) aus dem höchsten Teil der *Manticoceras*-Stufe. *Neues Jahrbuch für Geologie und Paläontologie, Abhandlungen*, **108**(1): 75-80.

ZIEGLER, W., 1962. Taxionomie und Phylogenie Oberdevonischer Conodonten und ihre Stratigraphische Bedeutung. *Abhandlungen des Hessischen Landesamtes für Bodenforschung*, **38**: 1-166.

ZIEGLER, W. & SANDBERG, C.A., 1990. The Late Devonian Standard conodont zonation. *Courier Forschungsinstitut Senckenberg*, **121**: 1-115.

Pierre BULTYNCK
Dept. of Palaeontology
Koninklijk Belgisch Instituut voor
Natuurwetenschappen
Vautierstraat 29, B-1000 Brussels,
Belgium

Stefan HELSEN
Afd. Historische Geologie-Instituut voor
Aardwetenschappen
Redingenstraat 16, B-3000 Leuven,
Belgium

Joanna HAYDUCKIEWICH
Geology Department
University of Wroclaw
Wroclaw, Poland

PLATE 1

All magnifications are x 78.

Figs. 1-7   – *Palmatolepis wildungensis* MÜLLER, 1956.
             I.R.Sc.N.B. N°b 3285, b 3286, b 3287, b 3288, b 3289, b 3290, b 3291, CFrE 1A.
Fig. 8   – *Palmatolepis barba* ZIEGLER & SANDBERG, 1990.
             I.R.Sc.N.B. N°b 3292, JH 11.
Fig. 9   – *Palmatolepis* aff. *P. jamieae* ZIEGLER & SANDBERG, 1990.
             I.R.Sc.N.B. N°b 3293, JH 42.
Figs. 10, 11 – *Palmatolepis wildungensis* MÜLLER, 1956.
             I.R.Sc.N.B. N°b 3294, b 3295, JH 20.
Fig. 12   – *Palmatolepis muelleri* KLAPPER & FOSTER, 1993.
             I.R.Sc.N.B. N°b 3296, CFrE 9.
Fig. 13   – *Palmatolepis jamieae* ZIEGLER & SANDBERG, 1990.
             I.R.Sc.N.B. N°b 3297, CFrW 4.
Fig. 14   – *Palmatolepis proversa* ZIEGLER, 1958.
             I.R.Sc.N.B. N°b 3298, JH 11.

PLATE 2

All magnifications are x 78.

Figs. 1-5 – *Palmatolepis hassi* MÜLLER & MÜLLER, 1957.
s.l.= sensu ZIEGLER & SANDBERG, 1990.
I.R.Sc.N.B. N°b 3299, b 3300, b 3301, b 3302, b 3303, JH 21 (transitional form to *P. nasuta)*, JH 21, JH 10, N12A'
(identification with?), N 12A'.

Fig. 6 – *Palmatolepis hassi* MÜLLER & MÜLLER, 1957.
s.s.= sensu KLAPPER & FOSTER, 1993.
I.R.Sc.N.B. N°b 3304, JH 42.

Fig. 7 – *Palmatolepis gigas* MILLER & YOUNGQUIST, 1947.
I.R.Sc.N.B. N°b 3305, N 12C.

Figs. 8, 9 – *Palmatolepis paragigas* ZIEGLER & SANDBERG, 1990.
I.R.Sc.N.B. N°b 3306, b 3307, CFrW 7, CFrE 1A.

PLATE 3

All magnifications are x 78.

Fig. 1 – *Palmatolepis hassi* MÜLLER & MÜLLER, 1957.
?s.s.= sensu KLAPPER & FOSTER, 1993.
I.R.Sc.N.B. N°b 3308, CFrW 2.

Fig. 2-7 – *Palomatolepis hassi* MÜLLER & MÜLLER, 1957.
s.s.= sensu KLAPPER & FOSTER, 1993.
I.R.Sc.N.B. N°b 3309, b 3310, b 3311, b 3312, b 3313, b 3314, CFrE 7, CFrW 7, L 4b, CFrW sample COEN F5, CFrE 7,
L 4b.

Figs. 8-13 – *Palmatolepis subrecta* MILLER & YOUNGQUIST, 1947.
I.R.Sc.N.B. N°b 3315, b 3316, b 3317, b 3318, b 3319, b 3320, JH 45, JH 32b, JH 40, L 3', N 16A, L sample COEN
HAN 26.

PLATE 4

All magnifications are x 78.

Figs. 1-11 – *Palmatolepis rotunda* ZIEGLER & SANDBERG, 1990.
I.R.Sc.N.B. N°b 3321, b 3322, b 3323, b 3324, b 3325, b 3326, b 3327, b 3328, b 3329, b 3330, b 3331, figs. 1-8 from
JH 42, CFrE 9, JH 32b, L 4a.

Fig. 12 – *Palmatolepis rhenana* BISCHOFF, 1956.
I.R.Sc.N.B. N°b3332, JH 42.

PLATE 5

All magnifications x 78, except fig. 4 x 39.

Figs. 1, 2 – *Palmatolepis linguiformis* MÜLLER, 1956.
I.R.Sc.N.B. N°b 3333, b 3334, NV 11, NV 9.

Figs. 3, 5-7 – *Palmatolepis nasuta* MÜLLER, 1956.
I.R.Sc.N.B. N°b 3335, b 3337, b 3338, b 3339, NV 9, JH 42, JH 42, CFrW 2.

Fig. 4 – *Palmatolepis rhenana* BISCHOFF, 1956.
I.R.Sc.N.B. N°b 3336, JH 42.

Figs. 8-10 – *Ancyrodella curvata* (BRANSON & MEHL, 1934) latest form.
I.R.Sc.N.B. N°b 3340, b 3341, b 3342, NV9, JH 42, NV 9.

PLATE 6

All magnifications are x 78.

Figs. 1, 2   – *Ancyrodella curvata* (BRANSON & MEHL, 1934) late form.
                I.R.Sc.N.B. N°b 3343, b 3344, JH 42.

Fig. 3   – *Ancyrodella curvata* (BRANSON & MEHL, 1934) latest form.
                I.R.Sc.N.B. N°b 3345, JH 42.

Fig. 4   – *Ancyrodella nodosa* ULRICH & BASSLER, 1926.
                I.R.Sc.N.B. N°b 3346, JH 23.

Fig. 5   – *Ancyrognathus sinelobus* (SANDBERG, ZIEGLER & DREESEN, 1992).
                I.R.Sc.N.B. N°b 3347, JH 42.

Figs. 6, 7   – *Ancyrognathus triangularis* YOUNGQUIST, 1945.
                I.R.Sc.N.B. N°b 3348, b 3349, JH 20, JH 39.

Fig. 8   – *Ancyrognathus* aff. *A. tsiensi* MOURAVIEFF, 1982.
                I.R.Sc.N.B. N°b 3350, JH 37.

Figs. 9a-b, 10a-b – *Ancyrognathus coeni* KLAPPER, 1990 - *Ancyrognathus tsiensi* MOURAVIEFF, 1982 group.
                I.R.Sc.N.B. N°b 3351, b 3352, JH 11, JH 17.

Fig. 11   – *Ancyrognathus tsiensi* MOURAVIEFF, 1982.
                I.R.Sc.N.B. N°b 3353, JH 42.

PLATE 7

All magnifications x 78, except fig. 1 x 234.

Figs. 1-5   – *Ancyrognathus asymmetricus* (ULRICH & BASSLER, 1926).
            I.R.Sc.N.B. N°b 3354, b 3355, b 3356, b 3357, b 3358, Fig. 1, detail of pit JH 40, Figs. 2-4 JH 40, Fig. 5 CFrE 7.

Figs. 6-8   – *Ancyrognathus asymmetricus* (ULRICH & BASSLER, 1926 - *Ancyrognathus uddeni* (MILLER & YOUNGQUIST, 1947).
            I.R.Sc.N.B. N°b 3359, b 3360, b 3361, L sample COEN Han 28, C 17, CFrW sample COEN F 6.

Figs. 9-11 – *Ancyrognathus amana* MÜLLER & MÜLLER, 1957.
            I.R.Sc.N.B. N°b 3362, b 3363, b 3364, C 16.

Fig. 12   – *Ancyrolepis cruciformis* ZIEGLER, 1959.
            I.R.Sc.N.B. N°b 3365, JH 47.

PLATE 8

All magnifications x 62.

Fig. 1   – *Palmatolepis wolskajae* OVNATANOVA, 1969.
             I.R.Sc.N.B. N°b 3366, JH 47.

Fig. 2   – *Palmatolepis tenuipunctata* SANNEMANN, 1955.
             I.R.Sc.N.B. N°b 3367, JH 47.

Fig. 3   – *Palmatolepis quadrantinodosalobata* SANNEMANN, 1955.
             I.R.Sc.N.B. N°b 3368, JH 47.

Fig. 4   – *Polygnathus xylus* STAUFFER, 1940.
             I.R.Sc.N.B. N°b 3369, JH 7.

Figs. 5, 6   – *Polygnathus aspelundi* SAVAGE & FUNAI, 1980.
             I.R.Sc.N.B. N°b 3370, b 3371, JH 11.

Figs. 7-9   – *Polygnathus pacificus* SAVAGE & FUNAI, 1980.
             I.R.Sc.N.B. N°b 3372, b 3373, b 3374, JH 40, JH 32, JH 40.

Fig. 10   – *Polygnathus* sp.
             I.R.Sc.N.B. N°b 3375, JH 10.

Figs. 11, 12 – *Polygnathus decorosus* STAUFFER, 1938.
             I.R.Sc.N.B. N°b 3376, b 3377, JH 42.

Figs. 13,17 – *Polygnathus* aff. *P. evidens* KLAPPER & LANE, 1985.

I.R.Sc.N.B. N°b 3378, b 3382, JH 45, JH 27.

Figs. 14,15 – *Polygnathus alatus* HUDDLE, 1934.
            I.R.Sc.N.B. N°b 3379, b 3380, JH 11.

Fig. 16   – *Polygnathus evidens* KLAPPER & LANE, 1985.
            I.R.Sc.N.B. N°b 3381, JH 27.

Figs. 18-21 – *Icriodus* aff. *I. excavatus* WEDDIGE, 1984.
            I.R.Sc.N.B. N°b 3383, b 3384, b 3385, b 3386, JH 2, JH 11, JH 11, JH 11.

Fig. 22   – *Icriodus alternatus alternatus* BRANSON & MEHL, 1934.
            I.R.Sc.N.B. N°b 3387, JH 37.

Fig. 23   – *Icriodus alternatus helmsi* SANDBERG & DREESEN3, 1984.
            I.R.Sc.N.B. N°b 3388, JH 37.

Fig. 24, 25 – *Icriodus symmetricus* BRANSON & MEHL, 1934.
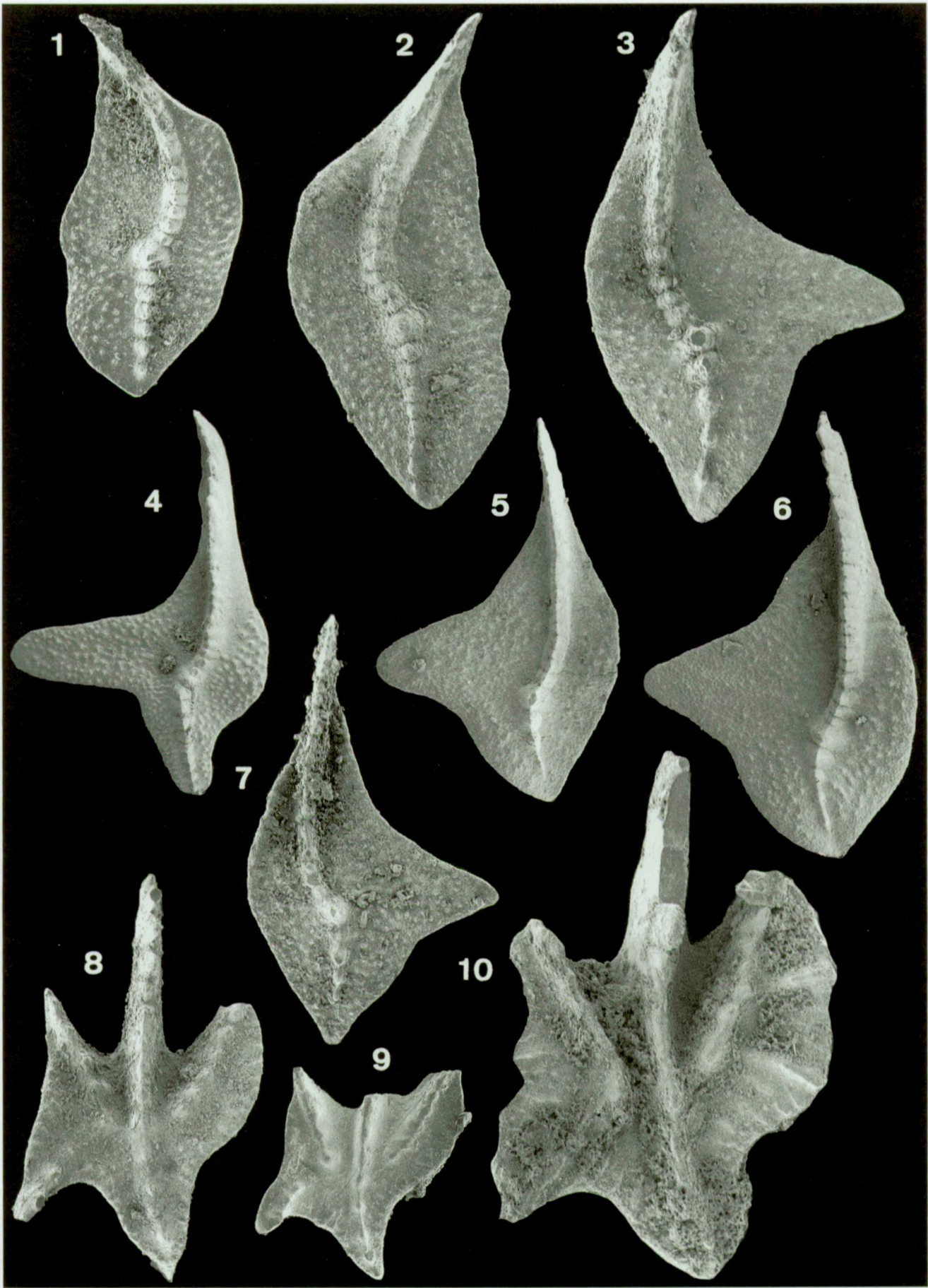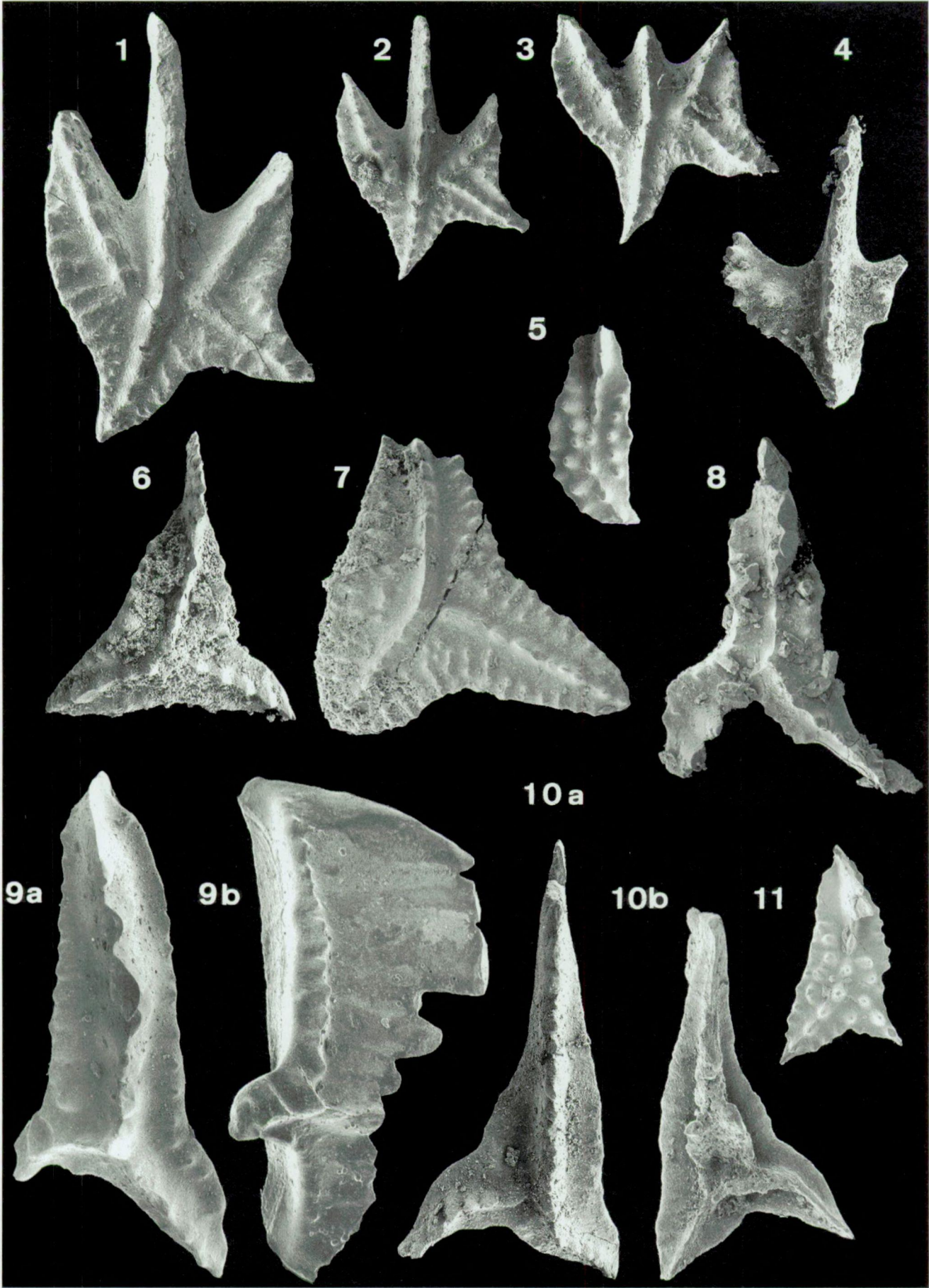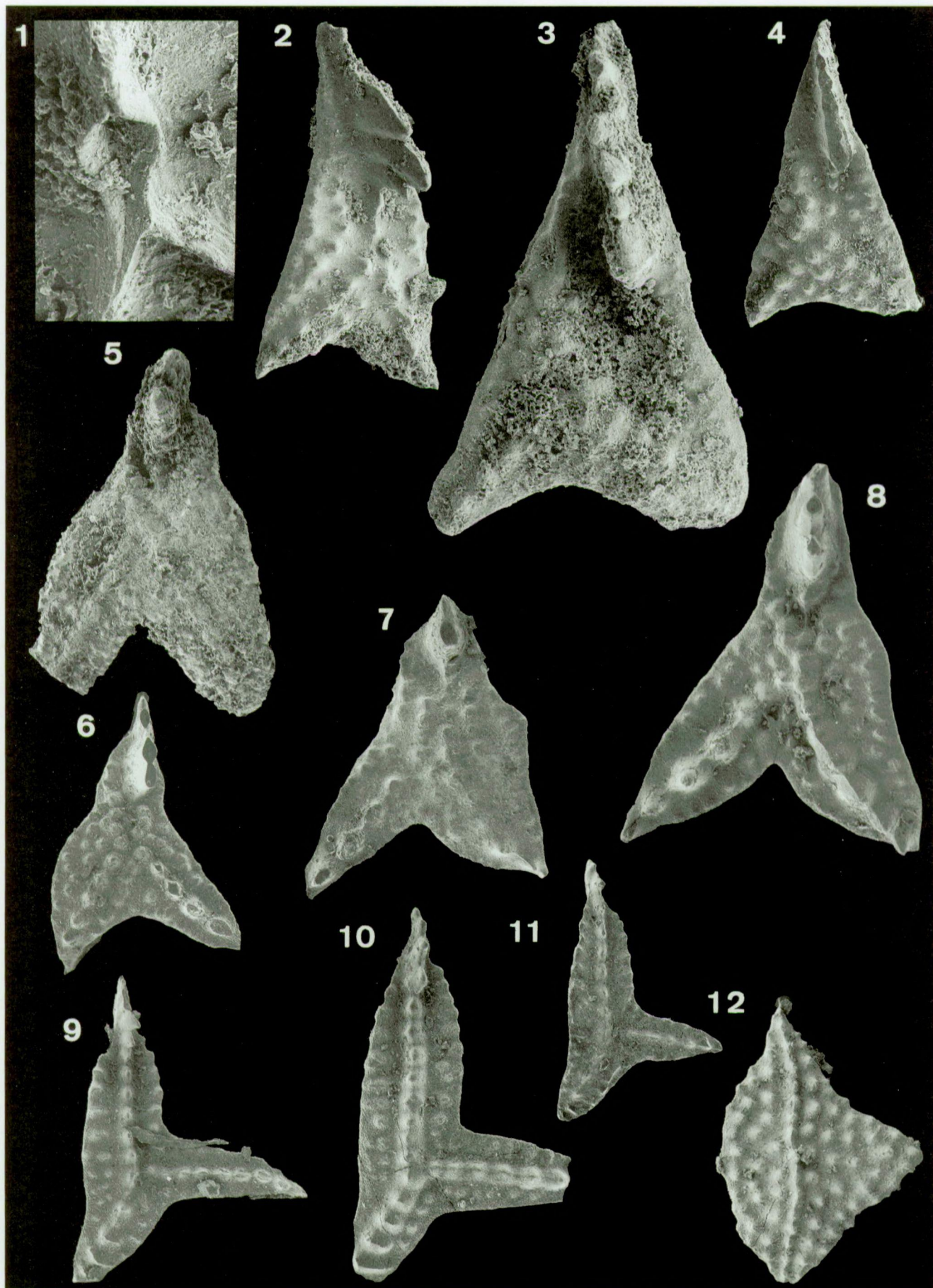   I.R.Sc.N.B. N°b 3389, b 3390, JH 11, JH 26.
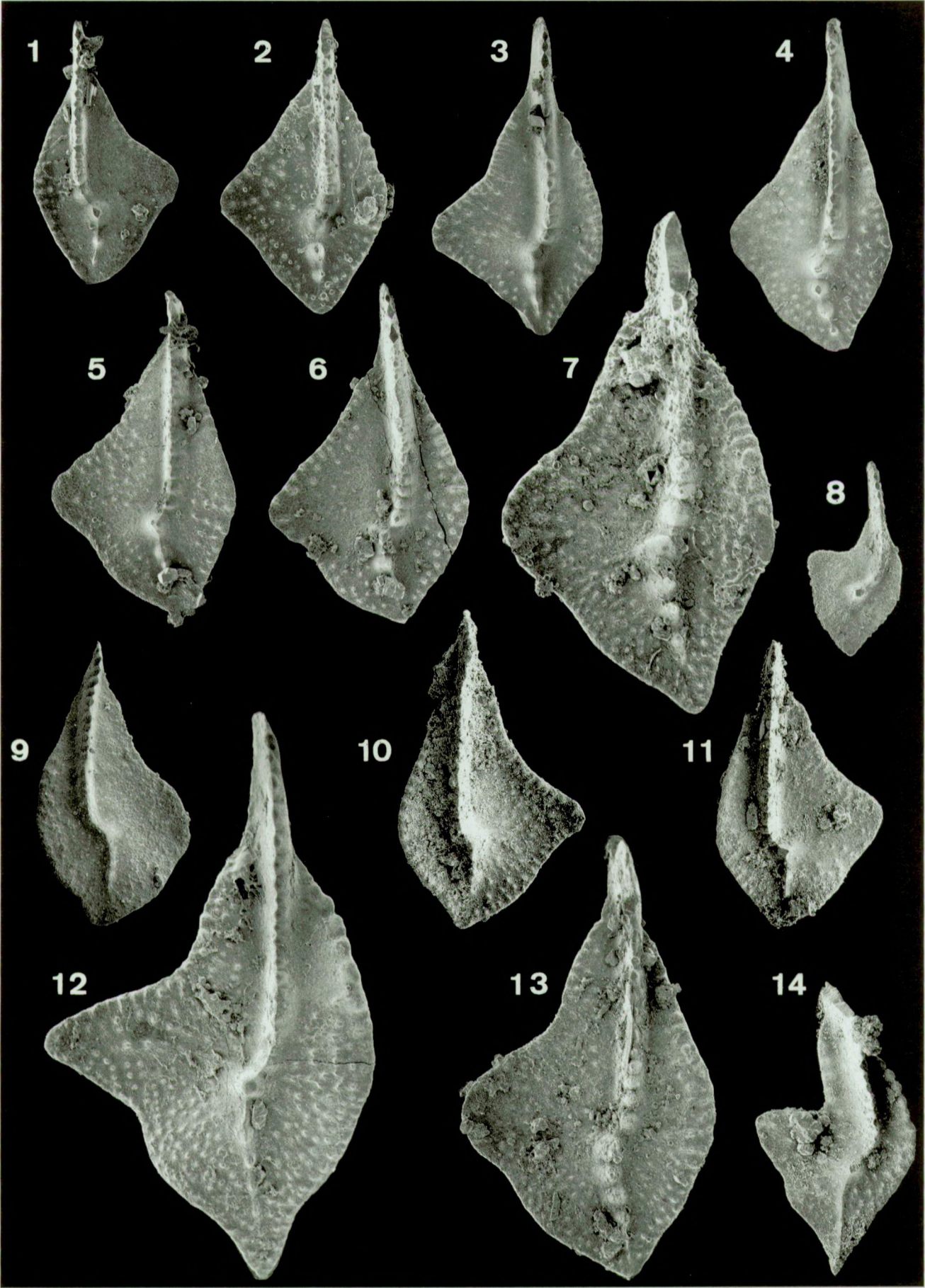
PLATE 1
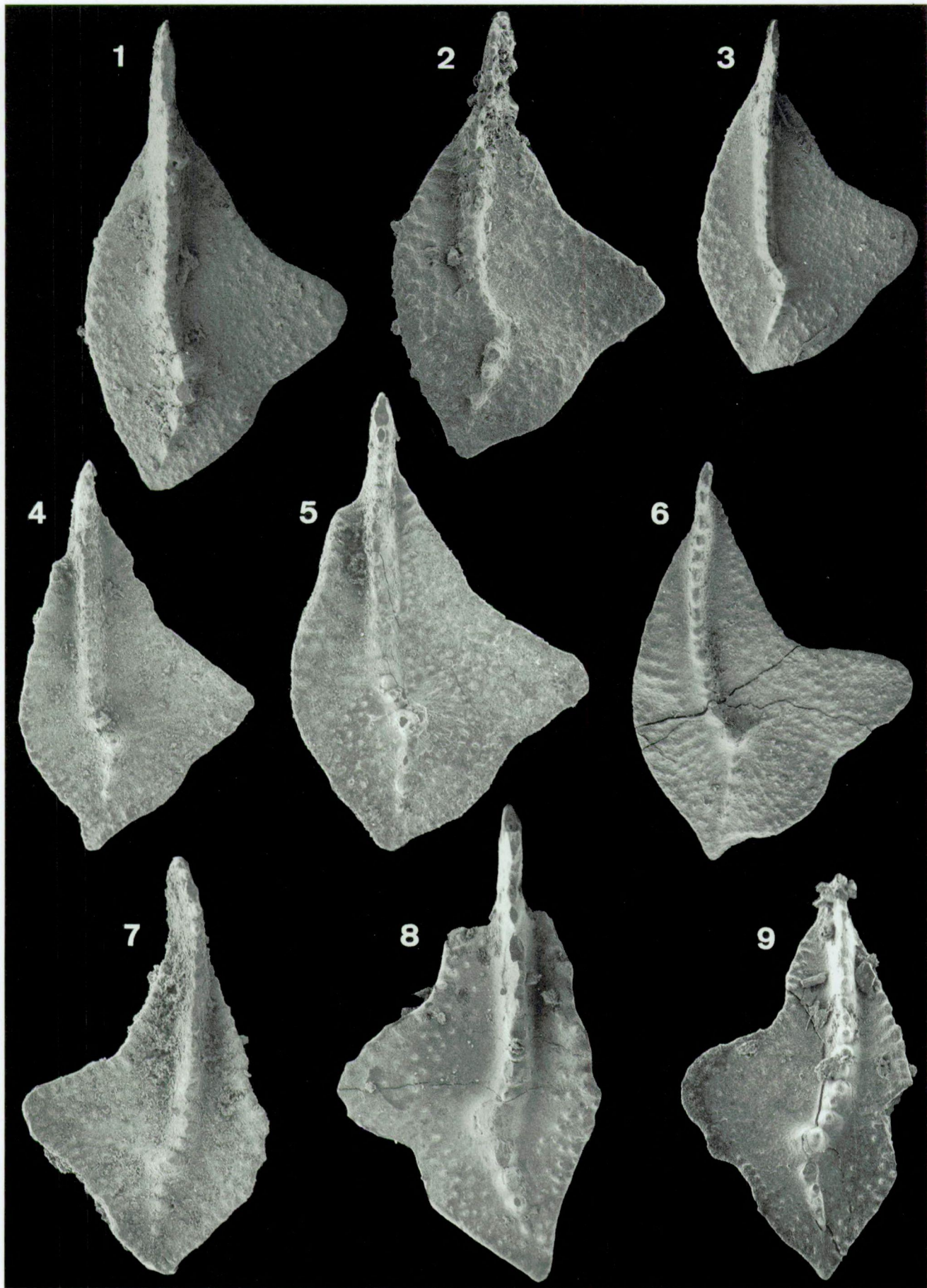
PLATE 2
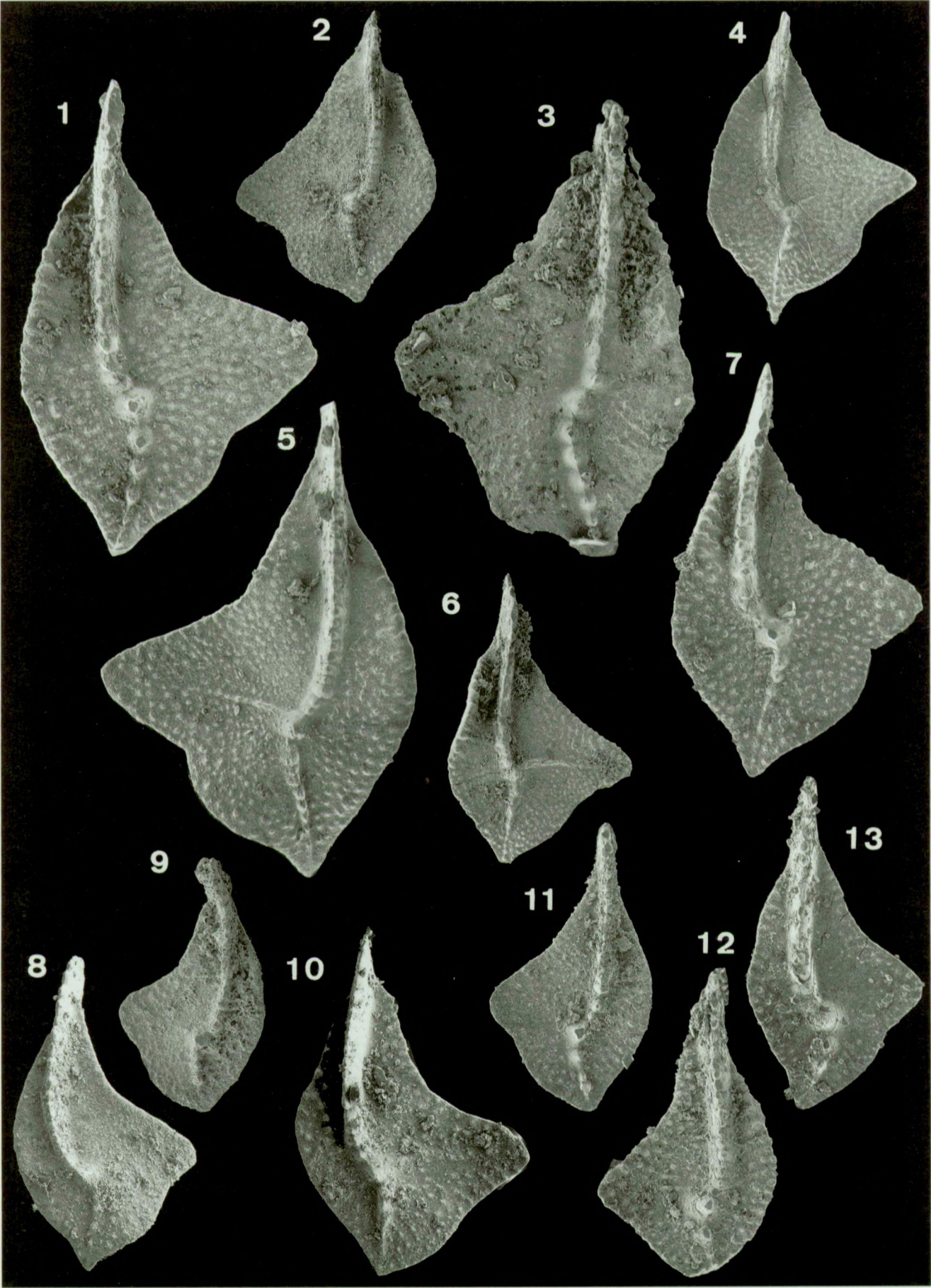
PLATE 3
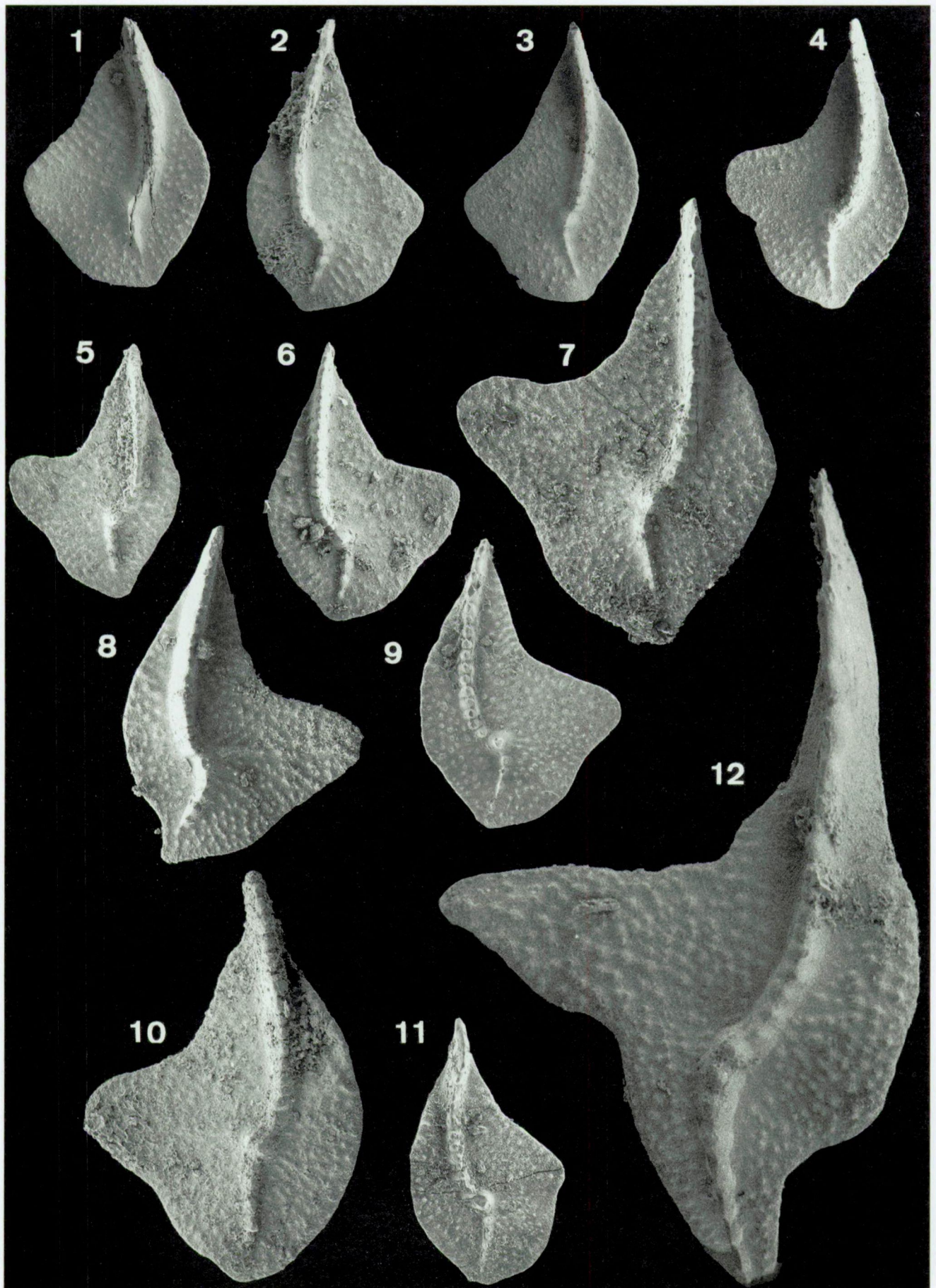
PLATE 4

PLATE 5

PLATE 6

PLATE 7

PLATE 8

*** blanco ***